CANADIAN THESES ON MICROFICHE

THÈSES CANADIENNES SUR MICROFICHE

National Library of Canada
Collections Development Branch

Canadian Theses on
Microfiche Service

Ottawa, Canada
K1A 0N4

Bibliothèque nationale du Canada
Direction du développement des collections

Service des thèses canadiennes
sur microfiche

NOTICE

The quality of this microfiche is heavily dependent upon the quality of the original thesis submitted for microfilming. Every effort has been made to ensure the highest quality of reproduction possible.

If pages are missing, contact the university which granted the degree.

Some pages may have indistinct print especially if the original pages were typed with a poor typewriter ribbon or if the university sent us an inferior photocopy.

Previously copyrighted materials (journal articles, published tests, etc.) are not filmed.

Reproduction in full or in part of this film is governed by the Canadian Copyright Act, R.S.C. 1970, c. C-30. Please read the authorization forms which accompany this thesis.

AVIS

La qualité de cette microfiche dépend grandement de la qualité de la thèse soumise au microfilmage. Nous avons tout fait pour assurer une qualité supérieure de reproduction.

S'il manque des pages, veuillez communiquer avec l'université qui a conféré le grade.

La qualité d'impression de certaines pages peut laisser à désirer, surtout si les pages originales ont été dactylographiées à l'aide d'un ruban usé ou si l'université nous a fait parvenir une photocopie de qualité inférieure.

Les documents qui font déjà l'objet d'un droit d'auteur (articles de revue, examens publiés, etc.) ne sont pas microfilmés.

La reproduction, même partielle, de ce microfilm est soumise à la Loi canadienne sur le droit d'auteur, SRC 1970, c. C-30. Veuillez prendre connaissance des formules d'autorisation qui accompagnent cette thèse.

THIS DISSERTATION
HAS BEEN MICROFILMED
EXACTLY AS RECEIVED

LA THÈSE A ÉTÉ
MICROFILMÉE TELLE QUE
NOUS L'AVONS REÇUE

Canada

Dispersion Band Height Characteristics in a Bench Scale Gravity Settler

by

John Atkinson

Department of Chemical Engineering
University of Ottawa, Ottawa, Ontario

December, 1984

A thesis
presented to the University of Ottawa
in partial fulfillment of the
requirements for the degree of
Master of Applied Science
in
Chemical Engineering

ABSTRACT

A bench scale, single stage, mixer settler unit has been designed to study dispersion band height characteristics. The system studied was the kerosene-adogen 364-sulphate solution with isodecanol modifier. Two types of mixing vessels were studied. 1) square,open, unbaffled. 2) cylindrical, closed, baffled. Dispersions produced were fed to a box type, variable area, gravity settler and the height of the dispersion bands in the settler were measured.

The effects of throughput, agitation intensity in the mixer, dispersed phase fraction in the feed to the mixer, and the area available for settling were investigated. Individual height-settling area relationships were established for runs at constant throughput, agitation intensity, and dispersed phase fraction.

A four parameter model was developed to represent all the data obtained using the square mixer. The parameters were related to the effects of throughput, agitation intensity, dispersed phase fraction in the feed, and settling area. A five parameter model was developed to represent the data at each of the throughput levels investigated using the cylindrical mixer. The parameters were related to the effects of agitation intensity, dispersed phase fraction in the feed, and settling area. The effect of throughput could not be determined using the data obtained and therefore a model to represent all the cylindrical mixer data was not determined.

The model developed for the square mixer data, and the models developed for the cylindrical data at each of the three throughputs levels investigated, were found to adequately represent the data in each case. The models also provided insight into the form of the effects of the process variables on the observed dispersion band heights.

ACKNOWLEDGEMENTS

The author would like to thank Dr. J.A. Golding of the University of Ottawa and Mr. G.M. Ritcey of CANMET for their guidance and the financial support of this project.

The author would also like to thank Dr. David McLean of the University of Ottawa for his help with the mathematical modelling.

A special thankyou also to M. Daniel Lefebvre for his excellent craftsmanship when constructing the equipment used.

CONTENTS

Abstract ii

Acknowledgements iii

Chapter I: Introduction 1

Chapter II: Phase Separation in Gravity Settlers 6

Prediction of Dispersion Band Height in Vertical Settlers 9
Prediction of Dispersion Band Heights in Horizontal Settlers 22

Chapter III: Experimental 25

Apparatus 25
Phase composition 28
Experimental method 30
Experimental Proceedure 31

Chapter IV: Results and Discussion 32

Dispersion Bands in the Laboratory Settler using the Square Mixer 32
Experimental Results Using the Square Mixer 34
Modelling the Square Mixer Results 41
Dispersion Bands in the Laboratory Settler using the Cylindrical Mixer 59
Experimental Results Using the Cylindrical Mixer 60
Modelling the Cylindrical Mixer Results 74
Summary 84

Conclusions 86

Recommendations 87

Nomenclature 89

References 90

Appendix A: Experimental data 92

Appendix B: Statistical Analyses and Modelling 94

Non Linear LeastSquares 100
Minimizing the Sum of Squares of Residuals for a Nonlinear Model 100

Appendix C: Residual Plots for H=(T1/RPM+T2 Q)EXP(T3ϕd/A),Square Mixer 104

Appendix D: Plots of ln H vs 1/A for the Cylindrical Data 108

Appendix E: Plots of ln H vs ln (1/A) for the Cylindrical Data 117

Appendix F: Plots of V/Q vs H for the Cylindrical Data 125

Appendix G: Equipment 135

FIGURES

2.1 H vs Q/A , Stoenner and Wohlers proposal. 21

2.2 Wedge Shaped Dispersion Band 23

3.1 Experimental Equipment 26

3.2 Photographs of Experimental Equipment 27

4.1 Dispersion Band Height vs 1/A 35

4.2 Dispersion Band Height vs 1/A 36

4.3 Dispersion Band Height vs 1/A 37

4.4 The Effect of Dispersed Phase Fraction Q=1500 RPM=500 39

4.5 The Effect of Dispersed Phase Fraction Q=1500 RPM=250 40

4.6 ln H vs ln Q/A and ln H vs Q/A , Square Mixer Run 12 43

4.7 Model parameters vs. Impeller rpm 46

4.8 Model Parameters vs. Throughput 47

4.9 Model Parameters vs. Dispersed Phase Ratio in the Feed 48

4.10 Model Parameter T1 vs. 1/RPM 49

4.11 Residuals vs. Throughput H=(T1/rpm + T2 Q)exp(T3 ϕd/A) 54

4.12 Residuals vs. Predicted Response H=(T1/rpm + T2 Q)exp(T3 ϕd/A) 56

4.13 H vs. 1/A Q=2000 ϕd=.6 61

4.14 H vs. 1/A Q=2000 ϕd=.5 62

4.15 H vs. 1/A Q=2000 ϕd=.4 63

4.16 H vs. 1/A Q=1500 ϕd=.6 64

4.17 H vs. 1/A Q=1500 ϕd=.5 65

4.18 H vs. 1/A Q=1500 ϕd=.4 66

4.19 H vs. 1/A Q=1000 ϕd=.6 67

4.20 H vs. 1/A Q=1000 ϕd=.5 and .4 68

4.21 Plots of Five Parameters vs Q. Cylindrical Data 82

B.1 Joint Confidence Region for Run 13 SofS< 18.95 . . 96

B.2 Joint Confidence Region for Run 1 SofS< 1.22 . . . 97

C.1 Residuals vs. Impeller RPM H=(T1/rpm + T2 Q)exp(T3 ϕd/A) 105

C.2 Residuals vs. Dispersed Phase Ratio H=(T1/rpm + T2 Q)exp(T3 ϕd/A) 106

C.3 Residuals vs. Run Order H=(T1/rpm + T2 Q)exp(T3 ϕd/A) 107

D.1 ln H vs 1/A, Q=2000 ϕd=.6 109

D.2 ln H vs 1/A, Q=2000 ϕd=.5 110

D.3 ln H vs 1/A, Q=2000 ϕd=.4 111

D.4 ln H vs 1/A, Q=1500 ϕd=.6 112

D.5 ln H vs 1/A, Q=1500 ϕd=.5 113

D.6 ln H vs 1/A, Q=1500 ϕd=.4 114

D.7 ln H vs 1/A, Q=1000 ϕd=.6 115

D.8 ln H vs 1/A, Q=1000 ϕd=.5,.4 116

E.1 ln H vs ln (1/A) Q=2000 ϕd=.6 118

E.2 ln H vs ln (1/A) Q=2000 ϕd=.5 119

E.3 ln H vs ln (1/A) Q=2000 ϕd=.4 120

E.4 ln H vs ln (1/A) Q=1500 ϕd=.6 121

E.5 ln H vs ln (1/A) Q=1500 ϕd=.4 122

E.6 ln H vs ln (1/A) Q=1000 ϕd=.6 123

E.7 ln H vs ln (1/A) Q=1000 ϕd=.5,.4 124

F.1 1/H vs A Q=2000 ϕd=.6 127

F.2 V/Q vs H Q=2000 ϕd=.6 128

F.3 V/Q vs H Q=2000 ϕd=.5 129

F.4 V/Q vs H Q=2000 ϕd=.4 130

F.5 V/Q vs H Q=1500 ϕd=.6 131

F.6 V/Q vs H Q=1500 ϕd=.4 132

F.7 V/Q vs H Q=1000 ϕd=.6 133

F.8 V/Q vs H Q=1000 ϕd=.5,.4 134

TABLES

4.1 Experimental Conditions 34

4.2 Parameters for the Model H = T1 exp(T2 1/A), Square Mixer 44

4.3 Experimental Conditions using the Cylindrical Mixer 60

4.4 Dispersed Phase Fraction in the Mixer at Steady State 73

4.5 Variance from Replicate Runs 76

4.6 Parameters for the Model lnH=T1+T2(ln(1/A)), Cylindrical Mixer 79

4.7 Model Parameters for Five Parameter Model 81

4.8 Results of 5 Parameter Model Fit using 1/A instead of ln(1/A) 83

A.1 Run Conditions and Dispersion Band Heights with Square Mixer 92

A.2 Run Conditions and Dispersion Band Heights for Cylindrical Mixer 93

Chapter I

INTRODUCTION

This work was part of a research program involving the University of Ottawa, and CANMET, a division of Energy, Mines, and Resources Canada. The provision of laboratory space and materials by CANMET dictated directing research towards topics of interest to the Canadian hydrometallurgical industry while still meeting the thesis requirements at the University of Ottawa.

Recent work in the University of Ottawa-CANMET program (1,2) has involved the recovery of uranium from uranium bearing ores in the production of yellow cake. In the Canadian uranium processing industry, the uranium is usually recovered from the ore by first crushing the ore followed by leaching with acid or alkali. Either liquid-liquid extraction or ion exchange is used to recover the uranium from the leach liquors.

The "AMEX" process (3), in the case of solvent extraction, uses a selective tertiary amine present in an organic phase to extract the uranium from the aqueous leach liquor. This is followed by ammonium sulphate stripping to recover the uranium from the organic phase.

Sulphuric acid reacts with the dissolved uranium as follows:

$$UO_3 + 2H^+ = UO_2^{+2} + H_2O$$
$$UO_2^{+2} + SO_4^{-2} = UO_2SO_4$$
$$UO_2SO_4 + SO_4^{-2} = (UO_2(SO_4)_2)^{-2}$$
$$(UO_2(SO_4)_2)^{-2} + SO_4^{-2} = (UO_2(SO_4)_3)^{-4}$$

The uranium may occur in any of the above forms .

In solvent extraction, a transfer of the uranium occurs between the aqueous and the organic phases. This transfer of uranium from the leach liquor to the organic phase is called extraction and the recovery of the uranium to a second aqueous phase is called stripping. The use of an amine which is highly selective allows the extraction of a single metal ion. The amine used in the solvent extraction of uranium is chosen for its selectivity towards uranium and its ability to leave undesirable impurities behind.

The amine must be in its sulphate form for efficient extraction. This is effected by contacting the organic phase containing the amine with sulphuric acid.

$$2\ R_3N + H_2SO_4 = (R_3NH)_2SO_4$$

When the aqueous and organic phases are contacted the amine sulphate extracts the uranium,

$$\overline{2\ (R_3NH)_2SO_4} + UO_2(SO_4)_3^{-4} = \overline{(R_3NH)_4\ UO_2(SO_4)_2} + 2\ SO_4^{-2}$$
$$\overline{(R_3NH)_2SO_4} + UO_2(SO_4)_2^{-2} = \overline{(R_3NH)_2\ UO_2(SO_4)_2} + SO_4^{-2}$$

where the overbar indicates the organic phase.

The loaded organic is stripped at high pH with ammonium sulphate,

$$\overline{(R_3NH)_4UO_2(SO_4)} + 4\ NH_4OH = \overline{4\ R_3N} + UO_2SO_4 + 4\ H_2O + 2\ (NH_4)_2SO_4$$

The stripped organic is then contacted with sulphuric acid before recycle to the extraction stage.

To perform the liquid liquid contacting, mixer-settlers are commonly used in the international and Canadian uranium processing industries (1.4,5,6). A dispersion of one phase in the other is created in the mixer and then allowed to separate in a gravity settler. The process is usually multistage with the number of stages dictated by the efficiency of extraction or stripping desired.

The design of mixer settler equipment and the prediction of mixer settler performance when applied to a specific process, involves many uncertainties at present. This has led to "oversizing" of equipment to ensure process requirements are met. In stagewise operations such as liquid liquid extraction, where many mixer settler units are used in series, capital costs are very high for such equipment and the ability to accurately predict settler size would be of great benefit.

Previous University of Ottawa-CANMET work by Howell, Ritcey, and Golding (1), concentrated on developing a continuous operation single stage mixer settler unit to study the

processes occurring in a single stage of a liquid liquid extraction circuit (extraction, scrub, or stripping). This work used synthetic leach, extraction, and strip solutions in a small scale mixer settler unit with relatively short operating times (approximately 6-20 minutes). Howell, Ritcey, and Golding (1) noted the potential use of bench scale apparatus to examine dispersion band characteristics in the gravity settler with respect to several process parameters.

Attempts have been made to use bench scale and pilot plant apparatus to assist in equipment selection and design, as well as to study the chemical aspects of liquid liquid extraction. In the case of the design and selection of gravity settlers this involves prediction of the height of the dispersion band which occurs at the interface of the two phases.

Most of the work concerning the dispersion band characteristics in small scale gravity settlers has dealt with the effect of total throughput or dispersed phase throughput. Using throughput per unit cross sectional area is a commonly recommended scale up procedure.

A model of the form,

$$H = C\,(Q/A)^{y} \quad .$$

H = dispersion band height
Q = total throughput of the phases
A = settler cross sectional area

has been proposed for use as a basic scale up procedure when designing gravity settlers from bench and pilot plant data by Ryon et. al. (9,10,11), and Barnea and Mizrahi (12). C and y are experimentally determined constants. Glasser et.al.(4) report that y is usually between 2.5 and 7. Problems have been encountered (12), when working with bench scale gravity settlers. These include lack of reproducibility of results and the unsuitability of the $H = c\,(Q/A)^{y}$ model.

It was decided, with the cooperation of CANMET, to continue the development of a single stage mixer settler and to focus on the investigation of the dispersion band characteristics with respect to process parameters such as agitation intensity, throughput, and settler cross sectional area. It was hoped that the effects of these parameters on the height of the dispersion band could be determined. In addition, if reproducible results could be obtained, a model representative of the dispersion band characteristics in a small scale gravity settler could possibly be developed.

Chapter II

PHASE SEPARATION IN GRAVITY SETTLERS

The thermodynamically stable state of two immiscible liquids is their bulk form with a minimum of interface.

The gravity settler as used in liquid-liquid extraction processes separates a light organic phase and a heavier aqueous phase by means of the liquid density difference. In a batch separation situation, the two phases will be separate with a single interface between them when separation is complete. Often in continuous mixer-settler operation a dispersion band exists at the interface between the two phases in the gravity settler. In a vertical settler, the dispersion band covers the entire settling area. This is in contrast to a horizontal settler, where the dispersion does not necessarily cover the entire cross sectional area available for settling.

The mechanism of separation of droplets of one phase dispersed in the other involves many processes. Dispersed phase droplets are forced towards the bulk dispersed phase by gravitational forces and continuous phase drains from between the drops. Drop-drop coalescence occurs, as does drop-bulk phase coalescence. Some continuous phase is carried with

the dispersed phase drops and some small dispersed phase drops are carried along with the draining continuous phase as it flows towards the bulk continuous phase-dispersion interface.

The rates at which the above processes occur appears to depend on the physical characteristics of the respective phases and the characteristics of the feed dispersion. The drop size distribution in the dispersion leaving the mixer and entering the gravity settler is dictated by the physical characteristics of the phases and the mixing (agitation intensity, impeller geometry, and mixer configuration). Physical characteristics thought to affect the rate of separation of the phases include phase density, density difference, phase viscosity, and interfacial tension.

The primary concern when selecting or designing a mixer for use in a liquid-liquid extraction process is that it provides the necessary drop residence time and surface area to allow the required mass transfer to take place. Also of importance is that the dispersion will readily separate so as to minimize the settling area required.

Much literature is devoted to the size of the drops produced in agitated vessels and to the distribution of drop sizes. An excellent review of the literature is given by Glasser et.al. (4)

The dependence of d32, the Sauter mean drop diameter, on impeller speed, N, and impeller diameter, D, has been expressed in the form,

$$d32 \quad N^{a} D^{b}$$

The exponent "a" varies between -1.5 and -.72. The exponent "b" varies between -2.45 and -.70.

The drop size distribution has been found to be a normal one by some investigators and many report log-normal distributions. The log-normal reports include Brown and Pitt (7) for kerosene-water systems. Kolarik and Pipkin (8) report the drop size distribution as the sum of two individual gaussian curves for the uranyl nitrate-tributyl phosphate extraction system.

The effect of drop size on drop-interface coalescence time was also reviewed by Glasser et. al. (4). They reported that it was generally accepted by most authors that single drop-interface coalescence times increase with drop diameter. It must be noted that these observations were for single drops and not for drops in a dispersion or packed bed.

2.1 Prediction of Dispersion Band Height in Vertical Settlers

A basic method for predicting the dimensions of a gravity settler required to separate the dispersion created in continuous flow extraction processes was proposed by Ryon,Daley, and Lowrie (9,10,11). They utilized single stage mixer settler units in which the effects of phase ratio, dispersion type, throughput, mixing power,and temperature on the dispersion band height were investigated.

Plots of H, the dispersion band height, against dispersed phase throughput on log-log coordinates yielded straight line plots. The authors also concluded that dispersion band height as a function of flowrate per unit cross- sectional area was virtually independent of settler size, and that the specific flowrate (Q/A) could be used as a reliable basis for design of larger scale equipment.

This exponential increase of dispersion band height with specific flowrate can be expressed as,

$$H = C(Q/A)^{y}$$

where C and y are constants determined experimentally

Since Ryon,Daley,and Lowrie, several authors have confirmed the specific flowrate method. Barnea and Mizrahi (12) developed a semi-theoretical explanation for the model. They lim-

ited their treatment of dispersion bands in gravity settlers and excluded the following cases;

1. continuous settler operation with very small dispersion bands. i.e. less than 15 cm.
2. feed dispersions containing less than 15% by volume dispersed phase.
3. dispersions consisting of more than two liquid phases.
4. continuous settlers operating in unsteady state conditions.
5. continuous settler operation with incomplete separation.

The authors described the structure of the dispersion band in deep settlers as consisting of two main sub-layers,

1. a "dense layer" adjacent to the coalescence front. The dispersed phase is predominant here and exists in packed form. The dense layer occupies only 10-20% of the total volume of the dispersion band.
2. an "even concentration layer" of which most of the dispersion band is composed. The concentration of the dispersed phase is nearly constant in this region.

The role of these two sub-layers in the mechanism of phase separation is as follows;

Considering the light phase dispersed, the feed dispersion enters the settler. The dispersed phase moves towards the coalescence front. The heavier continuous phase moves downwards due to gravity. Dispersed phase droplets are carried with the continuous phase. Drop-drop coalescence results in light phase droplets of sufficient size that boyant forces cause the light phase drops to rise against the draining continuous phase. The "even concentration layer" thus self adjusts to a height which provides an average residence time sufficient for droplets to grow through drop-drop coalescence to the critical size for movement countercurrent to the continuous phase flow.

The "dense layer" or packed layer is formed when more drops approach the coalesence front than are removed by drop-bulk dispersed phase coalescence. At steady state a total mass balance on the dispersed phase should be considered rather than a drop balance. Drop-drop coalescence within the packed layer occurs as does drop deformation and packing.

Barnea and Mizrahi (12) consider the "even concentration layer" to be the primary factor in determining the thickness of the dispersion band and that it is a fixed proportion of the volume of the dispersion band. In a continuously operated settler, the phase flow and coalescence in the "even concentration layer" can be used to develop the $H = (Q/A)^y$ model.

At steady state the volume of continuous phase entering the dispersion band is equal to the volume leaving the dispersion band through drainage to enter the bulk continuous phase. Therefore the average draining velocity over the whole area will be,

$$\frac{Q(1-\phi o)}{A} \qquad \text{or} \qquad \frac{Qc}{A}$$

ϕo is the dispersed phase fraction in the feed

Barnea and Mizrahi denote $U\phi$, the relative velocity between the two phases as the average vertical velocity of the continuous phase divided by the average fraction of horizontal area occupied by the continuous phase

$$U\phi = \frac{Q(1-\phi o)}{A} \cdot \frac{1}{(1-\phi)}$$

where ϕ is the local concentration of the dispersed phase in the even concentration layer

or $$U\phi \propto Q/A$$

Also, if the relative velocity between the phases is proportional to the i power of the average drop diameter,

$$U\phi \propto d^i$$

$$2 \geq (i = f(Re_\phi)) \geq 0.5$$

The average drop diameter is a function of the residence time in the "even concentration layer",

$$d \propto t^{1/j}$$

$$j > 3$$

1/j is a function of the rate of growth of the drops due to coalescence in the even concentration layer.

Combining the equations for relative velocity gives,

$$Q/A \propto d^{i}$$

The average residence time in the even concentration layer, t, is

$$t = V'/Q \cdot \phi o/\phi$$

V' is volume of the even concentration layer

Therefore,

$$t \propto V'/Q$$

as ϕo and ϕ are constants at steady state.

Barnea and Mizrahi also consider the even concentration layer to be a constant proportion of the total thickness of the dispersion band.

Therefore,

$$d \propto (V/Q)^{1/j}$$

or

$$d \propto (H/(Q/A))^{1/j}$$

rearranging gives,

$$d^j \propto H/(Q/A)$$

or $$H \propto d^j\ (Q/A)$$

from $(Q/A) \propto d^i$,

$$d \propto (Q/A)^{j/i}$$

therefore,

$$H \propto (Q/A)^{j/i}\ (Q/A)$$

or $$H \propto (Q/A)^y \qquad \text{where } y = (j/i+1)$$

$$j > 3, \quad 0.5 \leq i \leq 2$$

If $j > 3$ and $0.5 \leq i \leq 2$, then $y \geq 2.5$.

Unlike Barnea and Mizrahi, Allak and Jeffreys (13) state that a "packing zone" is where the significant phase separation process which determines the thickness of the dispersion band occurs. They observed that their dispersion bands were composed of three distinct zones; a flocculating zone, a packing zone, and an interfacial coalescence zone.

In the packing zone, the drops pack closely together and take the shape of regular pentagonal dodecahedra. Allak and Jeffreys considered the thickness of the dispersion band to depend on the rate of drainage of the continuous phase film from between adjacent faces of the dodecahedral drops and on

the thickness of the film when it ruptures resulting in drop-drop coalescence. The model for prediction of dispersion band height presented is not readily applicable. Experimentally observed dispersion band heights were used to determine the critical film thickness for coalescence in each system studied. The film thickness obtained for each system was then used to predict dispersion band heights at other flow rates .

Smith and Davies (14) determined that the separation of the phases in the dispersion band is controlled by coalescence. They found H to be a function of the size of the drops entering the dispersion band and that height increased as drop diameter decreased. Also shown to have an important effect on the separation rate were wall effects.
Smith and Davies correlated their results in terms of throughput, inlet drop diameter, interfacial tension, phase viscosity, and density difference,

$$H/do = f\ (\ T' \cdot Qd/do)$$

where T' is a coalescence time constant which is characteristic of the particular system. T' is a function of drop diameter, phase viscosity, interfacial tension, and the density difference. Information about the form of the effect of throughput, drop diameter, and the physical properties of the systems studied was limited.

Golob and Modic (15) studied coalescence in the Amex extraction process. Alamine 336, or Aliquat 336 in Shell Sol K with n-decanol present was used as the organic phase and sodium sulphate in water was the aqueous phase.

The relationship between batch and continuous coalescence was investigated. Results were presented as,

$$H = 1.45\ (Qd/A)^{3\cdot 1} = 1.45\ Vd^{3\cdot 1}$$

Vd is the batch coalescence rate of the dispersed phase

This indicated that the continuous phase throughput, in the range of phase ratios investigated, had no effect.

Vieler, Glasser, and Bryson (16) presented a study concerned with the relationship between batch and continuous phase disengagement.

They defined $\psi(\tau)dt$ as the volume of dispersion in the settler of "age" between t and t + dt. "Age" is the time since the volume element entered the system.

A phase disengagement rate, g (x,t), is the volume of dispersion disengaging per unit time when the age is t and the properties of the system are X. Vieler, Glasser, and Bryson say examples of the properties represented by g might be phase ratio and total dispersion band height.

$$\frac{d\psi(t)}{dt} = -\bar{g}(x,t)\psi(t) \qquad 2.1$$

They used the relation,

$$V/Q = aH + b$$

to represent their continuous data, where a and b are positive constants.

Mechanistically, they proposed the following to explain the form of the V/Q = aH + b model. A perfectly mixed, continuously operated, steady state mixer supplies a dispersion to a settler.

$G(X,\tau)$ is a phase disengagement rate which is the fraction of volume disengaging per unit time when the age is τ and the properties of the system are X.

X is defined as the volume element of dispersion in the settler of age τ. Integrating equation 2.1 with X independent of age (as the system is at steady state),

$$\psi(\tau) = V(\exp -\int_0^{\tau} G(\underline{X},\tau')d\tau'$$

$$= \int_0^{\infty} \exp\left(\int_0^{\tau} G(\underline{X},\tau')d'\tau\right)d\tau$$

Where V is the volume of the dispersion.

If Q is the total volumetric flowrate of dispersion, from steady state considerations,

$$Q = {}_0\int^{\infty} G\,(X,\tau)\,\psi(\tau)\,d\tau$$

$$= \psi(0) - \psi(\infty)$$

$$= \psi(0)$$

as $\psi(\infty)$ must be zero for steady state operation (i.e. no volume element of age ∞ is left)

The average residence time in the dispersion band is V/Q, and Vieler et. al. state,

$$V/Q = \left({}_0\int^{\infty} \exp - {}_0\int^{\tau} G(X,\tau')\,d\tau'\right) d\tau$$

Furthermore, they state that any volume element with small G will have a large contribution towards the mean residence time, or more specifically any slowly disengaging particles will tend to build up in the continuous settler and make a large contribution to the volume of the dispersion band while the rapidly disengaging section will make a small contribution.

Vieler, Glasser, and Bryson plotted their continuous settler operation results as V/Q vs H which yielded straight lines in their case, with the observation that if these plots were extrapolated to zero the mean residence time V/Q does not reach zero as $H \to 0$. This is of the form $V/Q = aH + b$.

One model for internal age distribution in the continuous settler is as follows,

Assume that there is no disengagement in the continuous settler for some time t, after which there is a constant rate, k.

$$\text{i.e. } g = k \underline{H} \, (t - t^{*})$$

Where $\underline{H}$ is a step function

t could be thought of as the time to reach the disengaging interface

$$\text{i.e. } t = C^{*} H$$

Using that form of g', Vieler, Glasser, and Bryson obtained

$$V/Q = C\ H + 1/k$$

which is of the form,

$$V/Q = aH + b$$

which fits their continuous results.

Stoenner and Wohler (17) describe the separation of phases in a gravity settler as a sequence of three steps.

1. coalescence of the small, virtually suspended, drops into large drops
2. sinking or rising of the large drops to the coalescing interface
3. coalescence of the large drops at the interface

For scale up, Stoenner and Wohler prefer $Q/A = C \cdot H/(H+d)$ over $Q/A = aH^b$ as the former equation has a limiting value for Q/A. The authors do not support their opinions with experimental evidence. Fig 2.1 illustrates the difference between the two models.

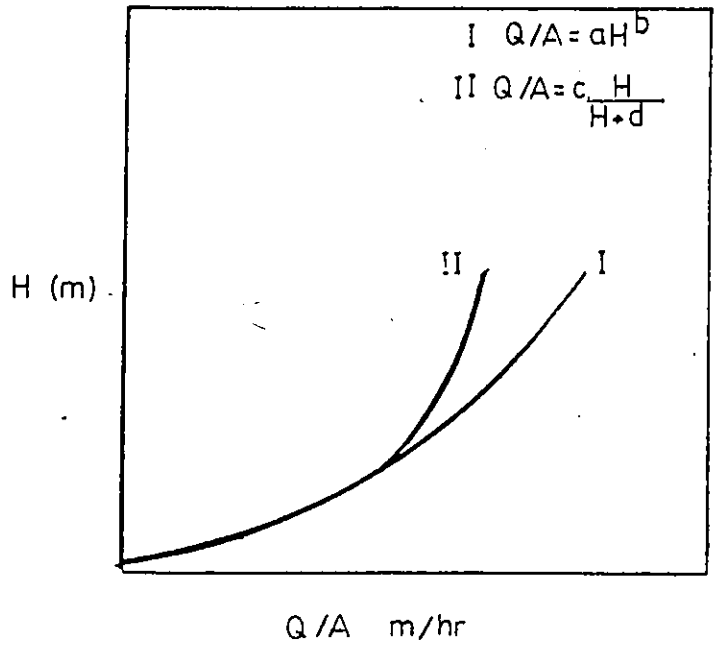

Figure 2.1: H vs Q/A , Stoenner and Wohlers proposal.

Gondo and Kusinoki (18) correlated their continuous settler results for a kerosene-water system as,

$$H = \phi^{4.9} (Uc + Ud)^{3.1} N^{2.8}$$

where N is the impleller rpm. Uc and Ud are the superficial velocities of the continuous and dispersed phases respectively in the settler (cm/min). ϕ is the dispersed phase ratio in the feed.

2.2 Prediction of Dispersion Band Heights in Horizontal Settlers

Horizontal settlers are not in use industrially because of the large settling area required. Capital expense is high as is the cost of the solvent inventory required. Some investigators, however, consider horizontal settlers to offer improvements in minimizing dispersed phase loss through entrainment by increasing the residence time in the settler and reducing the height of the dispersion in the settler.

Jeffreys, Davies, and Pitt (19) analyzed the behavior of wedged shaped dispersion bands. This analysis was based on a differential element model. A kerosene water system was studied. The authors showed that the length of a coalescing wedge in a gravity settler depends on the drop input rate and on the size of the drops entering the settler.

In the case of the light phase dispersed, the wedge will appear as in Fig 2.2 .

At steady state, the volume of dispersed phase entering the element will equal the volume of dispersed phase leaving. Jeffreys, Davies, and Pitt performed an overall material balance on the dispersed phase taking into account drop-drop coalescence, drop interface coalescence as well as drops entering and leaving the element.

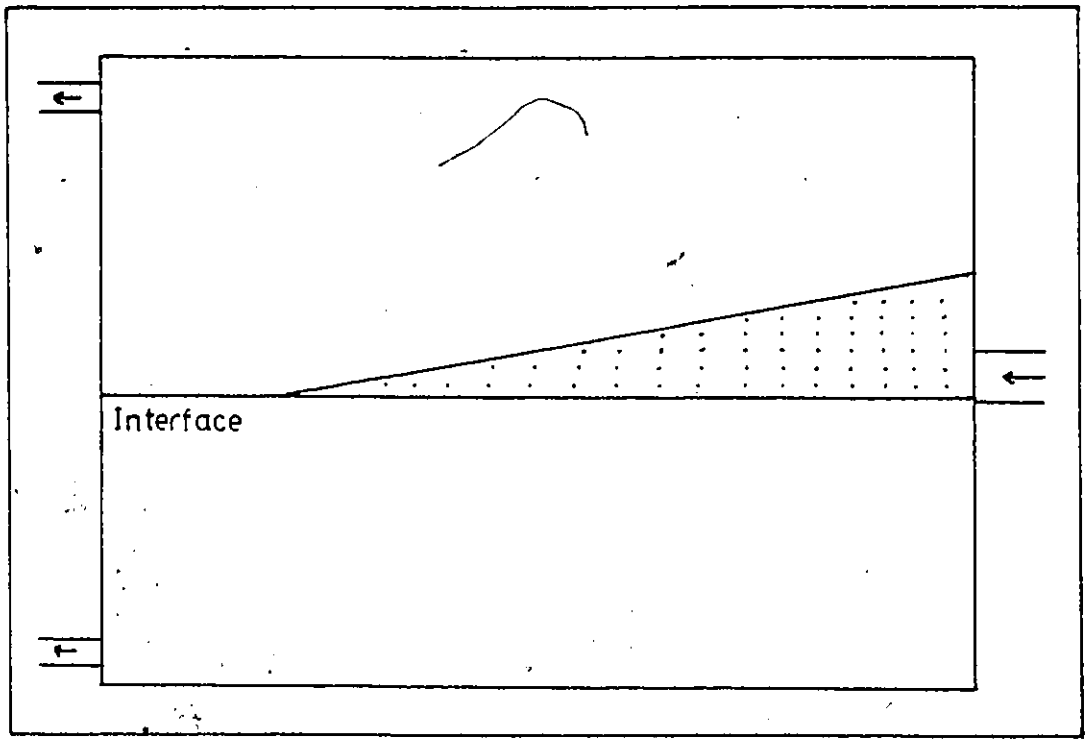

Figure 2.2: Wedge Shaped Dispersion Band

They presented a model which could be used to predict the mean drop size disribution in the wedge and the overall wedge length as a function of the flowrates of the phases to the settler. However, drop-drop and drop-interface coalescence time data as well as the mean drop size of the dispersion entering the settler have to be known before dispersion band heights can be predicted.

Vijayan and Ponter (20) also presented a study of wedge shaped bands but they also came to the conclusion that the

measurement of coalescence times is necessary in the prediction of the wedge characteristics. Their model could not be evaluated because of the difficulties in measuring the rates of coalescence in the wedge.

Chapter III

EXPERIMENTAL

3.1 Apparatus

The apparatus used is shown in Figures 3.1 and 3.2. A plexiglass settler was used to separate a dispersion produced in one of two plexiglass mixers. A movable full width baffle was inserted into slots in the settler side walls to provide different settling cross sectional areas as required.

Both mixers had a mixing volume of 2500 ml., but were quite different geometrically. Mixer A was square with an open top. No baffles were present. Mixer B was cylindrical with four vertical baffles and a closed top. In both cases the phases were fed to an inlet in the center of the bottom of the mixer. The square mixer allowed liquid to overflow the side wall closest to the settler along a walled trough into the settler. The cylindrical mixer overflowed around the impeller shaft and then down a walled trough into the settler. In the case of the cylindrical mixer, the overflow exited the mixer through a narrow opening through which the impeller shaft also passed, reducing the possibility of air entrainment through surface turbulence.

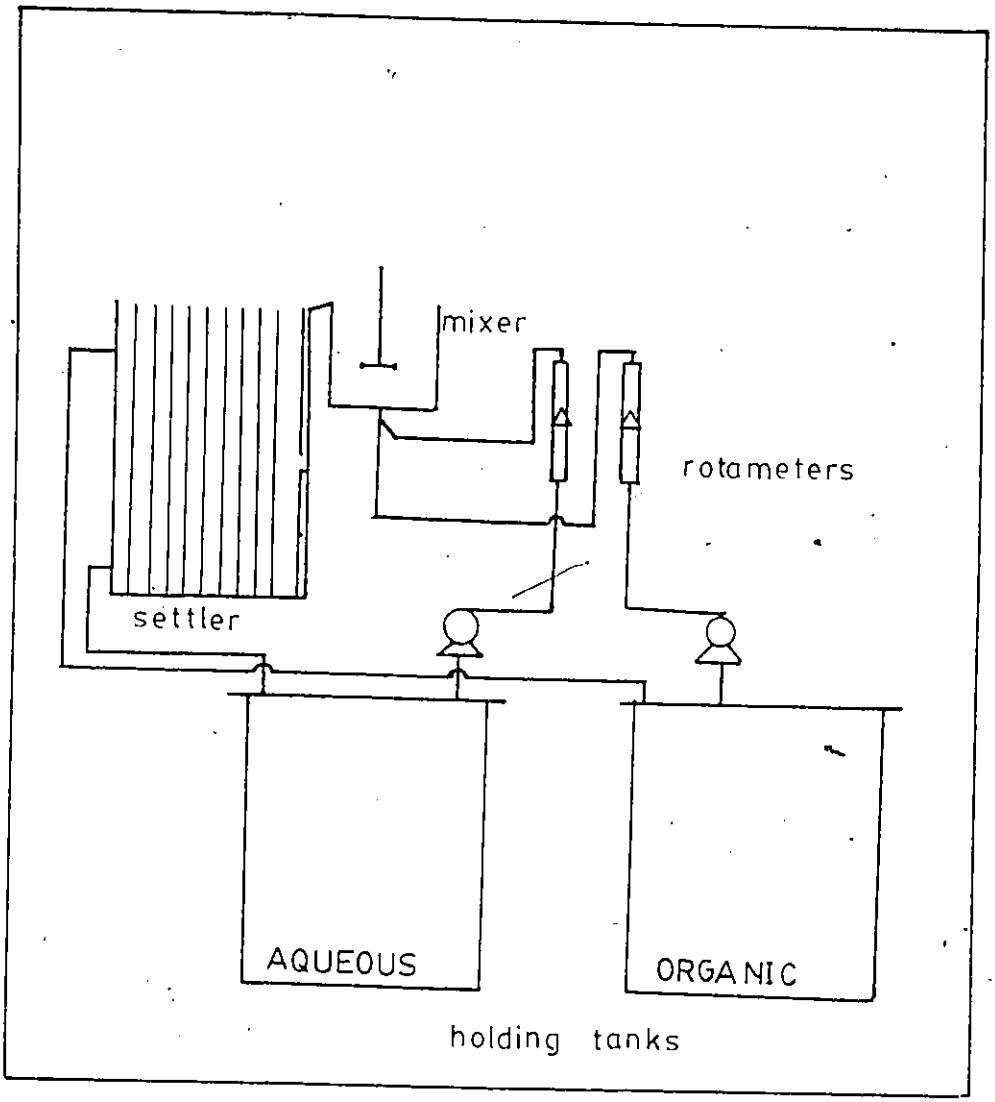

Figure 3.1: Experimental Equipment

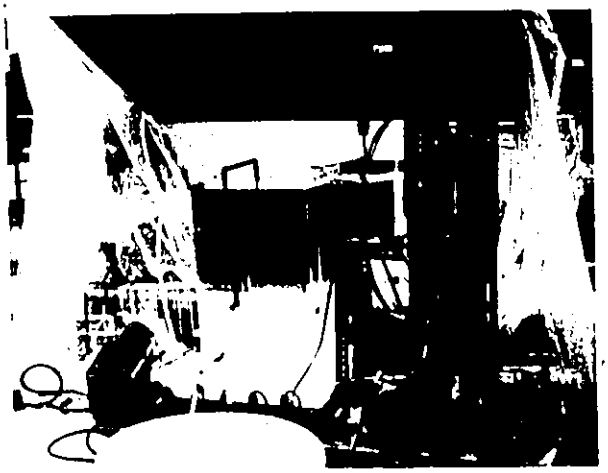

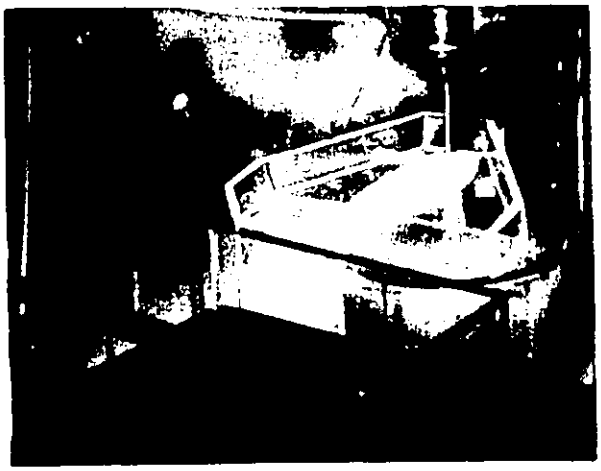

Agitation was provided by a 6-bladed turbine impeller which was rotated by a variable speed mixer. Rotational speed was set using a mechanical tachometer and was monitored during operation by a calibrated strobe light.

The organic and aqueous phases were recycled continuously from the settler to their respective holding tanks which were situated below mixer level.

The phases were then pumped to the mixer using peristaltic pumps. The phase flowrates were determined using inline glass rotameters which were calibrated for the experimental solutions. The phases were introduced into the mixers at a Y-joint placed at the mixer inlet. The dispersion then overflowed by gravity into the settler. The dispersion entered the coalesence area of the settler through a full width inlet, 2 cm. high, located a mid height.

The phases left the settler through cylindrical ports and flowed by gravity to the holding tanks. A flow restrictor was placed on the aqueous return line to allow adjustment of the aqueous phase level in the settler.

3.2 Phase composition

The aqueous and organic phases used experimentally were prepared in the laboratory.

City of Ottawa tap water acidified to pH=1.6 with concentrated sulphuric acid was used as the aqueous phase.

The organic phase was made up of 93% Shell 140 (an aliphatic kerosene), 3.5% isodecanol, and 3.5% Adogen 364. Adogen 364 is a commercially produced (Sherex) tertiary amine, R_3N , and is a 50% mixture of octyl and decylamines.

$$R = CH_2 (CH_3)_7$$

and $$R = CH_2 (CH_3)_9$$

Sixty litres of each phase was prepared.

The organic phase components were mixed together and then the combination was preacidified by contacting with 5% sulphuric acid in water. The two liquid phases were separated and the acidified water was discarded.

The pH=1.6 water solution and the acidified organic were then contacted by mixing with a marine impeller at high r.p.m. After settling, the pH of the aqueous phase was adjusted by the addition of concentrated sulphuric acid in small amounts followed by mixing and settling until the pH of the aqueous phase was once again 1.6 . The settled phases were allowed to remain in contact for several days.

The mutually saturated phases were stored in covered polyethylene containers to reduce contamination by dust over the course of experimentation.

3.3 Experimental method

Start up commenced with rinsing the settler with tap water and shaking dry. Continuous phase was pumped into the mixer and the flowrate was adjusted. When liquid began to enter the settler the impeller was started and the r.p.m. was set using the mechanical tachometer and the organic pump was started and adjusted to the required flowrate using the rotameter. This allowed the mixer to approach steady state operation while the settler was filling. The aqueous exit line from the settler remained closed until the aqueous level reached the height of the dispersion inlet. The flow constrictor on the aqueous exit line was then adjusted such that aqueous level remained at the height of the dispersion inlet.

Once the settler was full, the impeller r.p.m. was checked periodically with the strobe light and the flowrates of the two phases were adjusted as required. The apparatus was allowed to run for approximately one hour before the first measurements were made.

The flowrates of the two phases and the agitation intensity were constant for each run. The settler baffle was moved to adjust the cross sectional area available for the dispersion band to occupy. The baffle was moved to the different positions in a random order which varied from one run to the next.

After positioning the baffle in a specific slot, the dispersion band height was allowed to stabilize. The dispersion band height was not recorded until the height had remained at a constant level for approximately 20 minutes.

3.4 Experimental Proceedure

Two sets of experiments were performed. One with the square mixer and one with the cylindrical mixer. The remainder of the apparatus was used in both sets as were the liquid phases.

The first set of runs were performed using the square open top mixer. The cylindrical closed mixer was then constructed and subsequent runs were performed using it. A 3-level experimental design was employed with the square mixer to investigate the effects of agitation and throughput on the dispersion band height-cross sectional area relationship.

With the cylindrical mixer, another 3-level design was employed but feed phase ratio was also included as an independent parameter. In both series of runs the aqueous phase was continuous.

Chapter IV

RESULTS AND DISCUSSION

4.1 Dispersion Bands in the Laboratory Settler using the Square Mixer

For the preliminary 12 runs a range of height from < 2 cm to 16 cm was observed. The shape of the dispersion band varied from tall and narrow to flat and wide depending on the cross sectional area available. In every case however, the dispersion band occupied the total cross sectional area available for settling.

The surfaces of the dispersion bands were visible through the transparent sides of the settler and the upper and lower limits of the dispersion bands were well defined in all cases. The upper limit (coalescing front) was not uniform in height and contained peaks and valleys which were constantly growing and collapsing. It was possible to determine an average height as these topographic type features were not very large. The lower limit was much more uniform and could be indentified as a horizontal line.

When the dispersion band was relatively deep and narrow, H > L, where L is the length of the dispersion band, the physical characteristics appeared as Allak and Jeffreys (13)

described. Close packed drops existed at the top of the dispersion band. These drops appeared to be stationary. In the lower portion the drops were in constant motion due to turbulence from the incoming dispersion. When the dispersion band was low and long, H < L, a packed zone was visible at the end of the band opposite the inlet. This packed region occupied the band from top to bottom. Adjacent to the inlet, drops in turbulent motion occupied the dispersion band from top to bottom. There was no distinct division between the two regions and the height of the dispersion band was essentially uniform over the entire cross sectional area. Nine runs were performed using the factorial design. Two replicate runs were performed at the center point. Replicate runs were performed to obtain an estimate of the precision of the response being measured (height) over the operating region and to determine if the response varied with factors such as run order. The experimental conditions are presented in Table 4.1

In the square mixer, the upper surface of the mixed liquid was exposed to the atmosphere. It was observed that air was being entrained in the mixer in the form of small bubbles. These air bubbles were observed when continuous phase alone was being pumped through the mixer and into the settler. When both continuous and dispersed phase were being mixed together it was not possible to visually distinguish between the dispersed phase droplets and the air bubbbles.

Table 4.1: Experimental Conditions

Q	Aqueous	Organic	Impeller RPM
ml/min	ml/min	ml/min	
+	1200	800	750
0	900	600	500
-	600	400	250

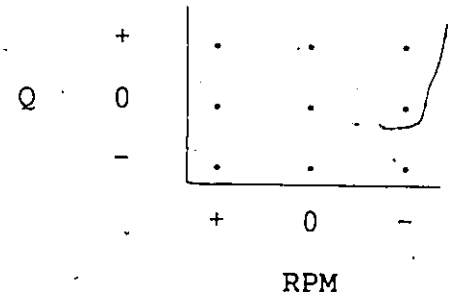

4.1.1 Experimental Results Using the Square Mixer

The experimental results are presented in figures 4.1 through 4.3 in the form of H vs. 1/A .

It is apparent that increasing the agitation intensity resulted in a decrease in disersion band height when the feed conditions were held constant.

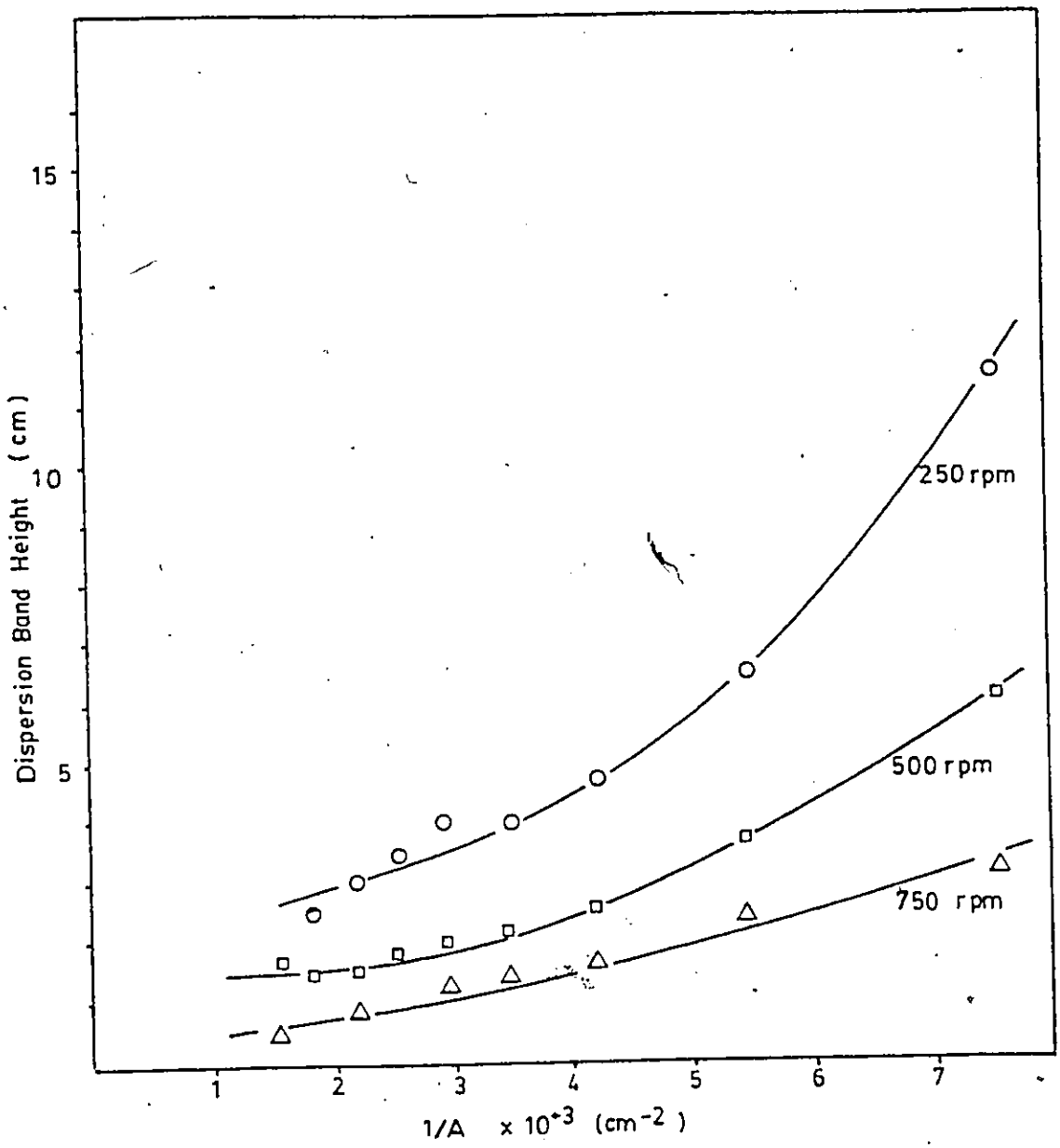

Figure 4.1: Dispersion Band Height vs 1/A
Q=1000, Square Mixer

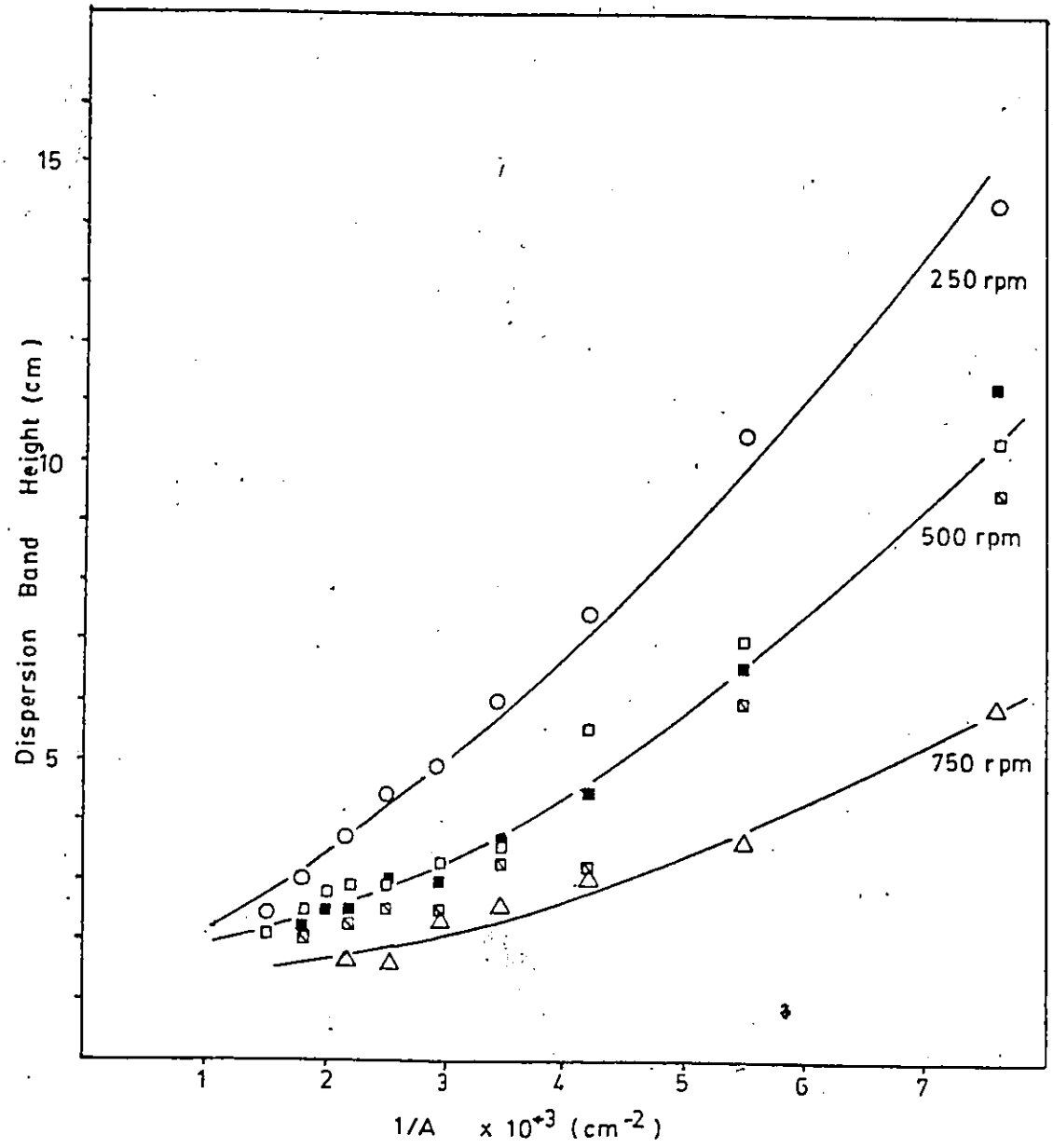

Figure 4.2: Dispersion band Height vs 1/A
Q=1500, Square Mixer

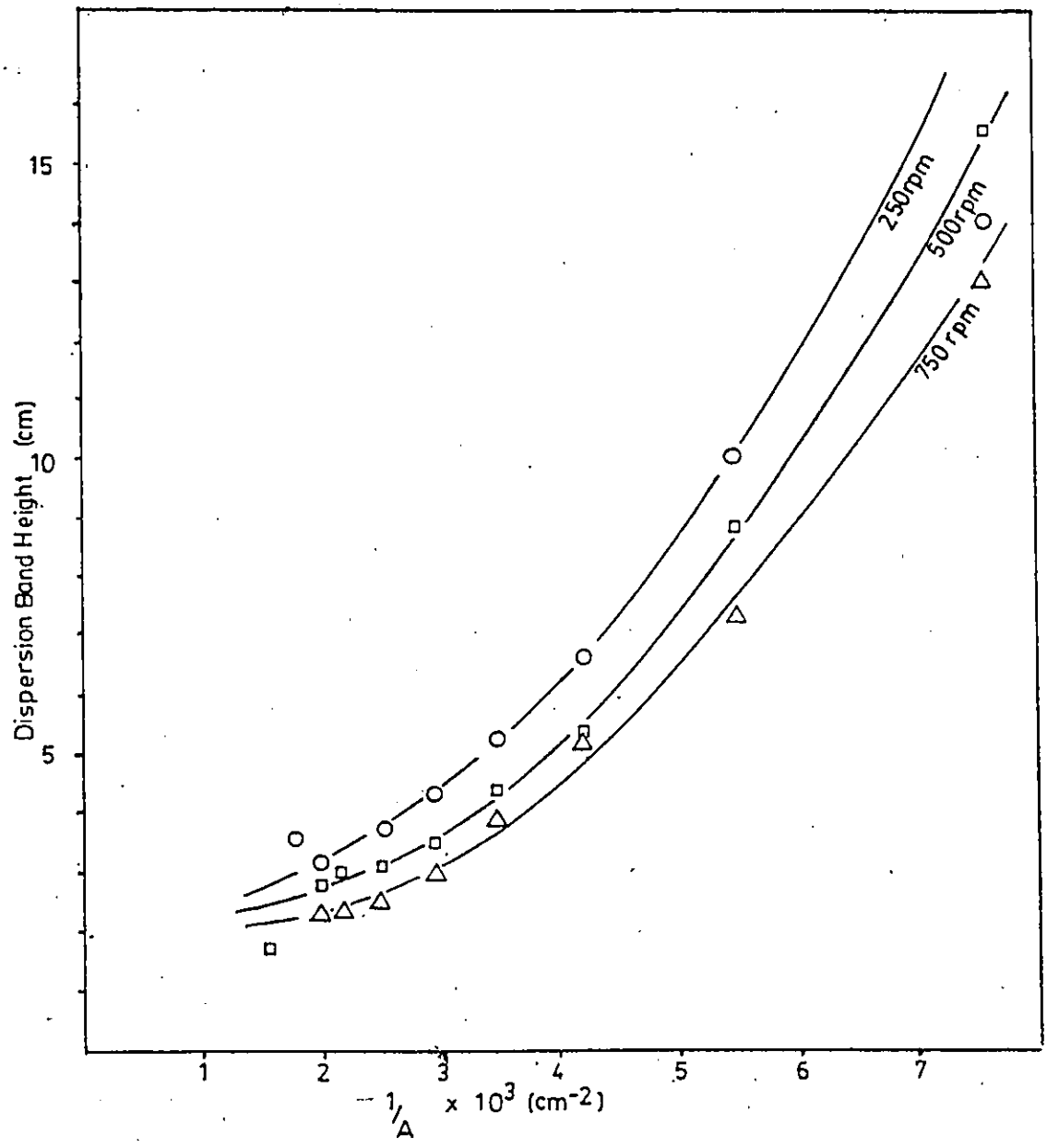

Figure 4.3: Dispersion Band Height vs 1/A
Q=2000, Square Mixer

This result is inconsistent with the majority of published results. In general (4) an increase in agitation intensity results in a smaller mean drop size leaving the mixer. A smaller mean drop size entering the settler usually results in an increase in dispersion band height (14). Ryon et. al. (9,10.11) observed that their systems were relatively insensitive to agitation intensity.

Additional runs were performed to determine the effect of feed phase ratio on the dispersion band height. When these runs were combined with the runs from the original 2^3 design, it was observed that an increase in the fraction of dispersed phase in the feed to the mixer resulted in larger dispersion bands in the settler. This effect is shown in Figure 4.4 and Figure 4.5

The effect of Q , the total throughput, on dispersion band height can be seen in Fig 4.1, Fig 4.2, and Fig 4.3 . Increasing the throughput while holding agitation and the feed phase ratio constant caused an increase in dispersion band height. This effect is pronounced at every agitation intensity except for the two runs Q=1500, rpm=250 and Q=2000, rpm=250 which appear to have the same dispersion band height-cross sectional area relationship.

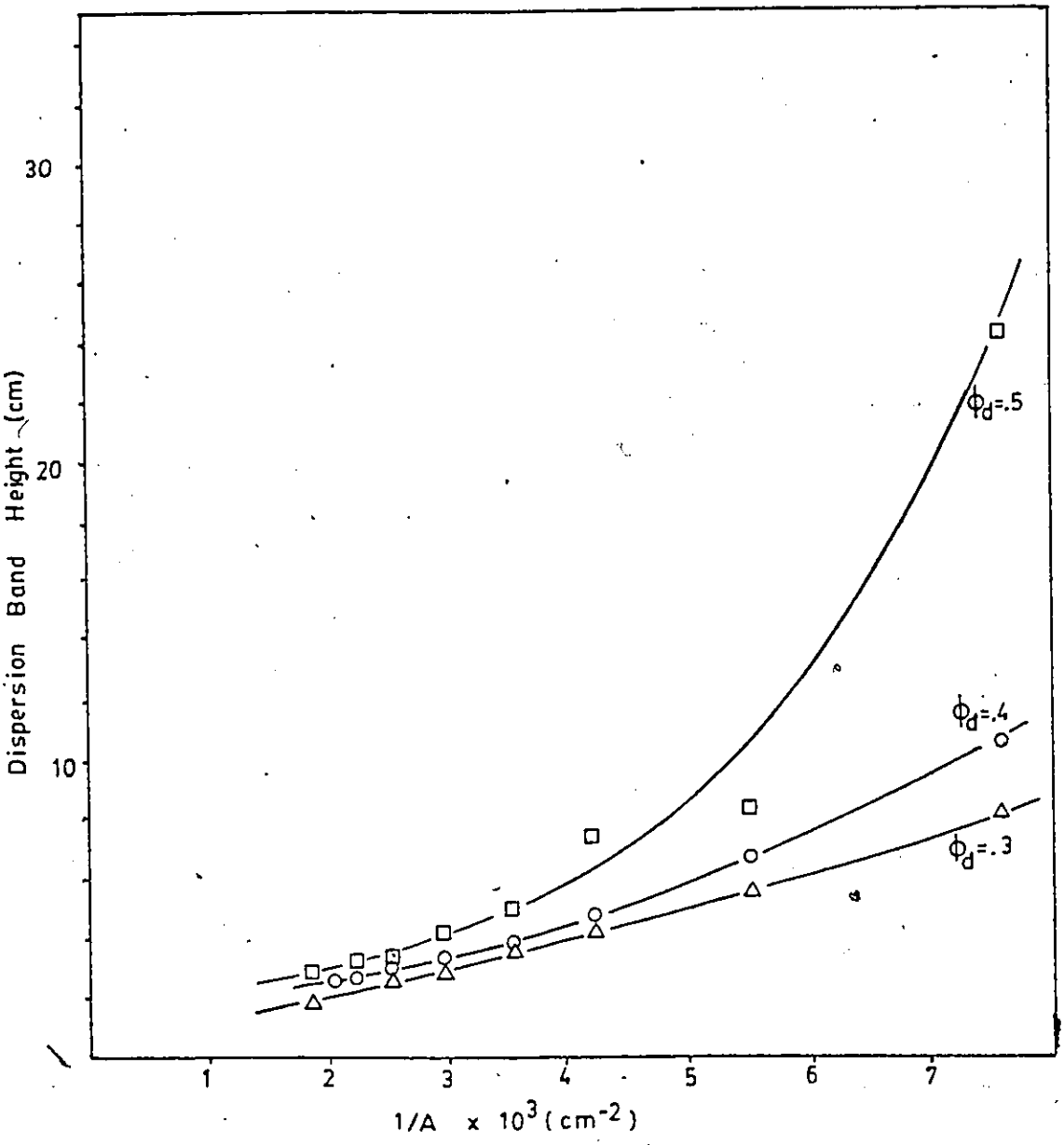

Figure 4.4: The Effect of Dispersed Phase Fraction in the Feed, Q=1500, Rpm=500

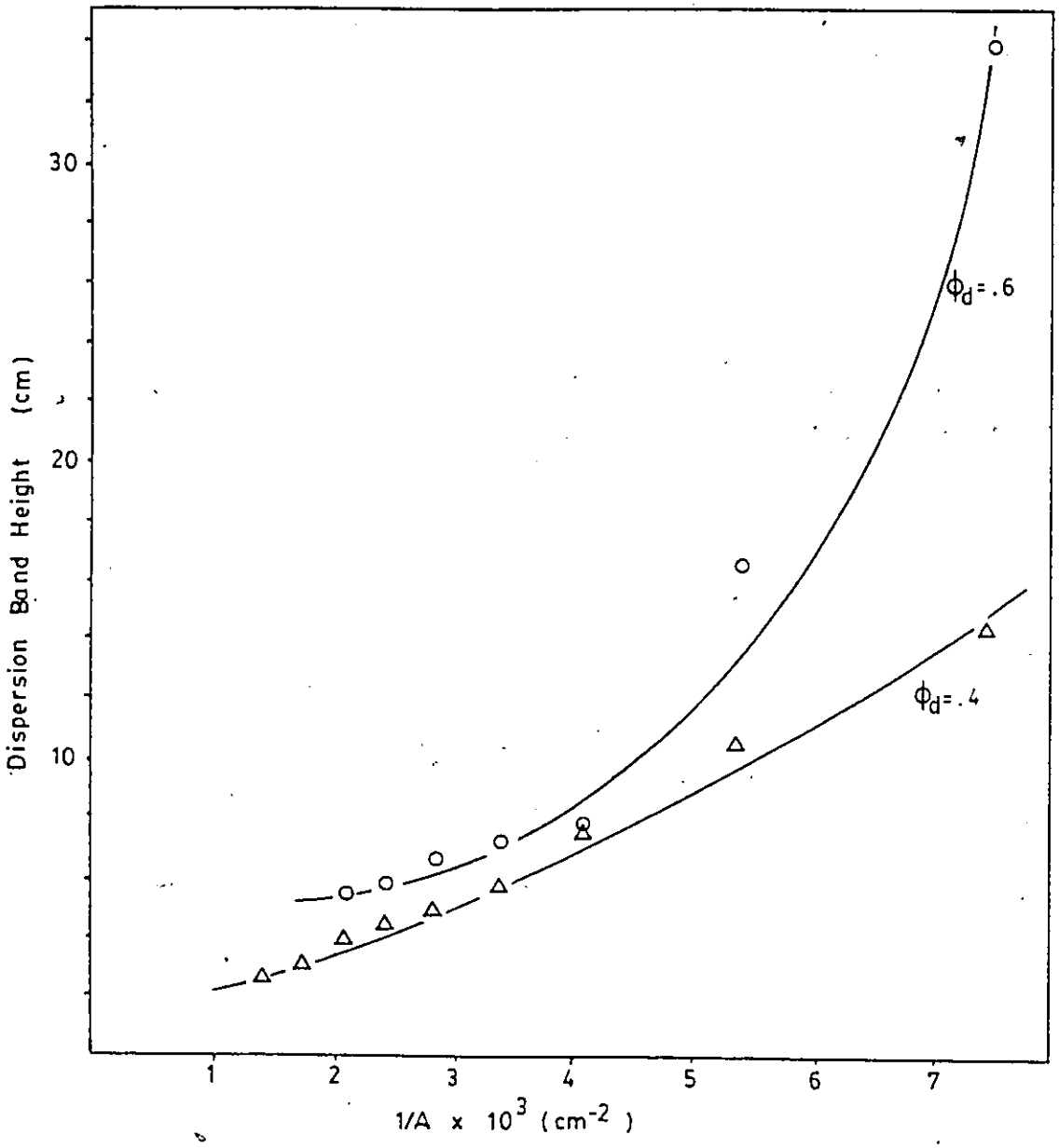

Figure 4.5: The Effect of Dispersed Phase Fraction in the Feed, Q=1500, rpm=250

4.1.2 Modelling the Square Mixer Results

Figures 4.1 through 4.5 showed that throughput, agitation intensity, and feed phase ratio had an effect on the dispersion band height for the system being studied.

To accurately predict the height of the dispersion band produced in the experimental settler , a model which incorporates the experimental variables (throughput, agitation intensity, and feed phase ratio) is necessary. The form of such a model should be determined from the experimental data and, if possible, theoretical considerations.

The models theoretically developed by Barnea and Mizrahi (12) and Vieler et. al.(16) were not found to adequately represent the experimental data. When plotted in the traditional log H vs log 1/A or log Q/A , the experimental results did not display the straight line behaviour that was described by Ryon et.al. (9,10,11) or Barnea and Mizrahi (12). The log-log plots showed upward concave curvature (see Figure 4.6) which had been noted by Barnea and Mizrahi as being observed mainly in systems where the dispersion bands were small or where a large range of dispersion band heights were observed. Barnea and Mizrahi noted that their own data displayed upward concave curvature at low dispersion band heights in one system. This type of behaviour was also observed by Warwick, Scuffham, and Lott (21). When V/Q was plotted against H as Vieler et.al. suggested,

straight lines were not observed. Plotting ln H vs. Q/A gave a straight line. This can be seen in Figure 4.6.

Because of this behaviour it was decided a suitable model to describe the H vs 1/A behaviour of the system being studied would be of the form.

$$H = T1 \exp (T2 \cdot 1/A)$$

where T1 and T2 are experimentally determined constants.

If such a model was found to adequately represent the data for the each individual run, the parameters may be distinct functions of the process variables and thereby assist in the identification of the process variables which have a significant effect on the dispersion band height and assist in the development of a model which represents the dispersion band height behaviour in terms of the process variables (22,23) The model $H = T1 \exp(T2 \cdot 1/A)$ was chosen rather than $H = T1 \exp(T2 \cdot Q/A)$ because the effects of agitation intensity, throughput, and feed phase ratio on the parameters T1 and T2 were of interest. If Q had an effect on T2 such that $H = T1 \exp(T2' \cdot Q/A)$ then T2 would be a strong function of Q.

For the model, $H = T1 \exp(T2 \cdot 1/A)$ or $H = T1 \exp(T2 \cdot Q/A)$ using ln H vs 1/A or Q/A and linear least squares analysis is not an appropriate method to determine the best estimates of T1 and T2 when fitting the

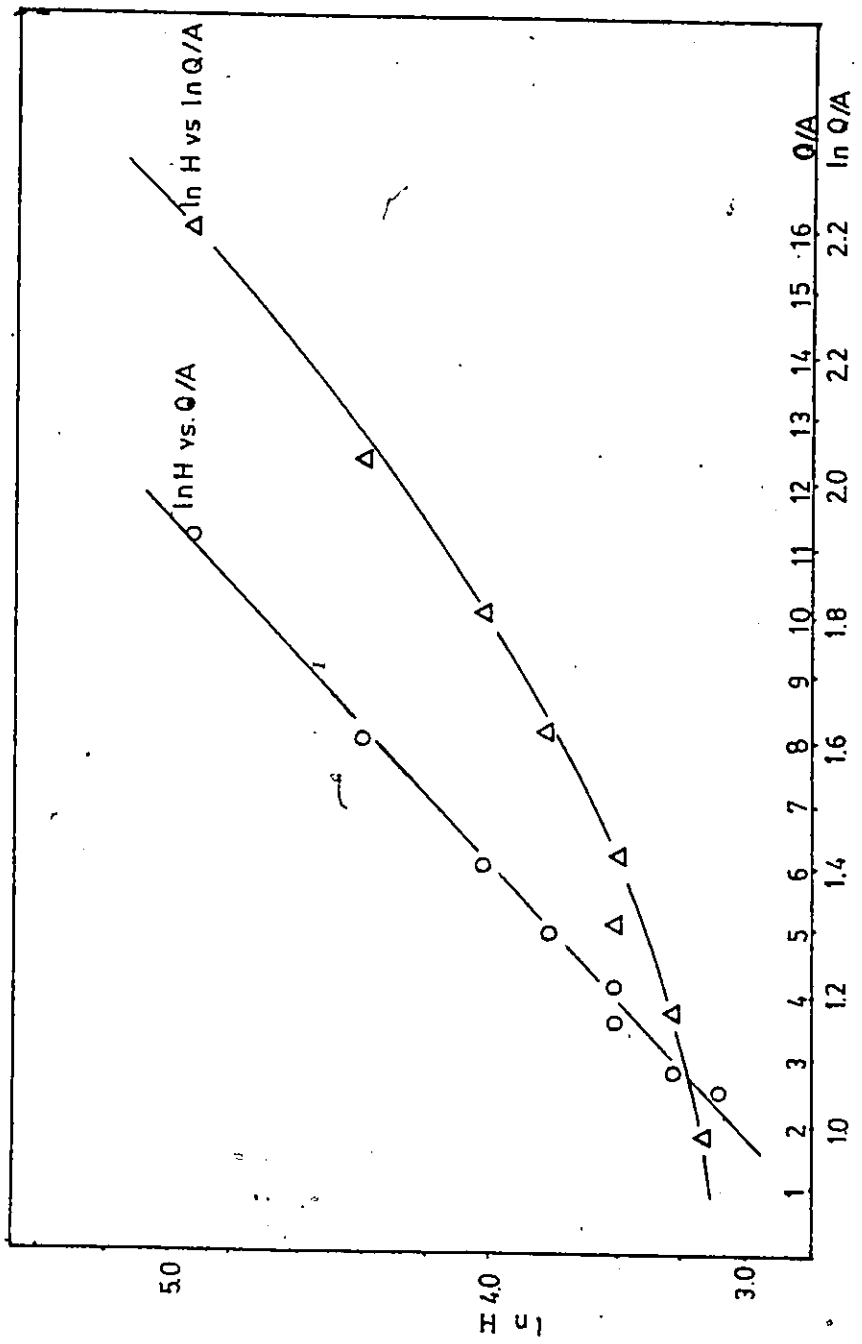

Figure 4.6: ln H vs ln Q/A and ln H vs Q/A
Square Mixer, run 12

model to the experimental data. Transforming the model logarithimically also transforms the error associated with the measured response. Therefore the model $H = T1 \exp(T2 \cdot 1/A)$ was fitted to the data for each run using nonlinear least squares. The parameters such that the sum of squares of residuals was minimized for each run are shown in Table 4.2

Table 4.2: Parameters for the Model $H = T1 \exp(T2 \ 1/A)$, Square Mixer

Q	RPM	T1	T2	
2000	250	2.31+/-.51	.24+/-.04	
2000	500	1.50+/-.18	.31+/-.02	
2000	750	1.36+/-.17	.30+/-.02	
1500	250	2.45+/-.60	.24+/-.04	
1500	500	1.46+/-.19	.26+/-.02	$\phi d=.4$
1500	750	1.14+/-.23	.22+/-.03	
1000	250	1.81+/-.31	.24+/-.03	
1000	500	0.97+/-.08	.24+/-.01	
1000	750	0.62+/-.23	.22+/-.06	
1500	500	1.28+/-.50	.39+/-.06	$\phi d=.5$
1500	500	1.29+/-.33	.24+/-.04	$\phi d=.3$
1500	250	2.11+/-.56	.37+/-.04	$\phi d=.6$

The three replicate runs at Q=1500 ml/min , 500 rpm , $\phi d=.4$ were grouped together and the model was fitted to the data from all three runs. Therefore 27 points were used to fit 2 parameters. The result of that fit was T1=1.46 and T2=.260 .

Plots of the fitted parameters vs the independent variables in the experiments (throughput, impeller rpm, and feed phase ratio) gave some insight into the effect of the independent variables on the model parameters.

Figures 4.7, 4.8, and 4.9 show the model parameters plotted against impeller r.p.m., throughput, and dispersed phase ratio in the feed.

The 95% confidence intervals for the parameter estimates were of use in determining the form of the effect of the independent variables on the model parameters and were also of use in eliminating some of the independent variables as having an effect on the fitted model parameters.

Impeller r.p.m. and throughput were identified as having a significant effect on the model parameter T1. Only dispersed phase ratio in the feed was identified as having an significant effect on the model parameter T2.

Figure 4.10 shows 1/rpm is a possible form of the effect of rpm on T1. The simplest form of the effect of throughput on T1 is linear. Due to the large parameter confidence intervals shown in figure 4.8, a more complicated form of the effect of Q on T1 is not justified.

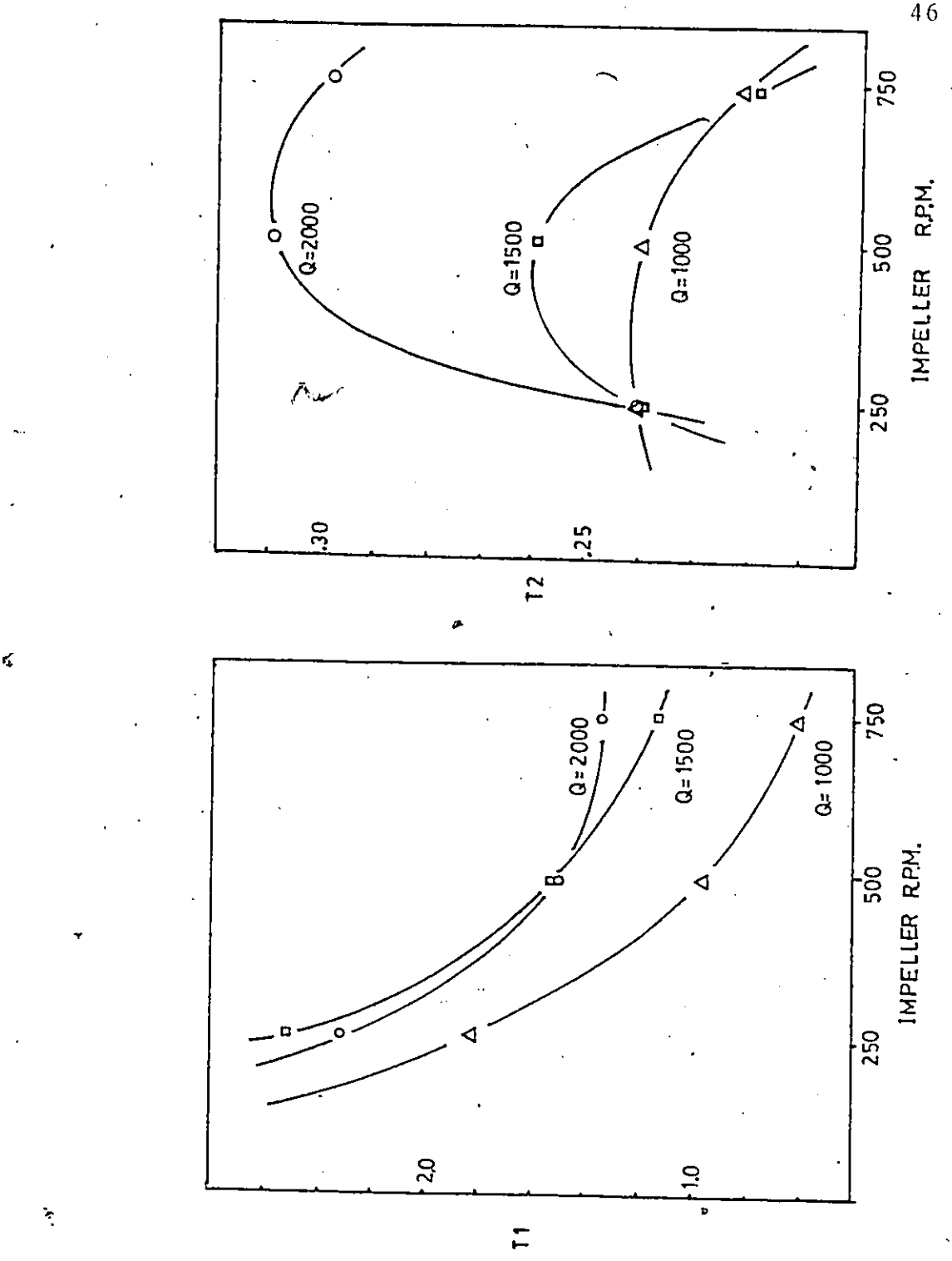

Figure 4.7: Model Parameters vs Impeller RPM

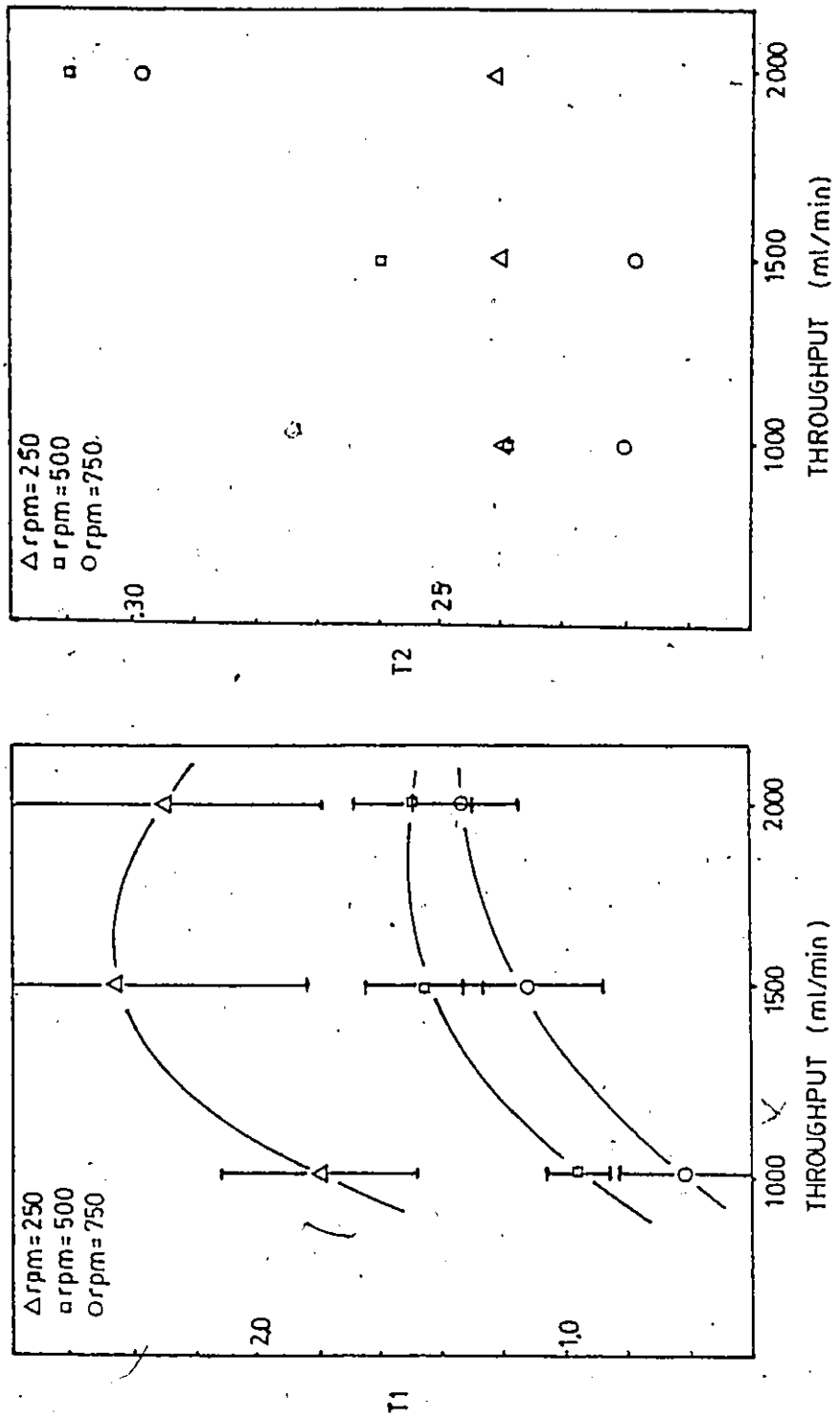

Figure 4.8: Model Parameters vs Throughput

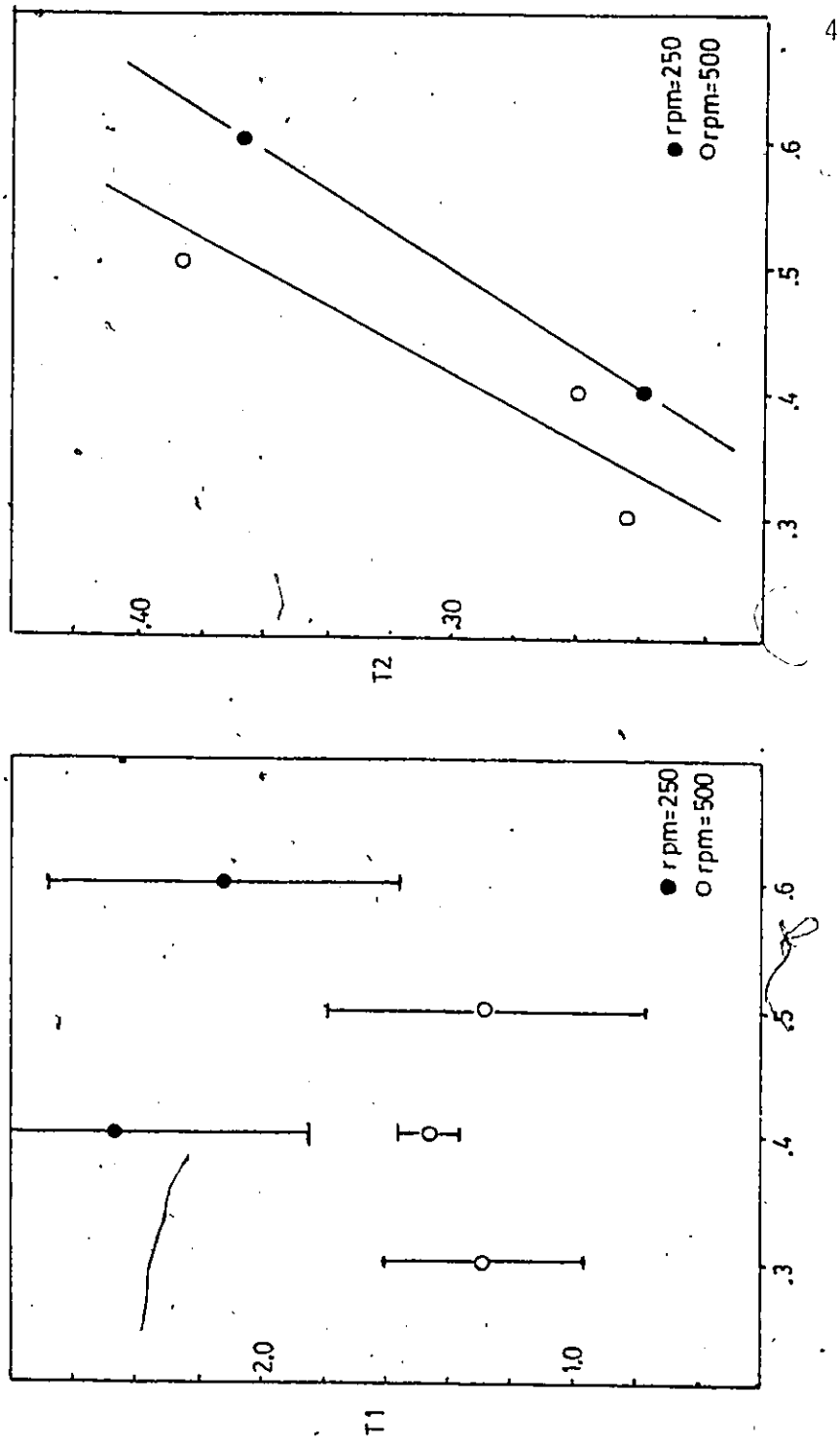

Figure 4.9: Model Parameters vs Dispersed Phase Fraction in the Feed

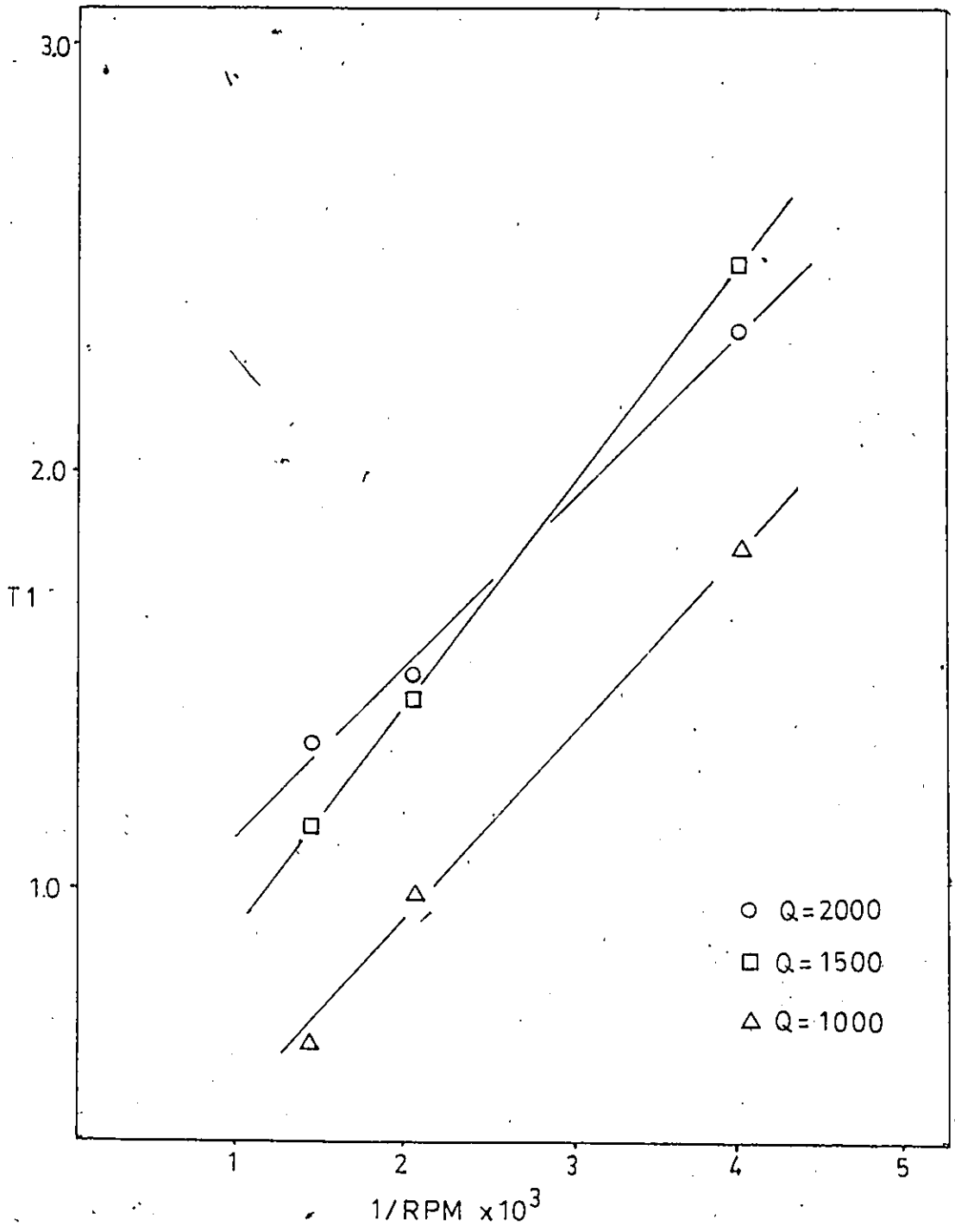

Figure 4.10: Model Parameter T1 vs 1/RPM

Therefore,

$$T1 = (T11/rpm + T12 \cdot Q)$$

A linear form of the effect of ϕd on T2 was chosen .

$$T2 = T21 \cdot \phi d$$

The model,

$$H = (T11/rpm + T12 \cdot Q) \exp(T21 \cdot \phi d/A)$$

was proposed.

The proposed model was then fitted to all the data using nonlinear least squares. The independent variables were scaled to facilitate model fitting.

The model,

$$H = (T11/X1 + T12 \cdot X2) \exp(T21 \cdot X3 \cdot X4)$$

was used where,

$X1 = rpm/250$

$X2 = Q/1000$

$X3 = \phi d$

$X4 = 1/A \times 10^3$

One noticably large residual was observed when the model was fitted to the data. At $1/A = 7.58 \times 10^{-3}$ cm^{-2}, Q=1500 ml/min, rpm=500, $\phi d = .5$, the observed response was H=24.5 cm. The height predicted by the model,

$$H = (T11/X1 + T12 \cdot X2) \exp(T21 \cdot X3 \cdot X4)$$

was 17.41 cm.

This outlier was removed from the data set and the model was fitted to the remaining data.

The parameters such that the sum of squares of residuals was minimized were found to be;

$$T11 = 1.05 \pm .21$$
$$T12 = .68 \pm .08$$
$$T21 = .62 \pm .02$$

The parameter precision was estimated using the parameter covariance matrix as described in Appendix B.

A quantitative lack of fit test performed indicated some doubt as to the adequacy of the model. As the data set contained replicate data points,an "R-Test" could be applied (24). R was found to be 1.80, the appropriate F distribution value is 1.77 at the 95% level. An R greater than the appropriate F indicates lack of fit. Since this test did not reveal any information about the nature of the possible inadequacy, residual (observed response - predicted response) plots were examined.

Residuals were plotted against the operating variables included in the model (Q, rpm, ϕd), run order, and predicted response.

Examination of these plots revealed no pronounced trends which would indicate lack of fit. In Figure 4.11 There is a possibility of a linear trend with increasing throughput.

However, if only those residuals contained within the 2 σ. limits are considered, no trend is apparent.

Models with different functions of Q were tested to verify that the residuals did not in fact indicate that another form of Q in the model was appropriate.

$$H = (T11/rpm + T12 \cdot Q^{0.5}) \exp(T21 \cdot \phi d/A)$$

$$H = (T11/rpm + T12 \cdot Q^{2}) \exp(T21 \cdot \phi d/A)$$

$$H = (T11/rpm + T12 \cdot Q) \exp(T21 \cdot Q \cdot \phi d/A)$$

resulted in poorer fits (greater sums of squares of residuals).

A four parameter model of the form,

$$H = (T1/rpm + T2 \cdot Q) \exp((T3 \cdot \phi d + T4 \cdot Q)/A)$$

was tested. The sum of squares of residuals was reduced using this model and when a quantitative lack of fit test was performed no lack of fit was evident.

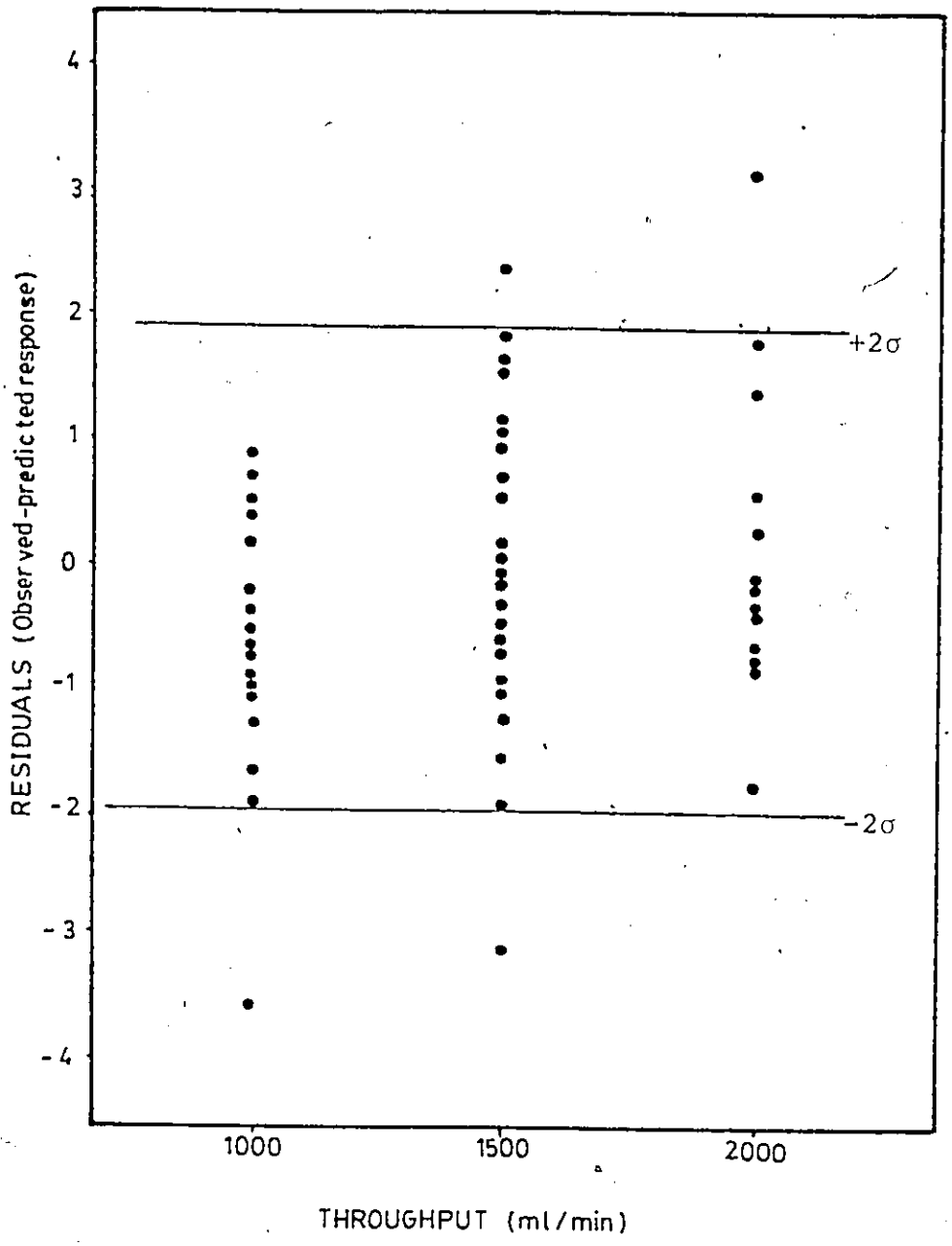

Figure 4.11: Residuals vs Throughput
$H=(T1/rpm+T2\cdot Q)\ \exp(T3\cdot \phi d/A)$

The fitted model parameters with 95% confidence intervals were,

$$T1 = 1.12 \pm .07$$

$$T2 = .593 \pm .04$$

$$T3 = .576 \pm .01$$

$$T4 = .018 \pm .003$$

In the residuals vs. predicted response plot in Figure 4.12 the possibility of increasing variance with increasing predicted response appeared when the three parameter model was used.

A transformed response model ,

$$\ln H = \ln (T1/rpm + T2 \cdot Q) + T3 \cdot \phi d/A$$

was tested to see if a change in the residual pattern would be realized using a model where the pure error variance is transformed. The use of a logarthmic transformation on the response would also transform the associated error logarithmically.

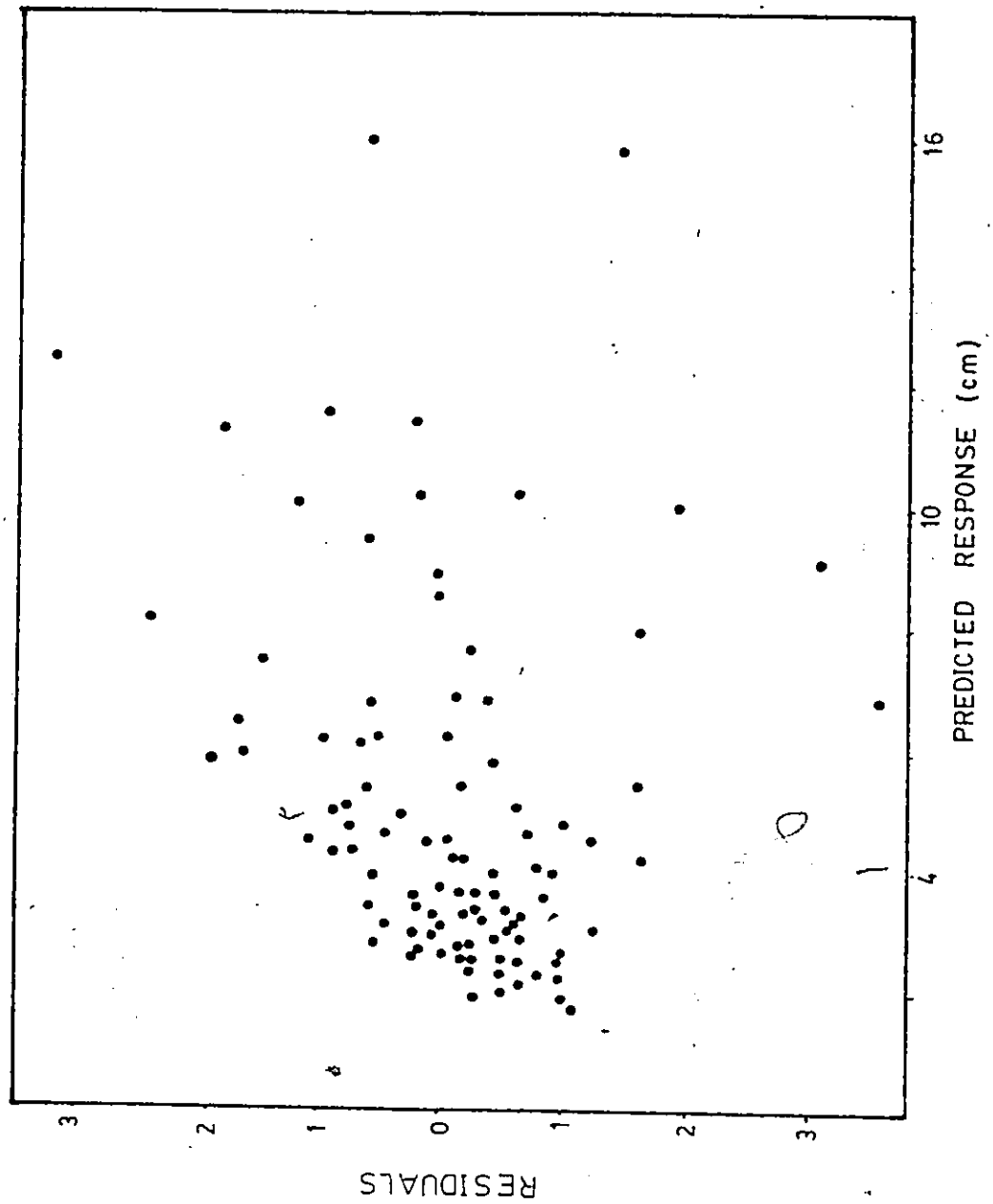

Figure 4.12: Residuals vs Predicted Response
$H=(T1/rpm+T2\cdot Q)\ \exp(T3\cdot \phi d/A)$

The fitted parameters were,

$$T1 = 1.13 \pm .26$$

$$T2 = .50 \pm .10$$

$$T3 = .66 \pm .05$$

When these parameters are compared to those for the

$$H = (T1/rpm + T2 \cdot Q) \exp(T3 \cdot \phi d/A)$$

model, only the T2 parameters differ by more than the calculated 95% confidence intervals.
To choose between the two forms of the model requires a decision about which form of the error is appropriate.

Overall it can be said that the model developed,

$$H = (T1/rpm + T2 \cdot Q) \exp(T3 \cdot \phi d + T4 \cdot Q)/A$$

displayed no evidence of lack of fit and is representative of the dispersion band height behaviour for the range of experimental conditions investigated. This four parameter model yielded the lowest sum of squares of residuals and the quantitative lack of fit test performed did not indicate any reason to question the adequacy of the model.

Although the four parameter model included throughput in the exponential portion of the model, a strong dependence on throughput in the form of Q/A was not evident. Neither the residual plots nor the T2 vs. Q plots presented earlier displayed strong evidence that Q needed to be included in exponential part of the model.

4.2 Dispersion Bands in the Laboratory Settler using the Cylindrical Mixer

To try and prevent air entrainment in the dispersion a new cylindrical mixer was constructed. In unbaffled form, this mixing configuration resulted in very low dispersed phase hold up in the mixer. When the four vertical baffles were installed hold up levels of greater than 50% were observed.

The mixing conditions possible with the cylindrical mixer were much different than those possible with the open square mixer. When operating at 400 rpm or greater it was difficult to discern the aqueous phase-dispersion band interface indicating organic phase was being entrained in the aqueous stream exiting the settler. The heights of the dispersion bands formed were much greater that those observed using the square mixer. Flooding occured at low settling areas in some instances, a phenomenon not observed when the square mixer was used.

A three level experimental design was set up using the three flowrates used in the square mixer runs , three levels of agitation intensity, and three levels of dispersed phase ratio in the feed. The experimental conditions are presented in Table 4.3

For many runs an additonal response was recorded. Dispersed phase holdup in the mixer was measured by allowing the dispersion in the mixer to separate after shut down. The heights of the two separated phases were then recorded.

Table 4.3: Experimental Conditions using the Cylindrical Mixer

	Q	Impeller RPM	ϕd
+	2000	350 300	.6
0	1500	250 200	.5
-	1000	150	.4

4.2.1 Experimental Results Using the Cylindrical Mixer

The experimental data in the form H vs. 1/A is presented in Figure 4.13 through Figure 4.20

The experimental design was augmented with four replicate runs at the center point of the design (Q=1500 ml/min, RPM=250, ϕd=.5) and with single replicates at two other locations in the design.

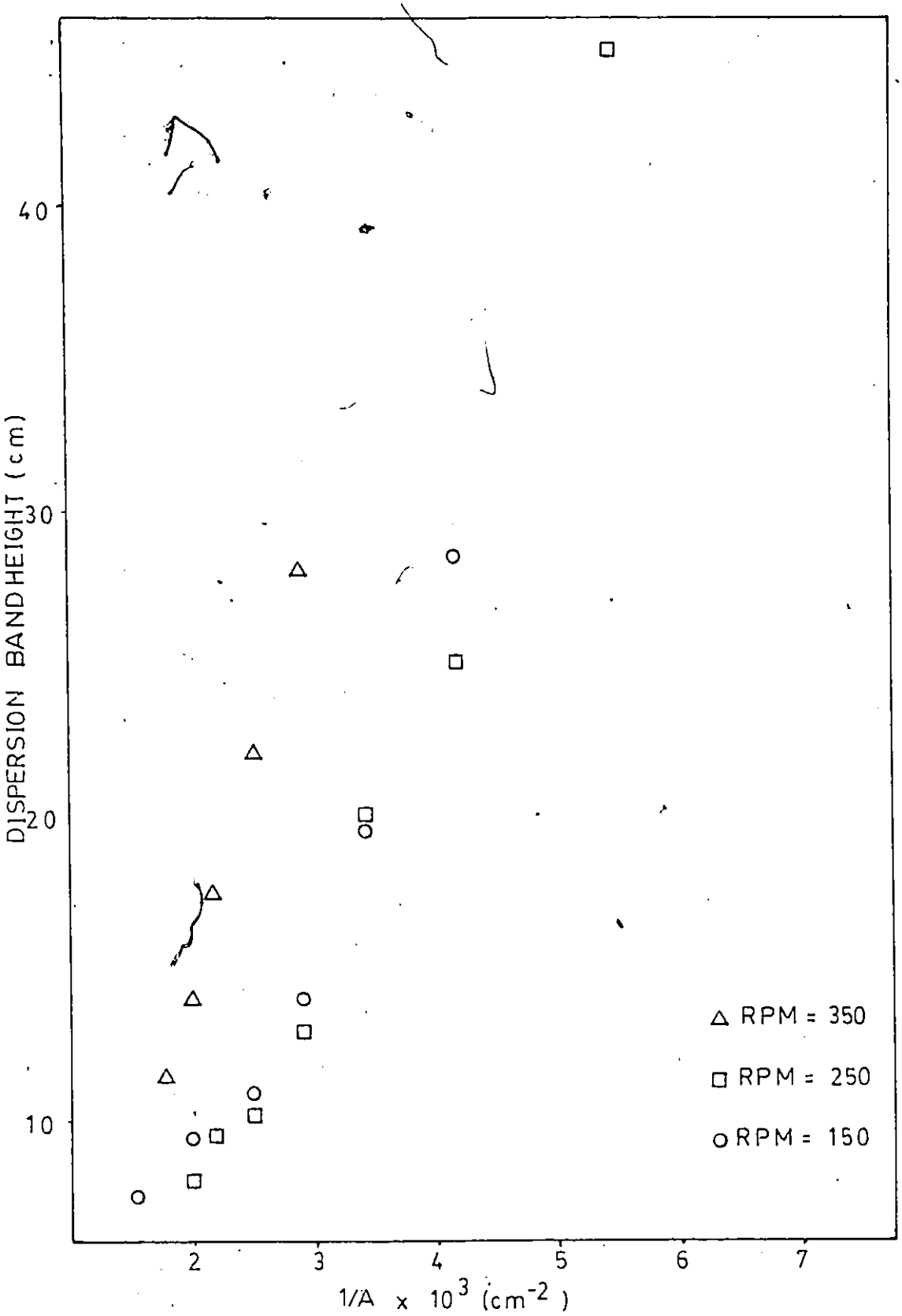

Figure 4.13: H vs 1/A Q=2000 ϕd=.6

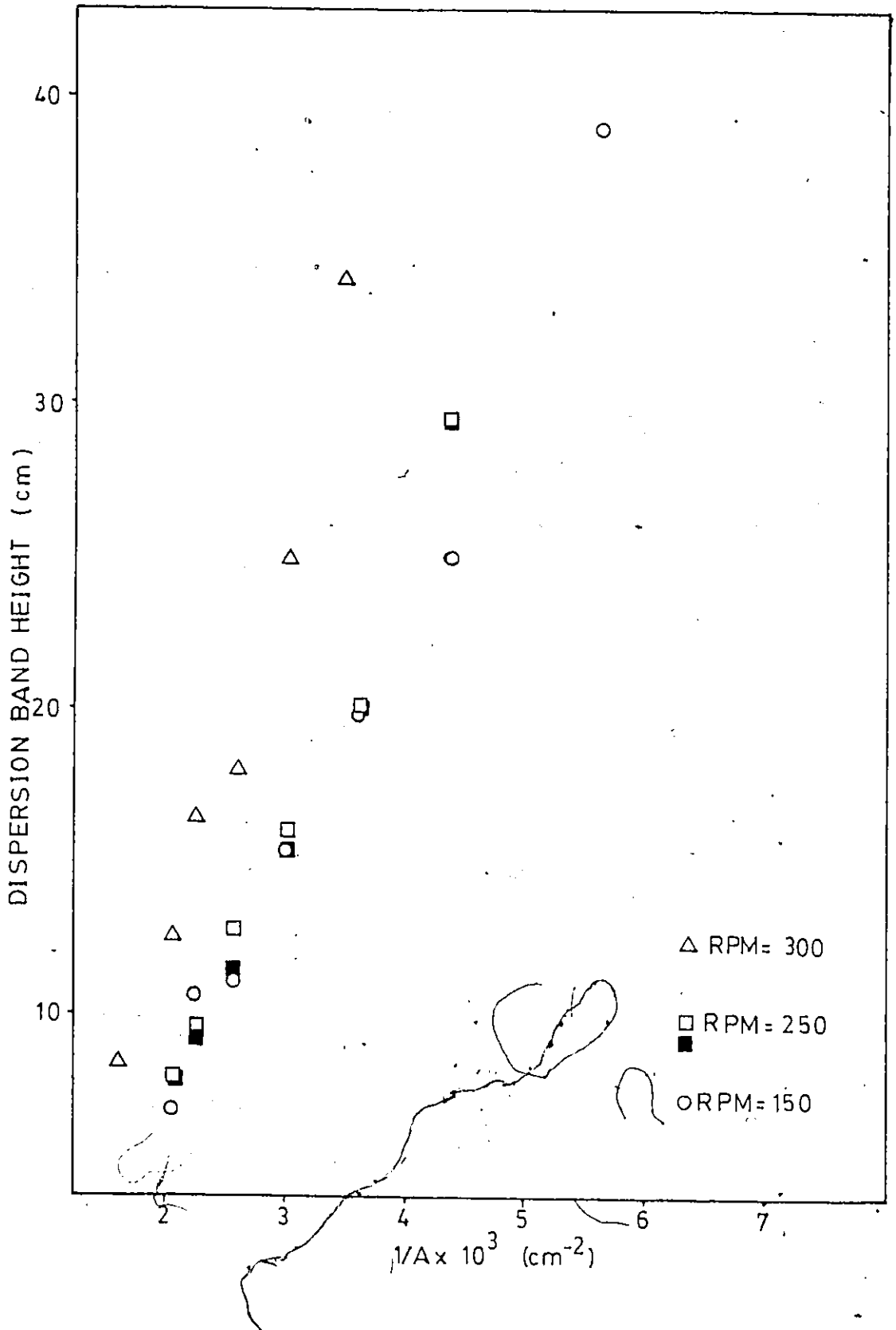

Figure 4.14 H vs 1/A Q=2000 $\phi d=.5$

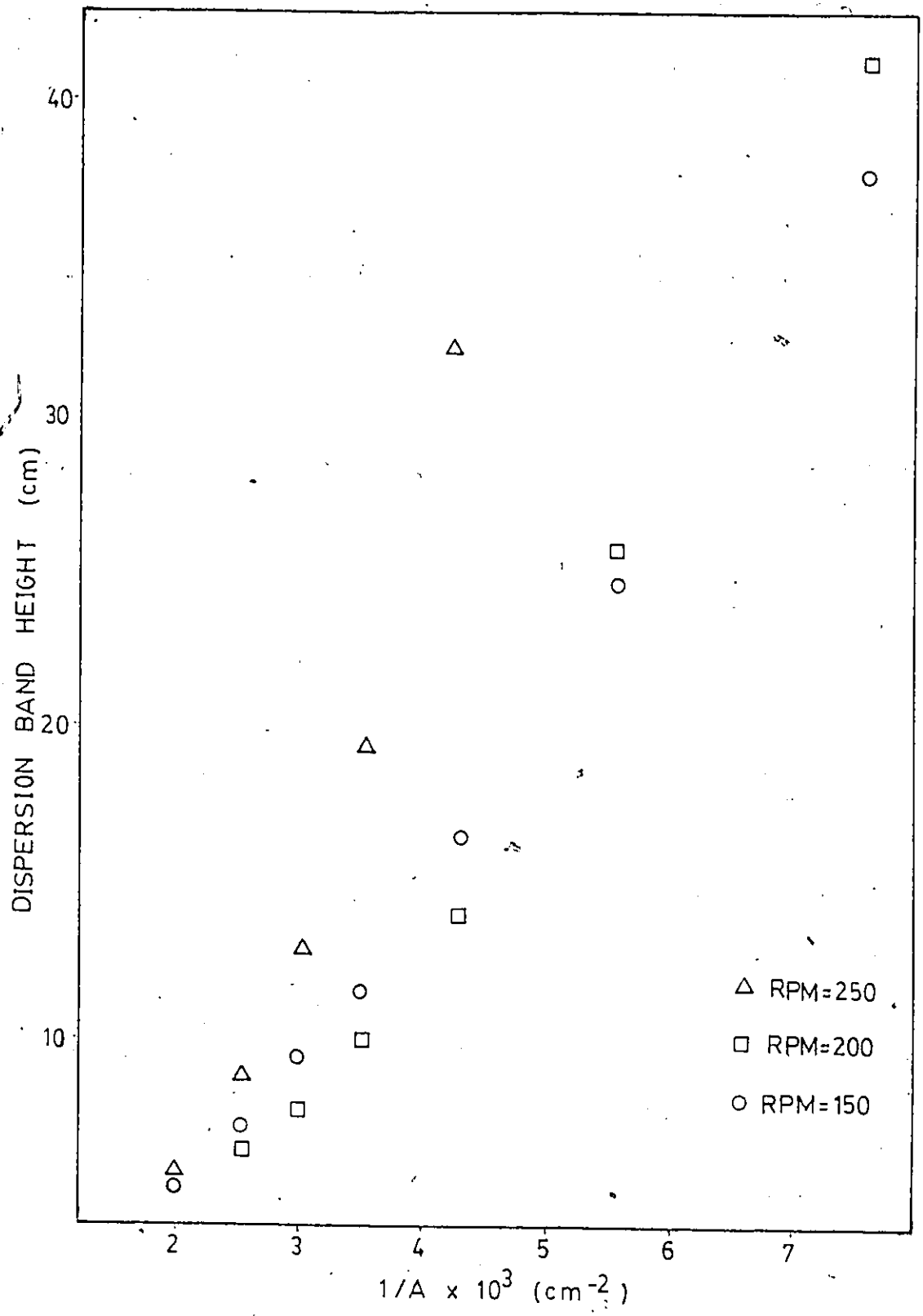

Figure 4.14: H vs 1/A Q=2000 $\phi d = .4$

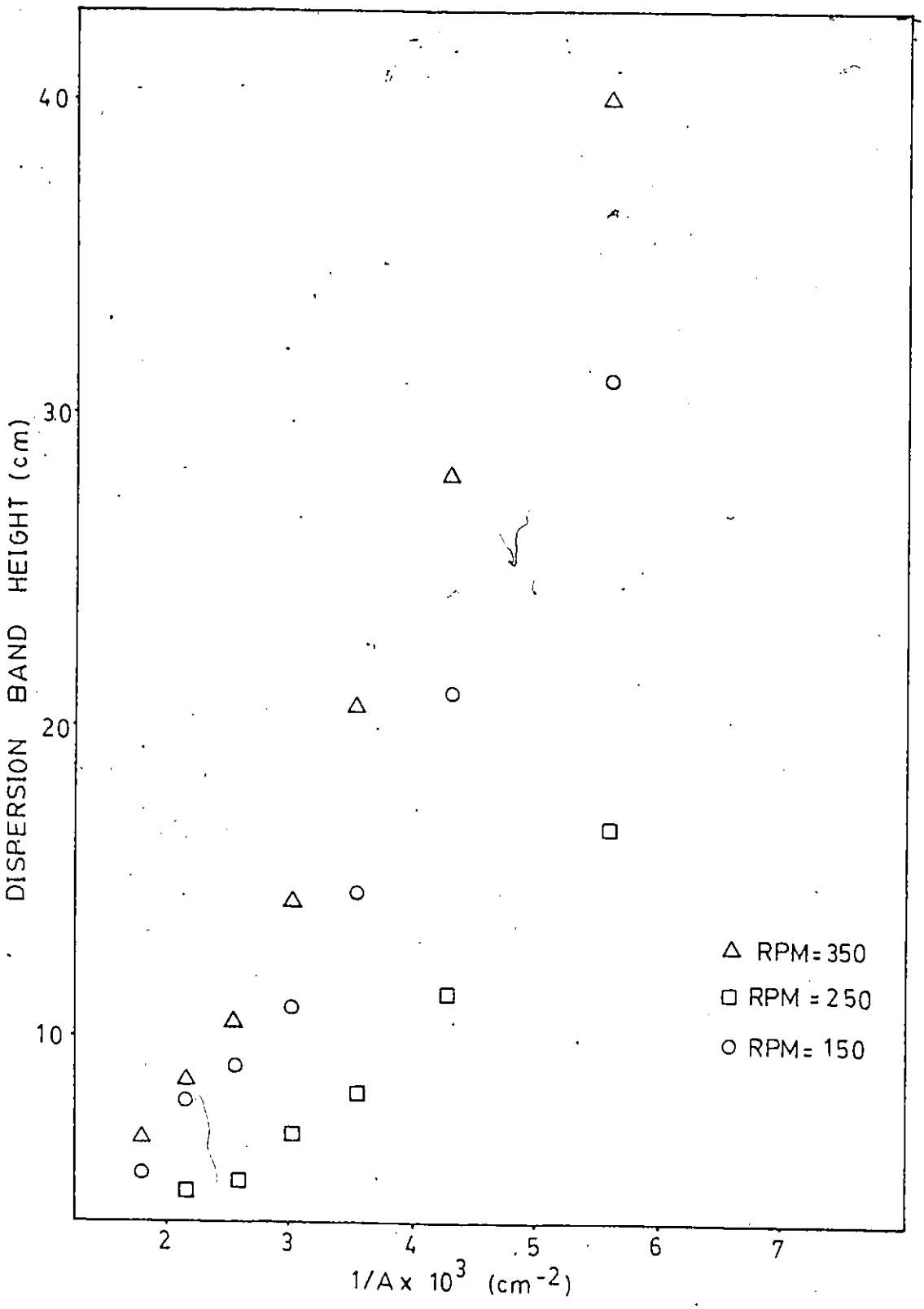

Figure 4.16: H vs 1/A Q=1500 $\phi d=.6$

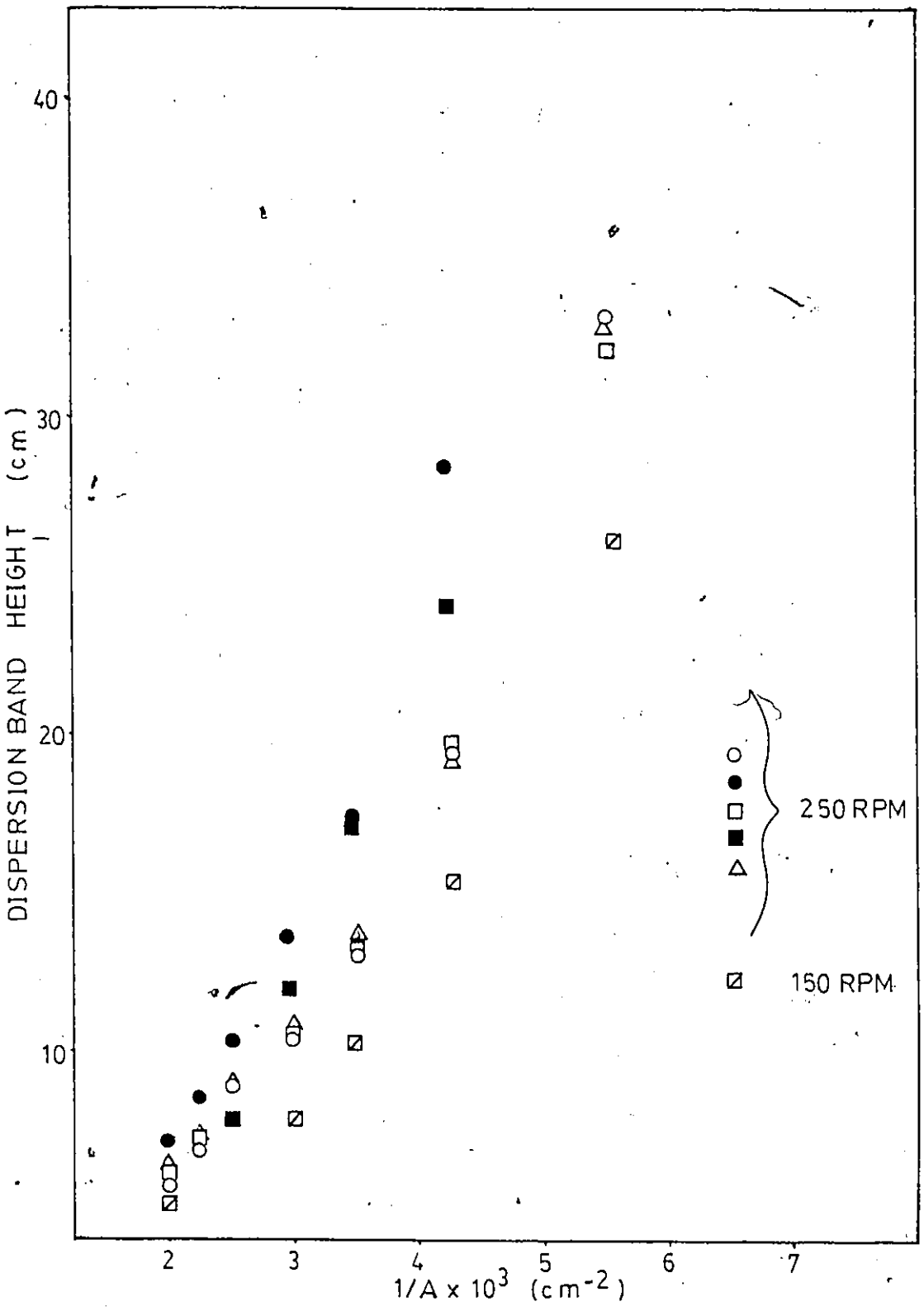

Figure 4.17: H vs 1/A Q=1500 ϕd=.5

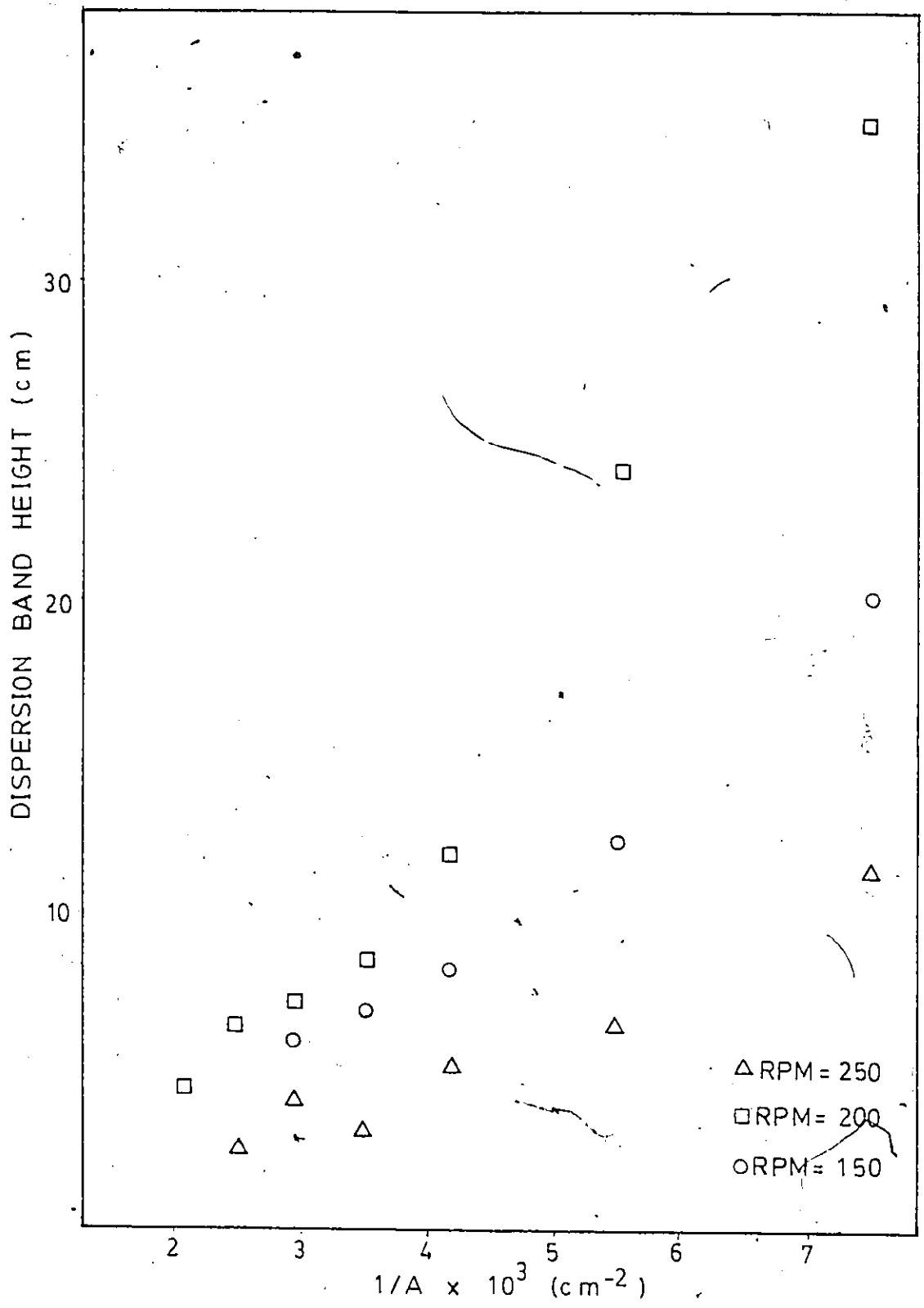

Figure 4.18: H vs 1/A Q=1500 ϕd=.4

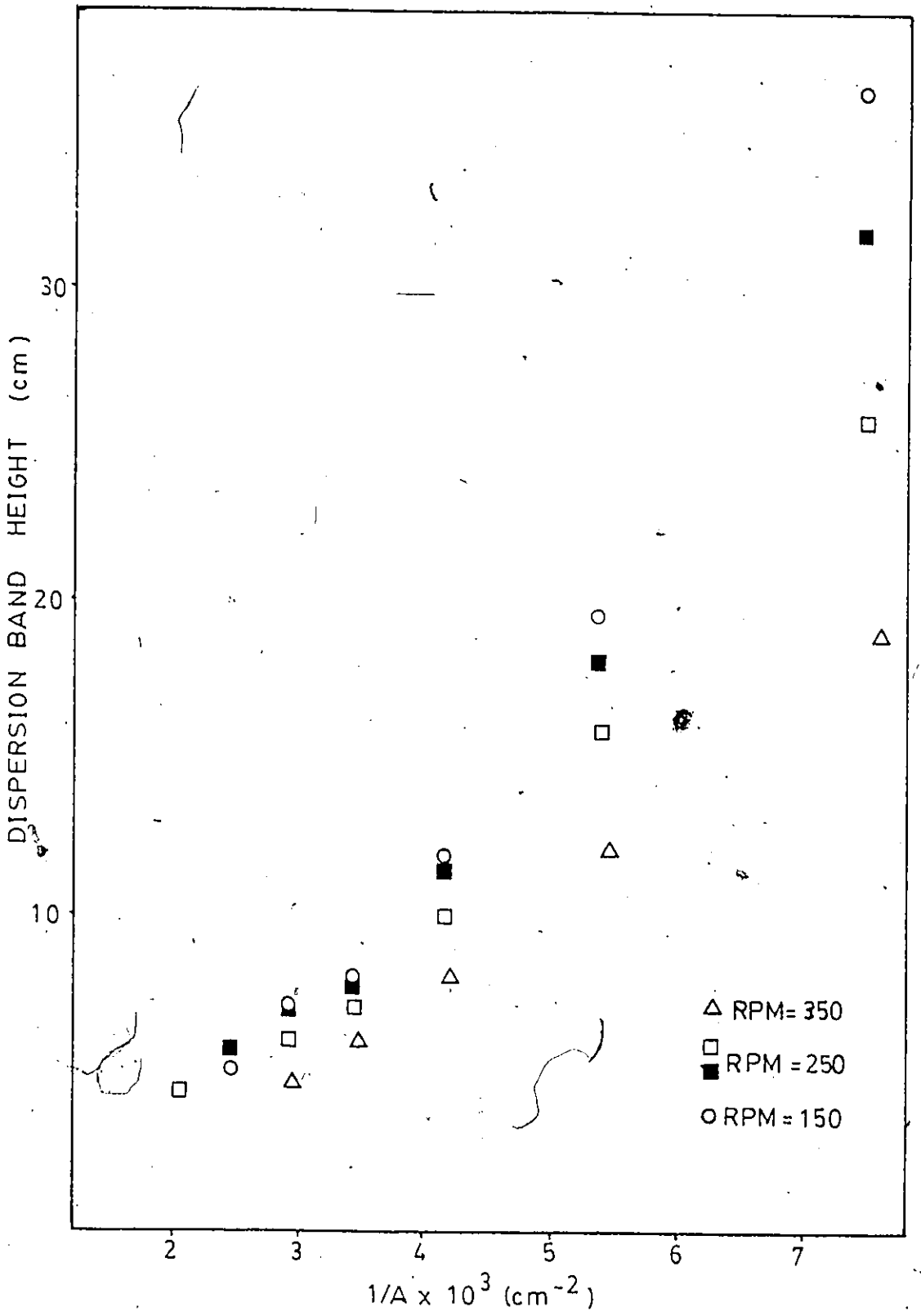

Figure 4.19: H vs 1/A Q= 1000 ϕd=.6

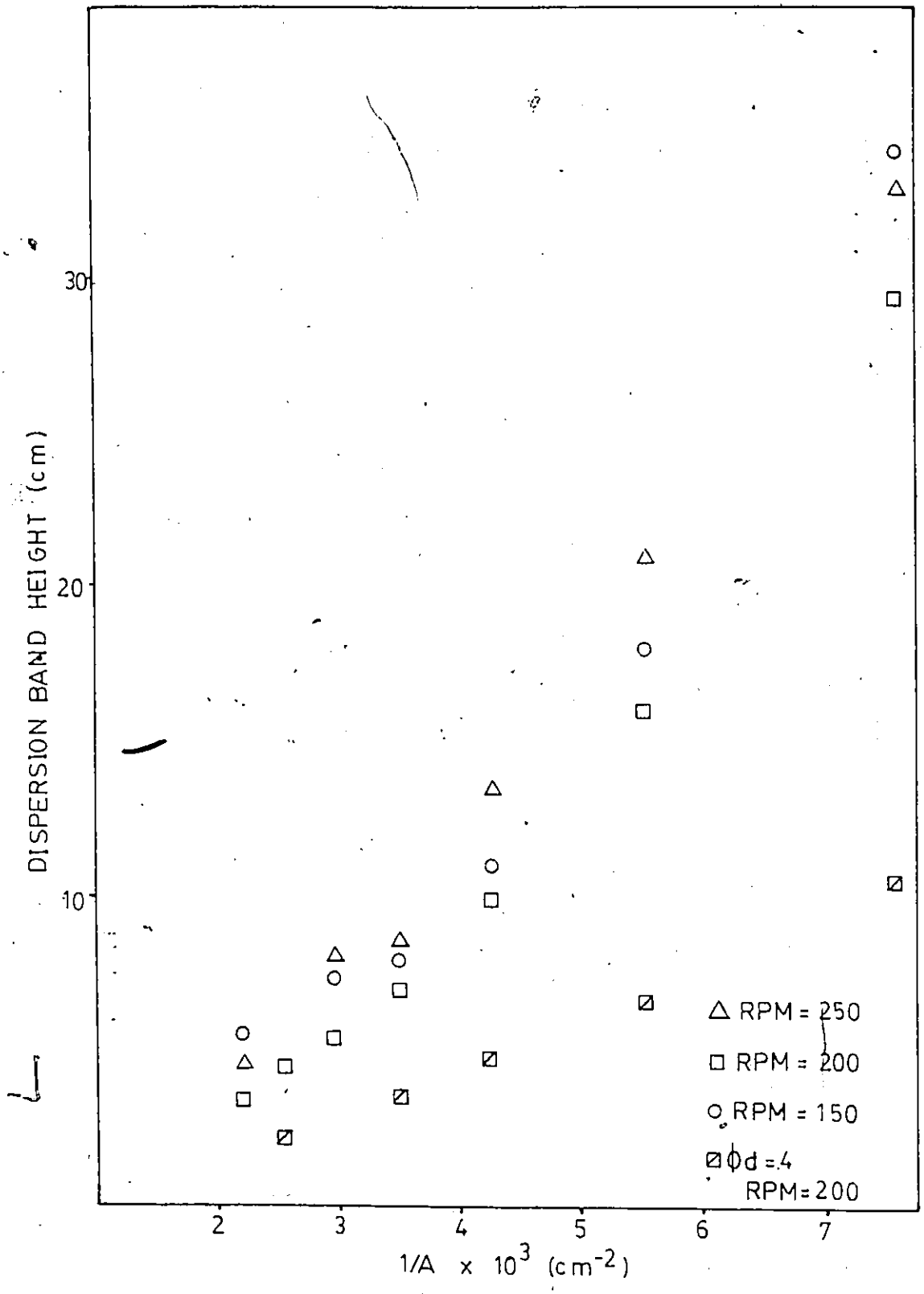

Figure 4.20: H vs 1/A Q=1000 ϕd=.5,.4

Two runs resulted in organic entrainment in the exit aqueous stream making it impossible to define the lower limit of the dispersion band. Thus no dispersion band height measurements were possible. A further run produced dispersion bands so small they could not be measured accurately. At some throughput conditions it was not possible to operate at the high end of the selected impeller rpm range due to organic entrainment in the aqueous stream leaving the settler. Therefore the range of impeller rpm used at a given Q and Od was reduced so that three levels of rpm were still recorded. The experimental design was therfore altered and incomplete. Further experimentation to effect a complete 3 level design was not possible due to contamination of the experimental phases by concrete dust during repairs to the laboratory. This also eliminated possible replication of early runs to study the variance in the observed dispersion band heights with time.

Unlike the square mixer runs, the dependence of dispersion band height on the experimental variables was not readily apparent from the H vs. 1/A plots presented in Appendix D. This raised the possibility of the dispersion band height being affected differently by the experimental variables in different portions of the experimental region.

The plots of ln H vs. 1/A displayed concave downward curvature. This indicated that the exponential model used to

represent the square mixer results would not be suitable to represent the cylindrical results. The downward curvature indicates that the observed dispersion band heights are lower at small settling areas than would be predicted if $\ln H = T1 + T2/A$ were representative of the behaviour. This observation, combined with the fact that the square mixer data which consisted of smaller dispersion band heights was adequately represented by $H = T1 \exp(T2/A)$, indicates that the coalescence rate in the dispersion band may be a function of dispersion band height. This possibility was noted by Vieler et. al. (16) and by Glasser et. al. (4).

Plotting the data in the form of ln H vs ln (1/A) as suggested by Ryon et. al.(9,10,11) and by Barnea and Mizrahi (12) resulted in a more linear representation of the data although slight curvature was observed. The ln H vs ln(1/A) plots are presented in Appendix E.

When the data was plotted in the V/Q vs H form as suggested by Vieler et. al. (16), the straight lines predicted by those authors were not observed. Pronounced curvature was observed in some cases. As this model can be rearranged into the form of 1/H vs A, the possibility of an effect of height on the coalescence rate again is raised. The plots of V/Q vs H are presented in Appendix F.

The effect of rpm on the dispersion band height was not consistent over the experimental operating region.

At Q=2000 ml/min, the effect of rpm on the dispersion band height was consistent at the three different ϕd levels and the expected behaviour of height increasing with increasing rpm is observed.

However, at Q= 1500 ml/min, ϕd=.6 rpm=250, and at ϕd=.4 rpm=250, the observed dispersion band heights are significantly lower than the heights observed at the other two rpm levels at the same Q and ϕd. In the case of ϕd=.6, increasing the impeller rpm from 150 to 250 to 350 appeared to cause an decrease in dispersion band height at rpm=250 followed by an increase at rpm=350. At Q=1500, ϕd=.4, increasing the impeller rpm from 150 to 200 to 250 appeared to cause an increase in dispersion band height at rpm=200 followed by a decrease at rpm=250. It must be noted that the two above mentioned runs were the first two performed in the cylindrical mixer experimental series and that the two runs were performed at the same impeller rpm.

At Q=1000 ml/min, an increase in impeller rpm appeared to cause a decrease in dipersion band height at ϕd=.6. At ϕd=.5, the effect of rpm is not clear due to the small differences in dispersion band heights observed at the different impeller rpm and the small range of rpm investigated.

The ratio of the volume of aqueous phase to organic phase in the mixer at steady state was measured. From this, the fraction of mixer volume the organic phase (dispersed phase)

occupied, was calculated. Table 4.4 shows the dispersed phase fraction in the mixer at steady state.

The dispersed phase fraction in the mixer data did not explain the inconsistencies in the effect of rpm on the dispersion band height. The effect of impeller rpm on the holdup of the dispersed phase in the mixer appears to be consistent over the entire operating region. And, when replicate runs were performed, the observed holdup values remained constant while the observed dispersion band heights diplayed significant variance.

Also of note is the very low dispersed phase fraction in the mixer at Q=1000 ml/min, ϕd=.4, rpm=200

Table 4.4

Dispersed Phase Fraction in the Mixer at Steady State

Q	RPM	ϕ_d	Dispersed Phase Fraction
2000	350	.6	.579
2000	250	.6	.550
2000	150	.6	.314
2000	300	.5	.500
2000	250	.5	N/A
2000	250	.5	.464
2000	150	.5	.229
2000	250	.4	.357
2000	200	.4	.350
2000	150	.4	.186
1500	350	.6	.550
1500	250	.6	.457
1500	150	.6	.279
1500	250	.5	.457
1500	250	.5	.464
1500	250	.5	.464
1500	250	.5	.457
1500	250	.5	.457
1500	150	.5	.214
1500	250	.4	.343
1500	200	.4	.321
1500	150	.4	.164
1000	350	.6	N/A
1000	250	.6	.543
1000	250	.6	.543
1000	150	.6	.279
1000	250	.5	.414
1000	200	.5	.386
1000	150	.5	.229
1000	200	.4	.071

4.2.2 Modelling the Cylindrical Mixer Results

The model,

$$H = T1 \exp(T2/A)$$

which was used to represent the square mixer runs was fitted to the individual cylindrical mixer runs. Inadequacies were observed using this model for some runs. These inadequacies took the form of a large residual at the second highest 1/A value. These residuals were positive meaning the model was predicting a dispersion band height less than that observed experimentally. This lack of fit was expected when it was observed that the ln H vs 1/A plots in Appendix D displayed concave downward behaviour. Other models investigated were,

$$H = T1(\exp(T2/A)-1)$$

$$H = T1\ (1/A)^{T2}$$

H = (exp(T2/A)-1) was chosen for consideration as a dispersion band height of H=0 is expected at a very large settling area. Plotting V/Q vs. H and 1/H vs. A,(Appendix F),did not result in straight lines, therefore excluding models of the form,

$$V/Q = T1 + T2 \cdot H$$

and

$$1/H = T1 + T2 \cdot A$$

The model $H = T1 \cdot (1/A)^{T2}$ provided a better representation of the H vs A behaviour of the individual runs than did either $H = T1 \exp(T2/A)$ or $H = T1(\exp(T2/A)-1)$.

The replicate runs performed provided an estimate of the pure error variance associated with the height readings taken. As with the square mixer data, it must be noted that individual points cannot be considered to be "true replicates" as each run was performed by varying A as Q, rpm, and ϕd were held constant. When the individual points at the same Q, Rpm, ϕd, and A were considered as replicates, an Sp^2 value of 4.28 was obtained. However, a constant variance over the range of cross sectional areas used was not observed.

The variances associated with the individual sets of replicate points (same 1/A, Q, ϕd, rpm) increased with increasing 1/A. As one of the assumptions made when using a least squares analysis is that the variance associated with the measured response is constant over the entire experimental region, transforming the response (H) to transform the associated error such that the variance of the measurement of H is constant over the operating region was necessary.

A logarithmic and a reciprocal transformation on the dispersion band height was performed and the variance for each set of replicates was calculated. These are presented in Table 4.5

Table 4.5: Variance from Replicate Runs

Response runs	1/A	H	ln H	$\sigma_i^2/(m_i-1)$ 1/H
38,44	5.5	.75	.0007	7.5 E-7
50,58	4.22	73	.124	2.17 E-4
62	3.48	31.4	.116	4.42 E-4
	2.93	15.5	.297	6.16 E-4
	2.53	8.5	.091	9.89 E-4
	2.2	3.0	.049	7.98 E-4
	2.01	2.82	.059	4.23 E-3
46,57	7.58	18	.022	2.59 E-5
	5.5	3.13	.011	3.53 E-5
	4.22	1.13	.010	8.45 E-5
	3.48	.32	.006	1.08 E-4
	2.93	.50	.012	2.83 E-4
45,59	4.22	0	0	0
	3.48	0	0	0
	2.93	.5	.002	8.82 E-6
	2.53	.5	.004	2.45 E-5
	2.2	.125	.002	1.68 E-5
	2.01	0	0	0

The reciprocal transformation resulted in increasing variance with decreasing 1/A. Therefore only the logarithmic transformation remained to be considered. Thus, for the purposes of prediction of the dispersion band heights in the laboratory settler, models with the response (height)* in the form of ln H would be more suitable than H or 1/H. This could also be applied to the square mixer results resulting in the model found to adequately represent that data, being transformed logarithimically.

Examination of the ln H vs 1/A and the ln H vs ln (1/A) plots in Appendix D and Appendix E suggested that models of the form,

$$\ln H = T1 + T2 \ln(1/A) + T3\ 1/(\ln(1/A))$$

or

$$\ln H = T1 + T2\ 1/A + T3 \cdot A$$

where T3 is negative in the case of the latter model, may adequately represent the individual runs in terms of the height-cross sectional area relationship. However, fitting the $\ln H = T1 + T2 \ln (1/A) + T3\ 1/(\ln(1/A))$ model to the individual runs resulted in parameter estimates with large 95% confidence intervals. This occured because of the small degree of freedom associated with the fits. Thus, information provided about the nature of the effect of the experi-

mental variables on the fitted parameters was limited in this case.

Although determining an adequate representation of the H vs A behaviour for the individual runs was important, it was also of interest to determine the effect of the other independent variables (Q, rpm, ϕd) on the dispersion band heights observed in the laboratory settler. Therefore, the results of fitting $\ln H = T1 + T2 \ln(1/A)$ were examined.

Because the error structure indicated that a logarithmic transformation of H was appropriate, $\ln H = T1 + T2(\ln(1/A))$ where 1/A was equal to 1/Area x $\cdot 10^3$ cm^{-2} was fitted to the individual runs. 1/A was scaled to obtain positive ln H values. As in the analysis of the square mixer results, the model parameters T1 and T2 were obtained by least squares analysis and their 95% confidence intervals were calculated. Because this is a linear model, the calculated 95% confidence intervals for the parameter estimates are accurate. T1 and T2 were then plotted against the experimental variables to determine the effect of Q, rpm, and ϕd on the model parameters. The parameters and their 95% confidence intervals are presented in Table 4.6

The effects of rpm and ϕd at each of the three throughput conditions were investigated using the model parameters in the same manner as was used to investigate the /effects of the variables on the dispersion band heights obtained using

Table 4.6: Parameters for the Model lnH=T1+T2(ln(1/A)), Cylindrical Mixer

Q	ϕd	rpm	T1	T2
2000	.6	350	1.33+/-.25	1.89+/-.30
2000	.6	250	0.83+/-.31	1.71+/-.27
2000	.6	150	0.98+/-.28	1.60+/-.27
2000	.5	300	1.38+/-.24	1.70+/-.26
2000	.5	250	0.86+/-.09	1.74+/-.08
2000	.5	150	0.98+/-.35	1.28+/-.30
2000	.4	250	0.08+/-.33	2.33+/-.30
2000	.4	200	0.19+/-.29	1.74+/-.20
2000	.4	150	0.59+/-.14	1.51+/-.10
1500	.6	350	.083+/-.17	1.71+/-.15
1500	.6	250	0.49+/-.24	1.34+/-.19
1500	.6	150	0.78+/-.15	1.55+/-.13
1500	.5	250	0.70+/-.14	1.63+/-.12
1500	.5	150	0.51+/-.30	1.57+/-.22
1500	.4	250	-0.23+/-.74	1.28+/-.51
1500	.4	200	0.33+/-.38	1.58+/-.28
1500	.4	150	0.37+/-.41	1.27+/-.22
1000	.6	350	-0.08+/-.14	1.49+/-.09
1000	.6	250	0.22+/-.26	1.52+/-.18
1000	.6	150	-0.10+/-.20	1.80+/-.14
1000	.5	250	0.25+/-.33	1.61+/-.23
1000	.5	200	-0.12+/-.15	1.71+/-.11
1000	.5	150	0.44+/-.48	1.46+/-.33
1000	.4	200	-0.54+/-.59	1.44+/-.39

the square mixer. The runs at Q=1500 ml/min, ϕd=.6, rpm=250 and Q=1500 ml/min, ϕd=.4 rpm=250 and Q=1000 ml/min. ϕd=.4, rpm=200 had the lowest dispersion band heights observed obtained using the cylindrical mixer. Replication of these runs would be beneficial. Justification for deleting these runs from the data set can only be obtained if replication of these runs provides dispersion band heights significantly higher than those observed.

When these three low dispersion band height runs were removed from the data set a model of the form,

$$\ln H = T1 + T2 \cdot \phi d + (T3 \cdot \phi d + T4 \cdot RPM^3 + T5 \cdot RPM \cdot \phi d) \cdot (\ln 1/A)$$

was found to adequately represent the data for each of the three throughput conditions. The model parameters and their 95% confidence intervals are presented in Table 4.7 Also included in Table 4.7 are the results of the T-test for each model fit,(24). In each case T is less than $F_{n-p, \nu sp^2}$, indicating no evidence of lack of fit from this test. These results were examined to determine the effect of Q on the dispersion band height.

If however, replication of the three runs indicated that the observed dispersion band height were in fact representative of the behaviour at any of the three run conditions then the model found to represent the remaining data should be reexamined.

Table 4.7

Model Parameters for Five Parameter Model

Q	1000	1500	2000
T1	2.59+/-.54	0.98+/-.27	1.23+/-.32
T2	-4.46+/-1.04	-0.66+/-.54	-0.68+/-.63
T3	2.81+/-.56	-0.88+/-.60	4.89+/-.84
T4	-0.01+/-.015	-0.04+/-.01	0.07+/-.02
T5	0.12+/-.34	1.51+/-.44	-1.48+/-.53
SSR	.78	.94	1.54
T	.97	.71	1.26
F $_{n-p,\nu}$ sp^2	1.69	1.53	1.64

The five model parameters were plotted against Q. These plots are shown in Figure 4.21 As can be seen from Figure 4.21 , the effect of Q on the dispersion band height appears to be quite complicated. Models of the form,

$$\ln H = T1 + T2 \cdot \phi d \cdot Q^{T3} + ((T4 \cdot \phi d + T5 \cdot rpm \cdot \phi d) Q^{T6} + T7 \cdot rpm \cdot \phi d \cdot Q^{T8}) \ln(1/A)$$

and others with similar configurations were tested but a model which adequately represented the entire data set was not determined. Including a term to take into account run order did not offer any significant improvement in fit. Of note however, is the fact that throughput did not appear to affect dispersion band height in the form of Q/A.

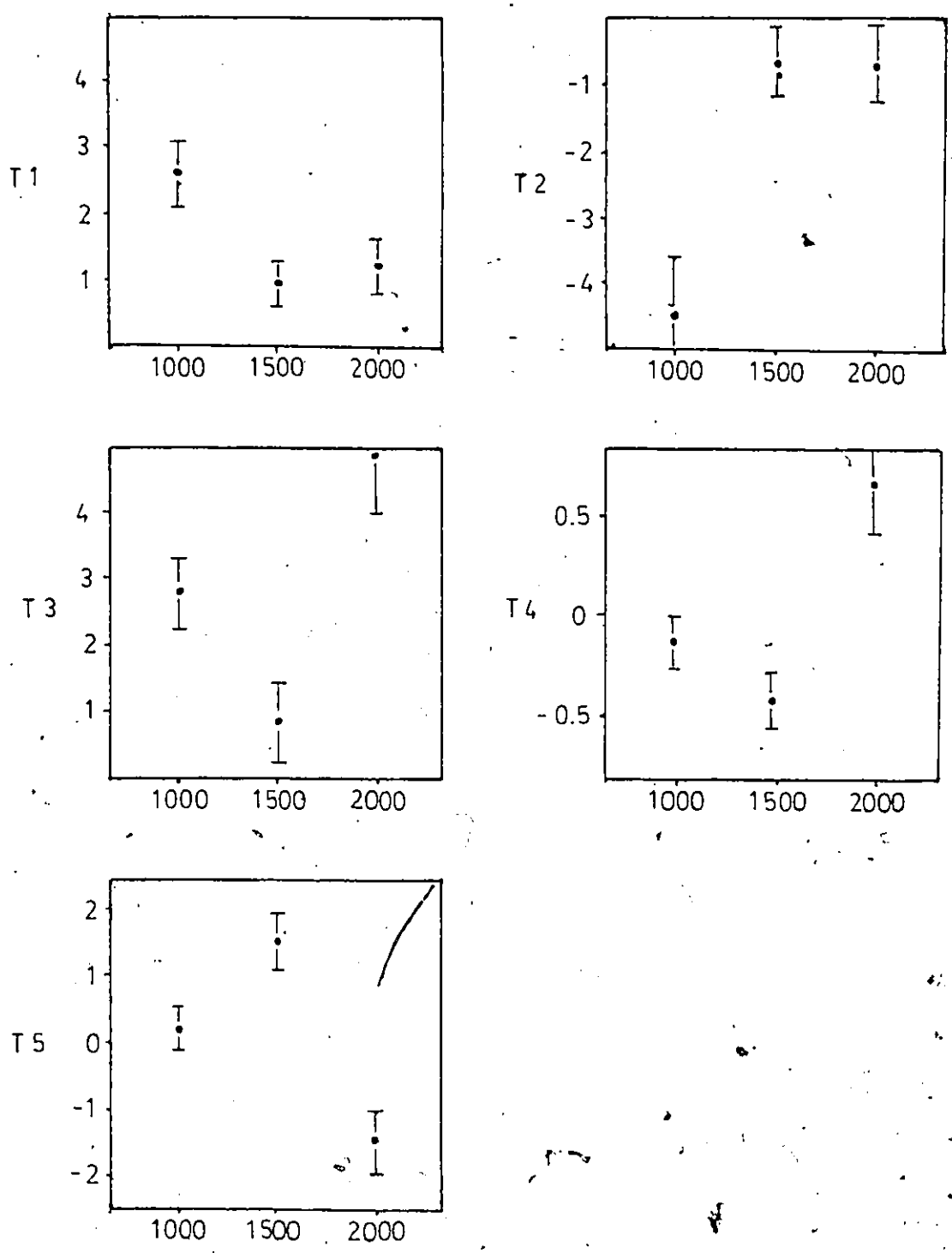

Figure 4.21: Plots of Five Parameters vs Throughput
Cylindrical Mixer Data

A five parameter model of the form,

$$\ln H = T1 + T2 \cdot \phi d + (T3 \cdot \phi d + T4 \cdot rpm^3 + T5 \cdot rpm\ \phi d)(1/A)$$

was fitted to the data for each throughput.

The runs previously deleted remained deleted from the data set. In each case a T-test was performed. No evidence of lack of fit was determined for any of the three throughputs investigated. The parameter estimates from these fits are presented in Table 4.8 The T and F n-p, νsp^2 values are also presented.

Table 4.8

Results of 5 Parameter Model Fit using 1/A instead of ln(1/A)

Q	1000	1500	2000
T1	2.46+/-.61	0.92+/-.27	1.21+/-.35
T2	-2.98+/-1.12	0.17+/-.53	-0.08+/-.68
T3	0.66+/-.19	-0.05+/-.20	1.41+/-.30
T4	.003+/-.005	-0.02+/-.005	0.02+/-.01
T5	-0.02+/-.12	0.61+/-.15	-0.45+/-.20
SSR	.98	.93	1.83
T	1.21	.70	1.50
F n-p,νsp^2	1.69	1.53	1.64

For predictive purposes, however, the model with the ln(1/A) term should be used, as the individual runs were better represented by $\ln H = T1 + T2 \ln(1/A)$.

4.2.3 Summary

The factorial design and the additional runs performed provided enought information to develop an adequate model to represent the cylindrical mixer data. It was found that all the experimental variables chosen for study had a significant effect on the observed dispersion band heights.

The form of the height-settling area relationship for the square mixer data was found to be different than the form found for the cylindrical data height-settling area relationship. The range of dispersion band heights observed in the two sets of data differed significantly indicating a possibility of the dispersion band height having an effect on the coalescence rates within the dispersion band.

The incomplete factorial design performed with the cylindrical mixer did not provide enough information to adequately model the entire data set. The five parameter model,

$$\ln H = T1 + T2 \cdot \phi d + (T3 \cdot \phi d + T4 \cdot RPM^3 + T5 \cdot RPM \cdot \phi d) \cdot (\ln 1/A)$$

was the simplest model which was found to represent the data at each of the three throughput conditions. All of the experimental variables investigated were found to have a significant effect on the dispersion band heights produced using the cylindrical mixer.

It is possible to investigate the effects of process variables on dispersion band heights using a bench scale mixer settler. After using a factorial experimental design to identify those variables which have a significant effect on the dispersion band height, more experimentation may have to be performed to investigate the form of the effects of the variables in more detail.

CONCLUSIONS

1. A model to predict the dispersion band height while using the square mixer was successfully developed. Attempts to model the data obtained using the cylindrical mixer were not successful.
2. $H = T1 \exp(T2/A)$ or $\ln H = T1' + T2/A$ appeared to adequately represent the individual runs obtained using the square mixer. The model parameters could be related to throughput, impeller rpm, and the dispersed phase fraction in the feed.
3. $\ln H = T1 + \ln(T2/A)$ appeared to best represent the individual runs obtained using the cylindrical mixer. This result is in agreement with previously published results by Ryon, Daley, and Lowrie, and by Barnea and Mizrahi among others. The model parameters did not reveal much information about the effect of the experimental variables on the dispersion band height.
4. There was no experimental evidence that the effect of throughput on dispersion band height was of the form Q/A.
5. Air entainment in a mixer settler apparatus may result in lowering the settling area required to effect phase separation.

RECOMMENDATIONS

1. in this study, the settler baffle was moved to vary the settling area while throughput, dispersed phase fraction in the feed, and agitation intensity were held constant at the chosen experimental conditions. This caused all the height measurements in a run to be correlated. Performing experiments where all the experimental variables, including settling area, are randomly varied over the experimental region would eliminate this height settling area dependence.
2. It would be of interest to construct a settler where a larger range of dispersion band heights could be studied. In this study, the range of heights observed in a specific run was limited by the settling areas available. Examining a larger range of dispersion band heights may provide insight into the nature of the effect of dispersion band height on the rates of coalescence in the dispersion band.
3. Perform more replication of runs to examine the variance of the observed dipersion band heights with time and run order. It was observed that there was some effect of time or run order in this study. The replicate runs performed indicated that dispersion band heights increased over the course of experimentation.

4. Expand the investigation to include organic continuous dispersions as they are common in industrial use as a means of reducing solvent loss through entrainment in waste aqueous streams.

5. Investigate different extraction systems e.g.LIX & extraction of copper.

NOMENCLATURE

A	settling area cm^2
H	dispersion band height cm
ϕd	dispersed phase fraction in the feed to the mixer
Q	total throughput of phases ml
R	R-test value
RPM	rotations per minute of impeller in mixer
SSR	sum of squares of residuals
T	T-test value
Ti	model parameter
Tij	model parameter
Xi	scaled experimental variable
V	volume of dispersion band cm^3

REFERENCES

1. Howell, W., Ritcey, G.M., Golding, J.A., Proceedings ISEC 1983, 1, 78, Denver, (1983).

2. Hopkins, J., M.A.Sc. Thesis, Univ. Of Ottawa (1984).

3. Ritcey, G.M., Ashbrook, A.W., "Solvent Extraction-Principles and Applications to Process Metallurgy Part 11 " Elsevier, p. 453 (1979).

4. Glasser, D., Arnold, D.R., Bryson, A.W., Vieler, A.M.S., Minerals Sci. Engng. 8, 23 (1976).

5. Carino, A.B., CIM Bullitin June 1979, p. 162.

6. Key Lake Mining Corp, "Key Lake Project:Process Development", Sherritt Gordon Mines, (1980).

7. Brown, D.E., Pitt, K., Chem. Eng. Sci. 27, 577 (1972) also Chem. Eng. Sci, 29, 435 (1974).

8. Kolarik, Z., Pipkin, N., Int. J. Hydromet. 9, 256 (1983).

9. Ryon, A.D., Daley, F.L., Lowrie, R.S., Chem. Eng. Prog. 55, 70 (1959).

10. Ryon, A.D., Daley, F.L., Lowrie, R.S., USAEC ORNL-2951 (1960).

11. Ryon, A.D., Lowrie, R.S., USAEC ORNL-3381 (1963).

12. Barnea, E., Mizrahi, J., Trans. Instn. Chem. Engrs. 53, 61 (1975).

13. Allak, A.M.A., Jeffreys, G.V., AIChE Journal 20, 564 (1974).

14. Smith, D.V., Davies, G.A., Can. J. Chem. Eng. 48, 628 (1970).

15. Golob, J., Modic, R., Trans. I. ChemE. 55, 207 (1977).

16. Vieler, A.M.S., Glasser, D., Bryson, A.W., Proceedings ISEC 1977, p. 399, Toronto (1977).

17. Stoenner, H., Wohler, F., " Hydrometallurgy IChE Symp Series 42 p. 14.1" (1975).

18. Gondo, S., Kusunoki, K., Hydrocarbon Processing 48, 209 (1969).

19. Jeffreys, G.V., Davies, G.A., Pitt, K., AIChE Journal 16, 823 (1970).

20. Vijayan, S., Ponter, A., Proceedings ISEC 1974 p.591 Lyons (1974).

21. Warwick, G.C., Scuffam, J.B., Lott, J.B., Proceedings ISEC 1971 p.1373 Hague (1971).

22. Box, G.E.P., Hunter, W.G., Technometrics 4, 301 (1962)

23. Scott, R.R., Sylvestre, E.A., J. Quality Tech. 11, 55 (1979)

24. Draper, N.R., Smith, H., "Applied Regression Analysis, 2nd Ed." John Wiley & Sons, New York (1981).

Appendix A

EXPERIMENTAL DATA

Table 1

Run Conditions and Dispersion Band Heights with Square Mixer

Run	Q	RPM	H(cm) at Settler Cross Sectional Area (cmxcm) A1	A2	A3	A4	A5	A6	A7	A8	A9	A10
1	2000	250	11.0	6.4	4.2	3.4	3.4	2.8	3.0			
2	2000	250	14.0	10.0	6.7	5.3	4.4	3.8	-	3.2	3.6	
3	1500	500	9.5	6.0	3.2	3.3	2.5	2.5	2.3	-	2.0	
4	1000	750	3.2	2.4	1.7	1.5	1.2	-	0.8	-	0.6	
5	1500	750	5.9	3.7	3.0	2.7	2.3	1.6	1.7			
6	2000	500	15.5	8.8	5.2	4.4	3.5	3.2	3.0	2.8	-	1.7
7	1500	500	10.3	7.0	5.5	3.5	3.3	2.9	2.9	2.8	2.5	2.1
8	1000	250	11.5	6.4	5.7	4.0	4.0	3.4	3.0	-	2.5	
9	1500	250	14.4	10.5	7.5	5.8	5.0	4.5	3.8	-	3.0	2.5
10	2000	750	13.0	7.3	5.2	3.9	3.1	2.6	2.4	2.4		
11	1000	500	6.0	3.7	2.6	2.2	2.0	1.8	1.5	1.5	1.7	
12	1500	500	11.3	6.7	4.5	3.7	3.0	3.0	2.5	2.5	2.2	
13	Φd=.5 1500	500	24.5	8.5	7.6	5.0	4.4	3.6	3.5	-	3.0	
14	Φd=.3 1500	500	8.0	5.2	4.0	3.2	2.5	2.3	--	--	1.4	
18	Φd=.6 1500	250	34.0	16.5	8.0	7.3	6.7	5.9	5.5			

Table 2

Run Conditions and Dispersion Band Heights for Cylindrical Mixer

				H(cm) at Settler Cross Sectional Area									
RUN	Q	RPM	ϕd	A1	A2	A3	A4	A5	A6	A7	A8	A9	A10
32	1500	250	.6	-	16.5	11.4	8.1	6.8	5.5	5.0			
33	1500	250	.4	11.5	6.5	5.0	3.2	4.0	2.5				
34	1500	350	.6	-	40	28	20.5	14.5	10.5	9.0	7.5		
35	2000	350	.6	-	-	-	-	28.0	22.0	17.5	14.0	11.5	
36	2000	250	.6	-	45.0	25.0	20.0	13.0	10.0	9.5	8.0		
37	1000	350	.6	19.0	12.0	8.0	5.8	4.7					
38	1500	250	.5	-	33.0	20.0	14.0	10.5	9.0	7.8	6.0		
39	2000	250	.4	-	-	32	19.5	13.0	8.8	-	5.8		
40	2000	150	.5	-	39.0	25.0	20.0	15.5	11.0	10.8	7.0		
41	1000	200	.4	10.5	6.5	4.8	4.0	-	2.0				
42	2000	150	.4	37	24.5	16.7	11.5	9.5	7.0	-	5.2		
43	1500	150	.5	41.0	26.0	15.5	10.5	8.0	7.5	-	5.5		
44	1500	250	.5	-	33.0	19.5	13.2	10.5	8.0	7.0	5.9		
45	2000	250	.5	-	-	29.5	20.0	16.0	12.5	9.5	8.0		
46	1000	250	.6	26.0	16.0	10.0	7.0	6.0	-	4.5			
47	2000	150	.6	-	-	28.5	19.5	14.0	11.0	9.5	-	7.5	
48	1500	150	.6	-	31.0	21.0	14.5	11.0	9.0	8.0	-	5.5	
49	1500	150	.4	20.0	12.0	8.5	7.0	6.0					
50	1500	250	.5	-	32.0	19.5	13.5	10.5	8.0	7.5	6.5		
51	1000	150	.6	36.0	19.5	12.0	8.0	6.5	5.0				
53	2000	200	.4	41.0	25.5	14.0	10.0	7.8	6.5				
55	1000	150	.5	34.0	18.0	11.0	9.0	7.5	-	5.5			
56	2000	300	.5	-	-	-	34.0	24.0	18.0	16.5	12.5	-	8.5
57	1000	250	.6	32.0	18.3	11.5	7.8	7.0	5.8				
58	1500	250	.5	-	-	28.5	17.5	13.7	10.5	8.7	7.5		
59	2000	250	.5	-	-	29.5	20.0	15.0	11.5	9.0	8.0		
60	1000	250	.5	33.0	21.0	13.5	8.5	8.0	-	4.5			
62	1500	250	.5	-	33	21.5	15.5	11.0	8.5	6.8			
63	1000	200	.5	29.5	16	10.0	7.0	5.5	4.5	3.5			
64	1500	200	.4	35.0	24.0	12.0	8.5	7.5	6.5	-	4.5		

Appendix B

STATISTICAL ANALYSIS AND MODELLING

The parameter precision estimates shown in table 4.1.2 were obtained using the parameter covarience matrix given approximately by,

$$V(\hat{T}) = (Xo^{T} Xo)^{-1} \sigma^{2}$$

Xo is the partial derivitive matrix

σ^{2} was estimated by $S(T)/n-p$

Therefore an approximate 95% confidence interval for the true value of the parameters is given by ,

$$\hat{T}i \; +/- \; t\nu, .05 \sqrt{V(\hat{T}i)}$$

where ν denotes the d.f. associated with the estimate of σ^{2}

To obtain some indication of the reliability of the estimates of the parameter confidence intervals in this nonlinear case, the sum of square contour for the 95% joint confidence region were plotted. These are presented for a run with a high sum of squares of residuals when the two parameter model was fitted to the data (Fig B.1) and for a run with a small sum of squares of residuals for the fitted model.(Fig. B.2)

The approximate 95% joint confidence region is given by,

$$S(T) \leq S(\hat{T})^{*}\left[1 + (p/n-p)\cdot F\ p,n-p,\right]$$

The shape of the joint confidence region is correct but the 95% confidence level is only approximate because of the nonlinearity of the model.

The contour plots are ellipsoid in shape and thus indicate there is no reason to doubt the reliability of the calculated 95% confidence intervals for the parameters. The three centre point replicate runs do not offer a true internal estimate of the pure error variance as each run has an individual H vs. A relationship. (i.e. each individual point is not a true replicate).

However, treating the data as such gives $Sp^2 = .54$ as an estimate of σp^2 when the sets of points at the cross sectional areas were treated as replicate sets.

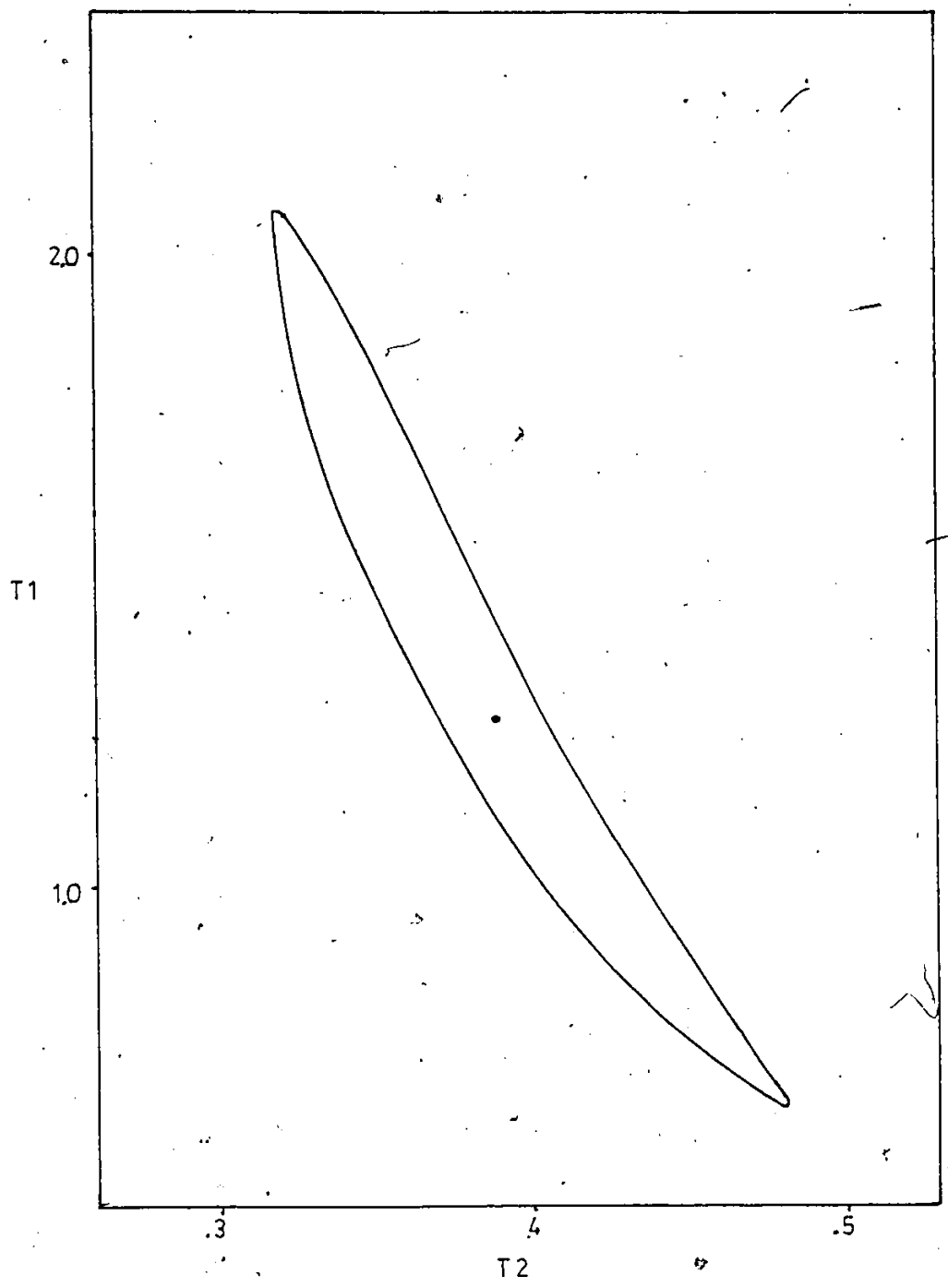

Figure B.1 Joint Confidence Region for Run 13 SofS > 18.95

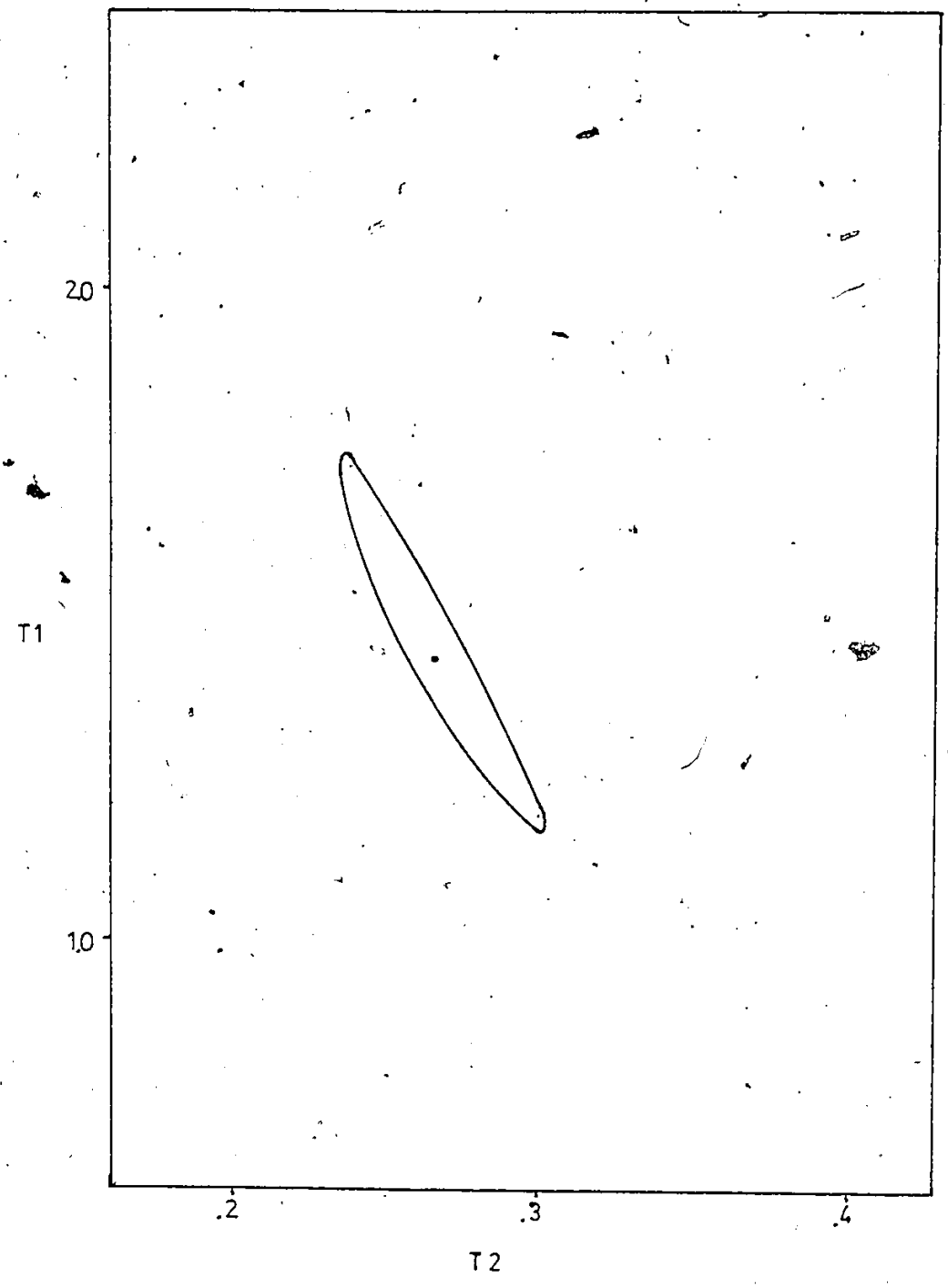

Figure B.2: Joint Confidence region for Run 1 SofS > 1.0

This allowed a quantitative lack of fit test to be performed.

$$R = \frac{\sum_{u=1}^{n} e_u^2 - Sp^2 \sum_{i=1}^{l} (m_i - 1)}{Sp^2} \Big/ (n-p-\nu p)$$

is compared to $F_{n-p-\nu p, \nu p, \alpha}$.

R can also be expressed as,

$$R = \frac{\sum_{u=1}^{n} (\bar{Y}_u - \hat{Y}_u)^2 \Big/ \{n-p- \sum_{i=1}^{l} (m_i - 1)\}}{\sigma p^2}$$

If the value of R is larger than the upper percent value of F, then the fitted model is said to display "lack of fit".

The experimental results yielded an R value of 1.80. The appropriate 95% F was F (93,16,.05) = 1.77. As this test is only approximate for nonlinear models, "lack of fit" is not apparant from this test.

The four parameter model,

$$H = (T1/rpm + T2 \cdot Q) \exp((T3 \cdot \phi d + T4 \cdot Q)/A)$$

yeilded a sum of squares of residuals of 89.88 when fitted to the data. The quantitative lack of fit test

$$R = \frac{89.88 - .54\ 16}{112-4-16} \Big/ .54 = 1.64$$

F (112-4-16, 16 ,.05) = 1.774, R < F . Therefore there is no evidence of lack of fit from this test.

Non Linear LeastSquares

$$H = T1 \exp(T2/A) + e$$

is a non linear function. Linearization of this model results in the transformation of the associated random error term , e .

$$\ln H = \ln T1 + T2/A + \ln e$$

Keeping the associated random error term constant is necessary when using least squares analysis whether it be of the linear or non linear form. If the associated random error term is of the form where a transformation will result in a constant random error over the entire data set then a least squares analysis may be performed. If not, then least squares analysis must be performed using the form of the function with which the associated random error is constant.

Minimizing the Sum of Squares of Residuals for a Nonlinear Model

There are several methods available. These include Steepest Descent, Grid Search, Gauss Method, Marqquart's comprimise , Box Modified Gauss, and direct search methods such as Powell's method.

For the model $H = T1 \exp(T2/A)$, the gauss method (also known as Gauss-Newton or Linearization method) was chosen to fit the model to the experimental data.

The method is as follows,

For the general non linear model,

$$yu = f(\underline{\zeta u}, \underline{\theta}) + \varepsilon u$$

yu- the expected response value (or the value predicted by the model) for the u^{th} run;

ζu vector of values of the operating variables for the u^{th} run $= (\zeta u_1, \zeta u_2, \ldots\ldots \zeta uk)$

$\theta = (\theta_1, \theta_2, \theta_3, \ldots\ldots \theta p)^T$ = vector of p parameters in the model

f response function

Expanding $f(\underline{\zeta u}, \underline{\theta})$ in a Taylors series expansion about θ_0 and neglecting second and higher order terms:

$$f(\underline{\zeta u}, \underline{\theta}) \simeq f(\underline{\zeta u}, \underline{\theta u}) + \sum_{j=1}^{p} (\theta j - \theta j_0) \left[\frac{\partial f(\underline{\zeta u}, \underline{\theta})}{\partial \theta j} \right]_{\theta = \theta_0} + eu$$

this is a linear model with form,

$$Zu = \sum_{j=1}^{p} \beta j_0 X j_0 + eu$$

where $Zu = yu - f(\underline{\zeta u}, \underline{\theta_0})$

$$\beta j_0 = \theta j - \theta j_0$$

$$X j_0 = \left[\frac{\partial f(\underline{\zeta u}, \underline{\theta})}{\partial \theta j} \right]_{\theta = \theta_0} \quad \text{a matrix}$$

β's are obtained by linear least squares which provides an estimate of $(\theta j - \theta j_0)$'s

Thus given data $(\underline{\zeta}u, yu)$, $u=1,2,3....n$

$$Z = \underline{X}_0\underline{\beta}_0 + \underline{e}$$

where $Z = \begin{bmatrix} y_1 - f(\zeta_1,\theta_0) \\ \vdots \\ yn - f(\zeta n,\theta_0) \end{bmatrix}$ n x 1 matrix

$$\beta_0 = \begin{bmatrix} \theta_1 - \theta_{10} \\ \vdots \\ \theta p - \theta p_0 \end{bmatrix}$$ p x 1 matrix

$$X = \begin{bmatrix} \left.\frac{\partial f(\zeta_1,\theta)}{\partial\theta_1}\right|_{\theta_0} & \cdots & \left.\frac{f(\zeta_1,\theta)}{\partial\theta p}\right|_{\theta_0} \\ \vdots & & \vdots \\ \left.\frac{f(\zeta n,\theta)}{\partial\theta_1}\right|_{\theta_0} & \cdots & \left.\frac{f(\zeta n,\theta)}{\partial\theta p}\right|_{\theta_0} \end{bmatrix}$$

n x p matrix

and $\hat{\beta} = (X_0^T X_0)^{-1} X_0^T Z$

and the new estimate of $\underline{\theta}$ is given by

$$\theta_1 = \theta_0 + \hat{\beta}_0$$

this is repeated until both $S\underline{\theta}$ and $\underline{\theta}$ converge.

Also used was a modified Gauss routine available through the University of Ottawa computing centre as SAS SIMNLIN which uses a scaled advance in the Gauss direction,

$$\hat{\beta} = 1/1+\lambda\{(X_0^T X_0)^{-1} X_0^T Z\}$$

Quantitative Lack Of Fit Test Applied to the Cylindrical Data Models

An sp^2 value of .0218 was determined from the replicate runs performed. Four replicate runs were performed at Q=1500 ml/min, and one replicate run at each of Q=1000 and Q=2000 was performed.

When models were fitted to the data at Q=1000 and Q=2000 ml/min, it was felt that the single replication did not provide an adequate estimation of the pure error variance. Therefore, the estimate of the pure error variance obtained from the whole data set was used.

Therefore a T-test as recommended by Draper and Smith (24), was performed. The R-test as applied to the models fitted to the square mixer data was not applicalble in this case as now the variance was estimated using replicates from all three flowrates and not just the throughput to which a model was being fitted.

$$T = \frac{\sum_{u=1}^{n} eu^2 /(n-p)}{\sigma E^2}$$

σE^2 is an external estimate of the variance

and is compared to $F_{n-p,\nu sp^2}$

where ν is the degree of freedom associated with the estimate of sp^2

In this case the estimate of the variance from the entire cylindrical mixer data set is not as reliable as would be an estimate obtained from many replicates at each of the throughputs investigated.

Appendix C

RESIDUAL PLOTS FOR H=(T1/RPM+T2

Q)EXP(T3ϕD/A),SQUARE MIXER

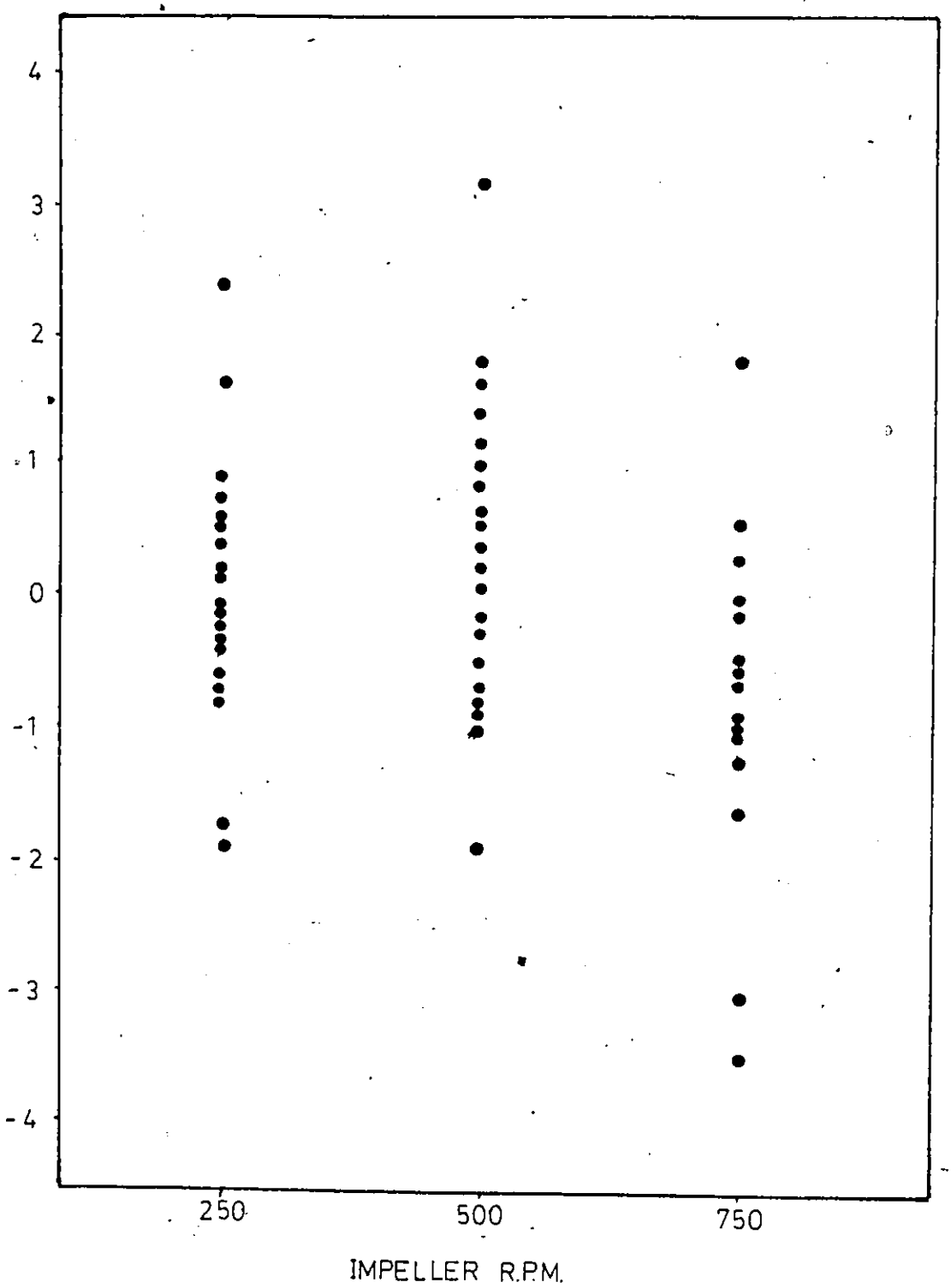

Figure C.1: Residuals vs Impeller RPM
$H=(T1/rpm+T2\cdot Q)\ \exp(T3\cdot \phi d/A)$

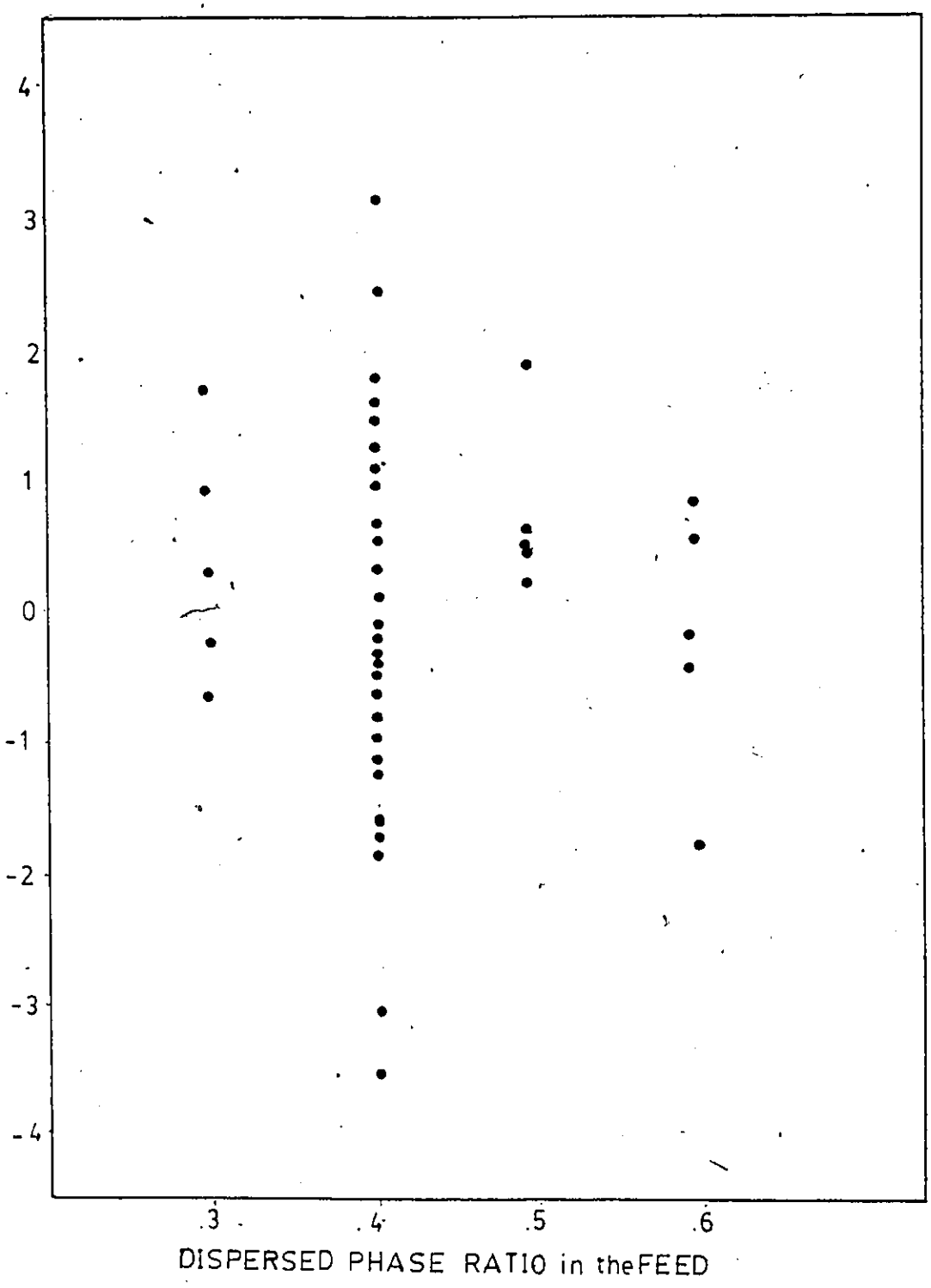

Figure C.2: Residuals vs Dispersed Phase Ratio
$H=(T1/rpm+T2\cdot Q)\ \exp(T3\cdot \phi d/A)$

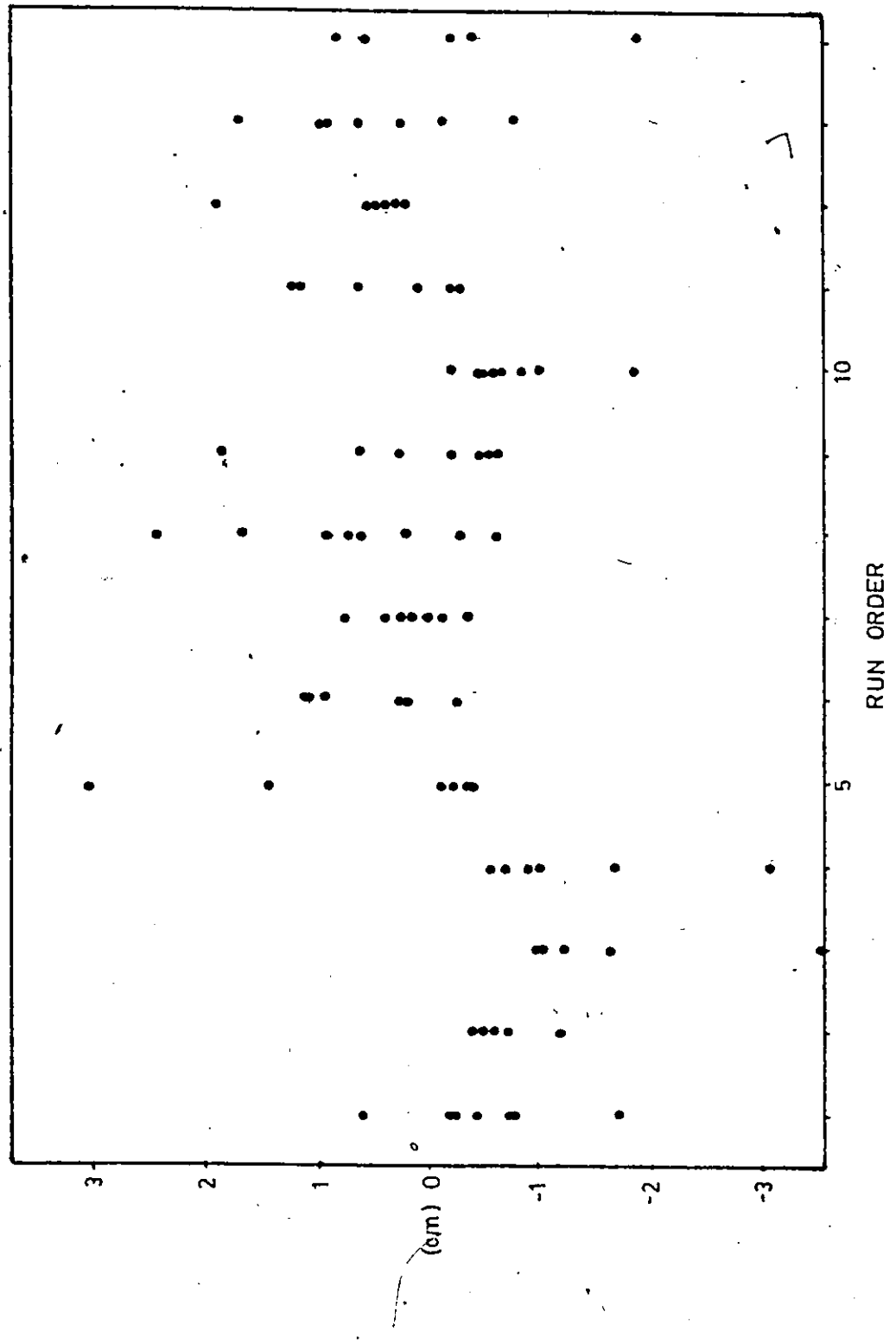

Figure C.3: Residuals vs run Order
$H=(T1/rpm+T2\cdot Q)\ \exp(T3\cdot \phi d/A)$

Appendix D

PLOTS OF LN H VS 1/A FOR THE CYLINDRICAL DATA

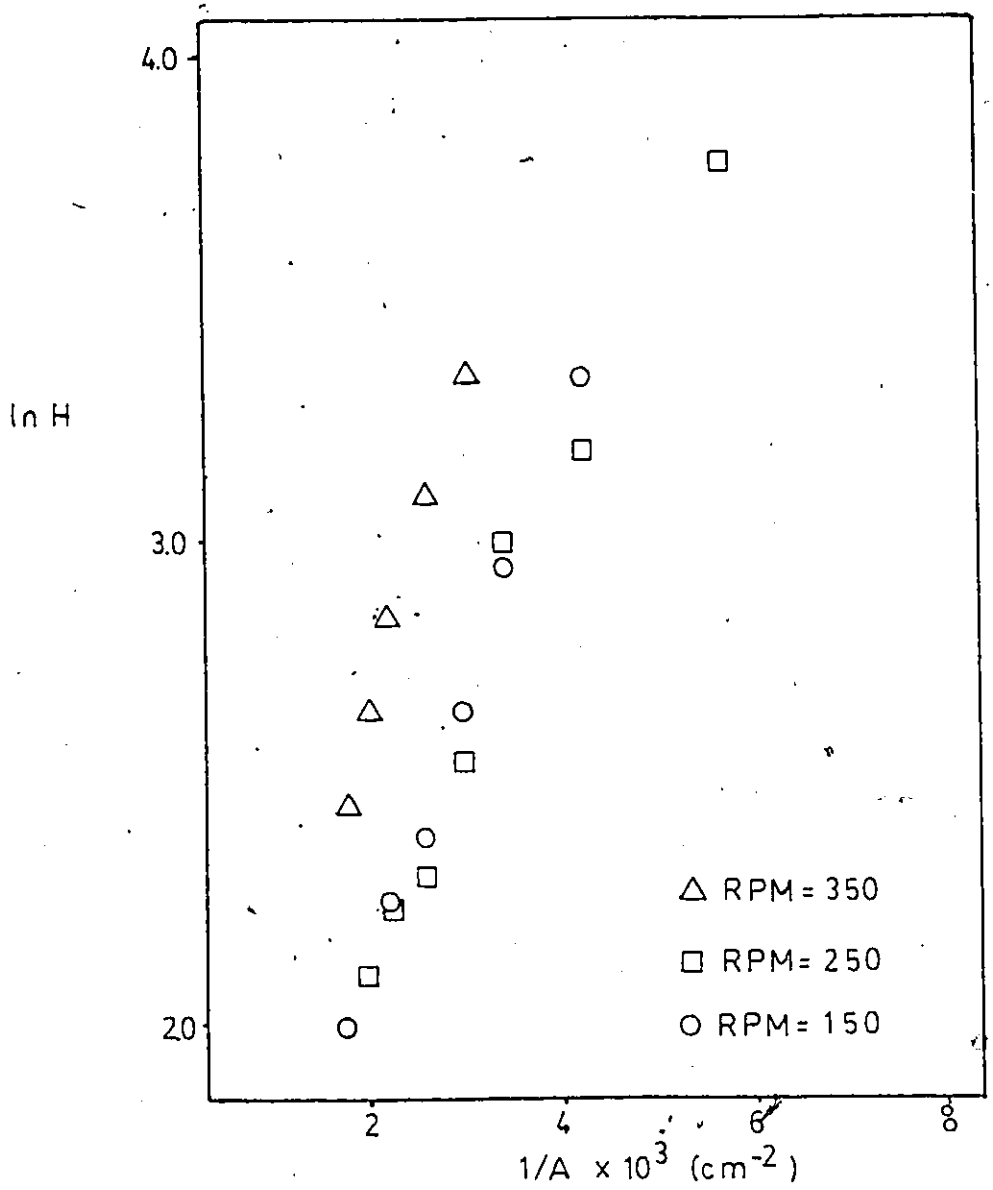

Figure D.1: ln H vs 1/A Q=2000 ϕd=.6

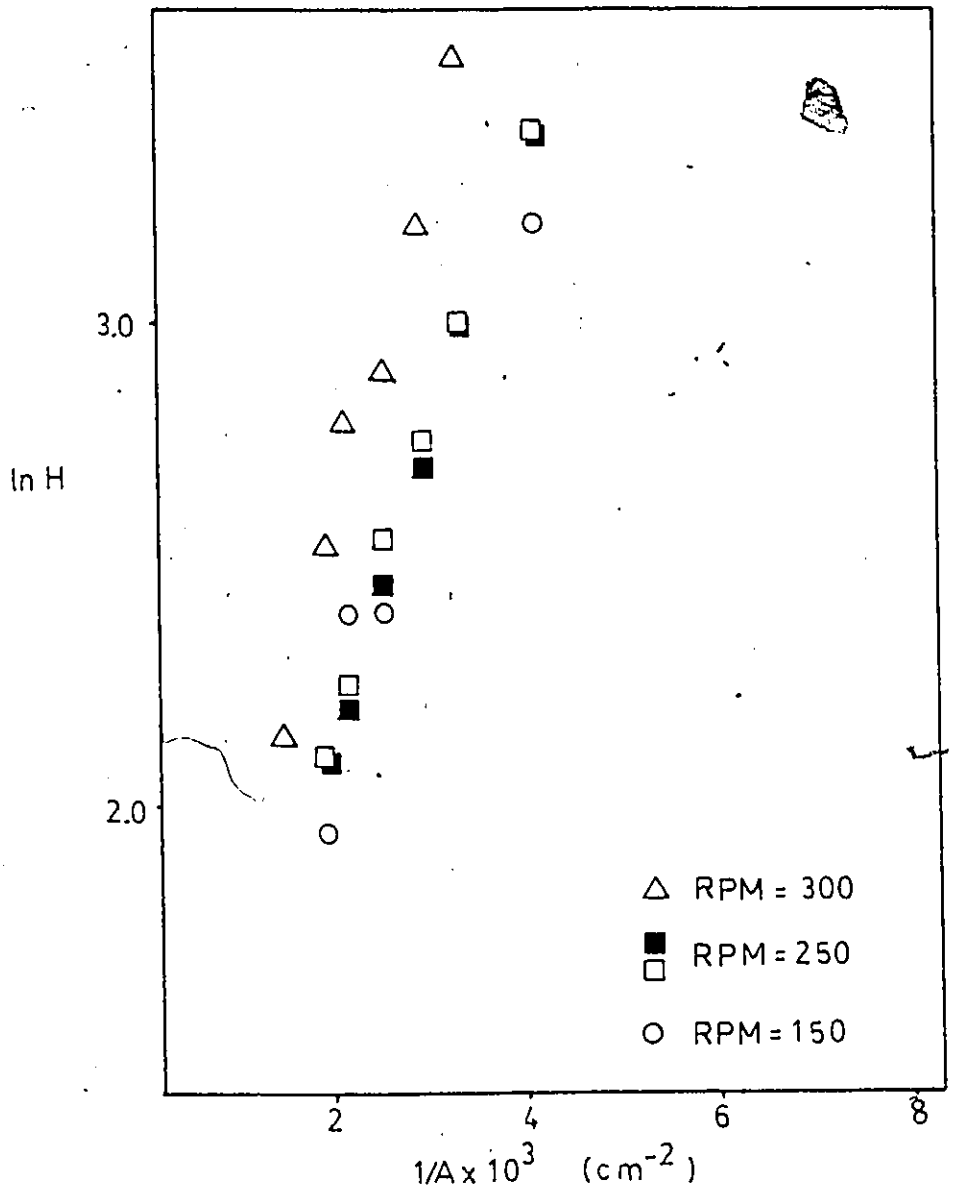

Figure D.2: ln H vs 1/A, Q=2000 $\phi d \leq .5$

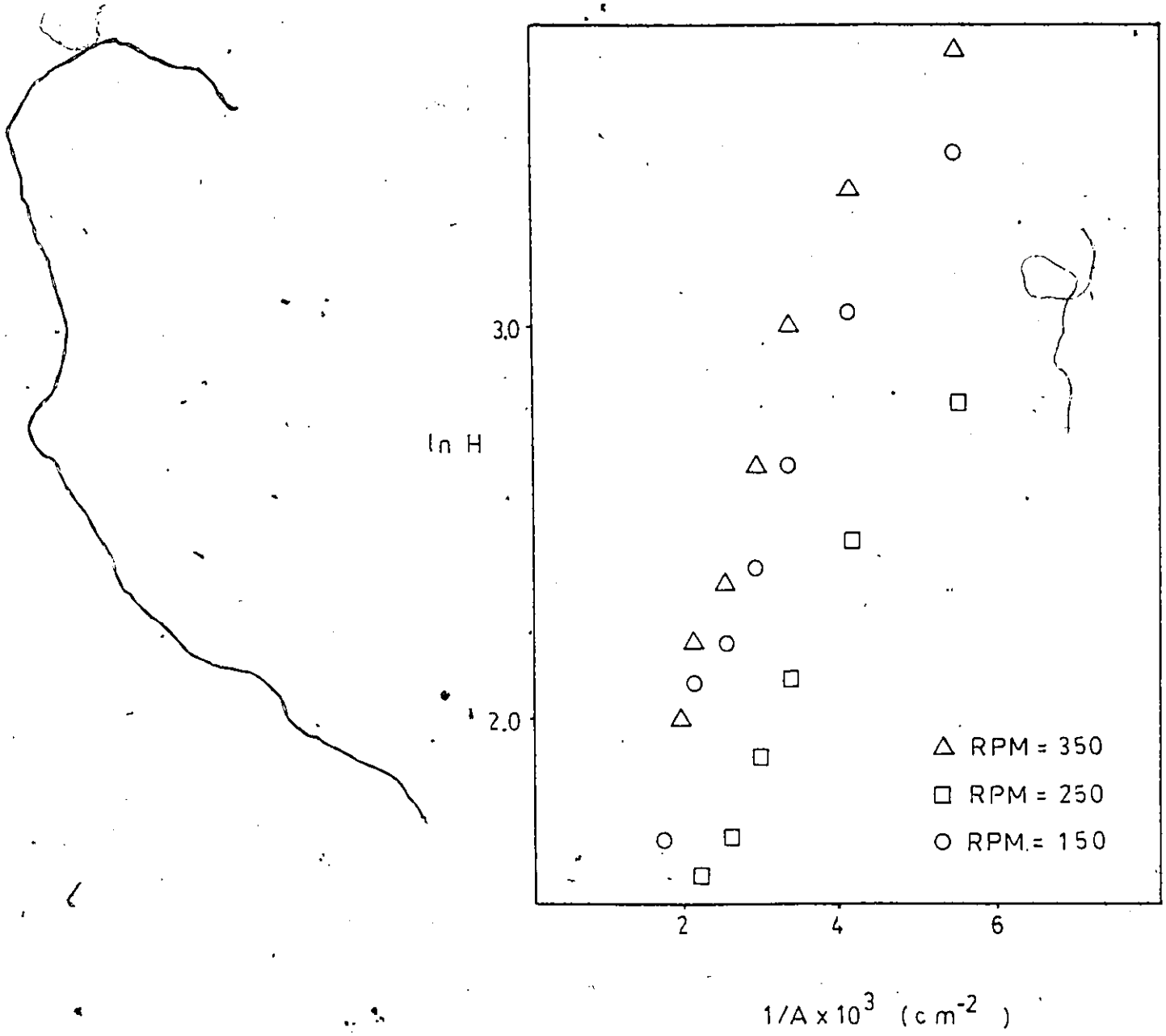

Figure D.3: ln H vs 1/A, Q=2000 ϕd=.4

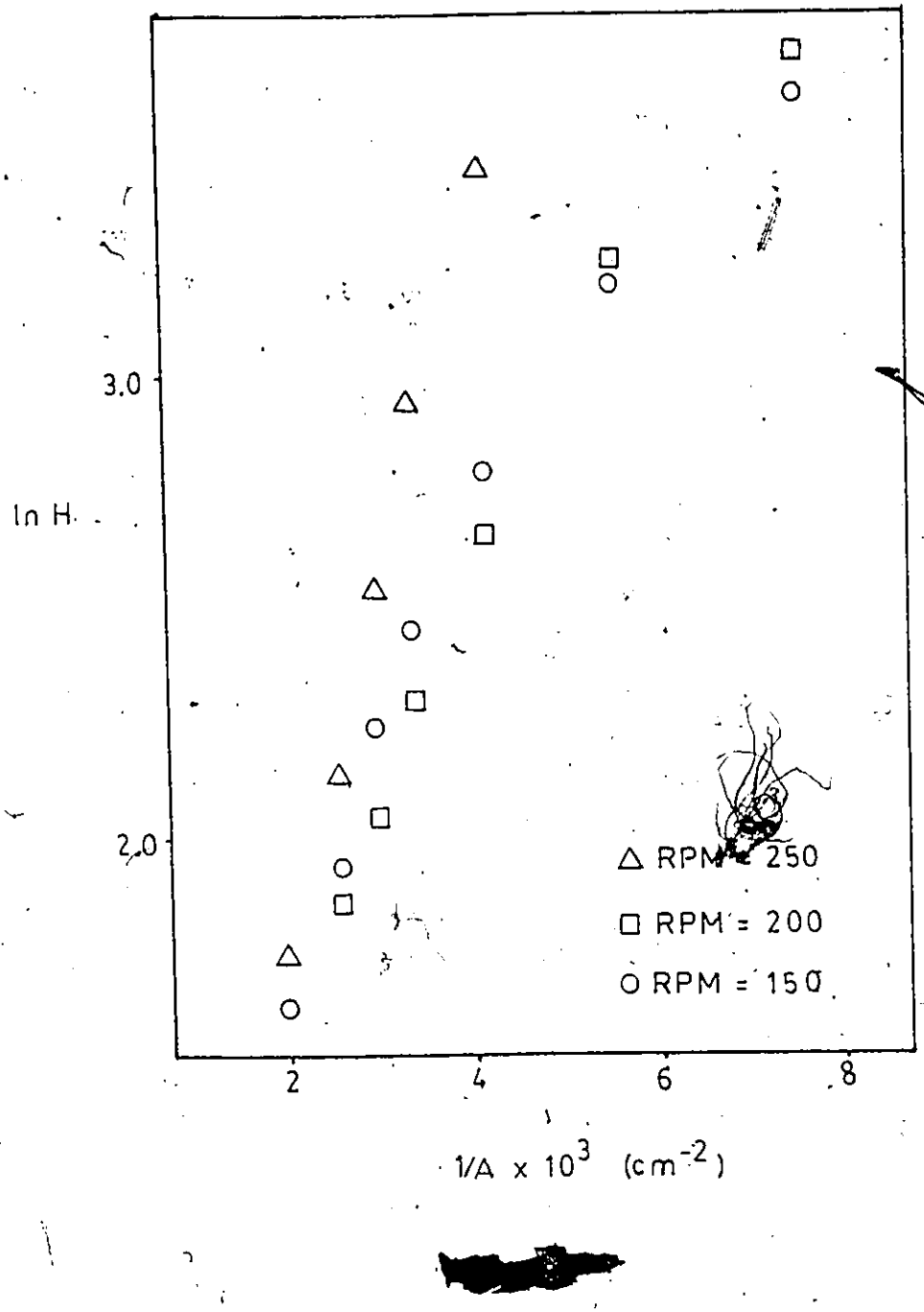

Figure D.4: ln H vs 1/A, Q=1500 ϕd=.6

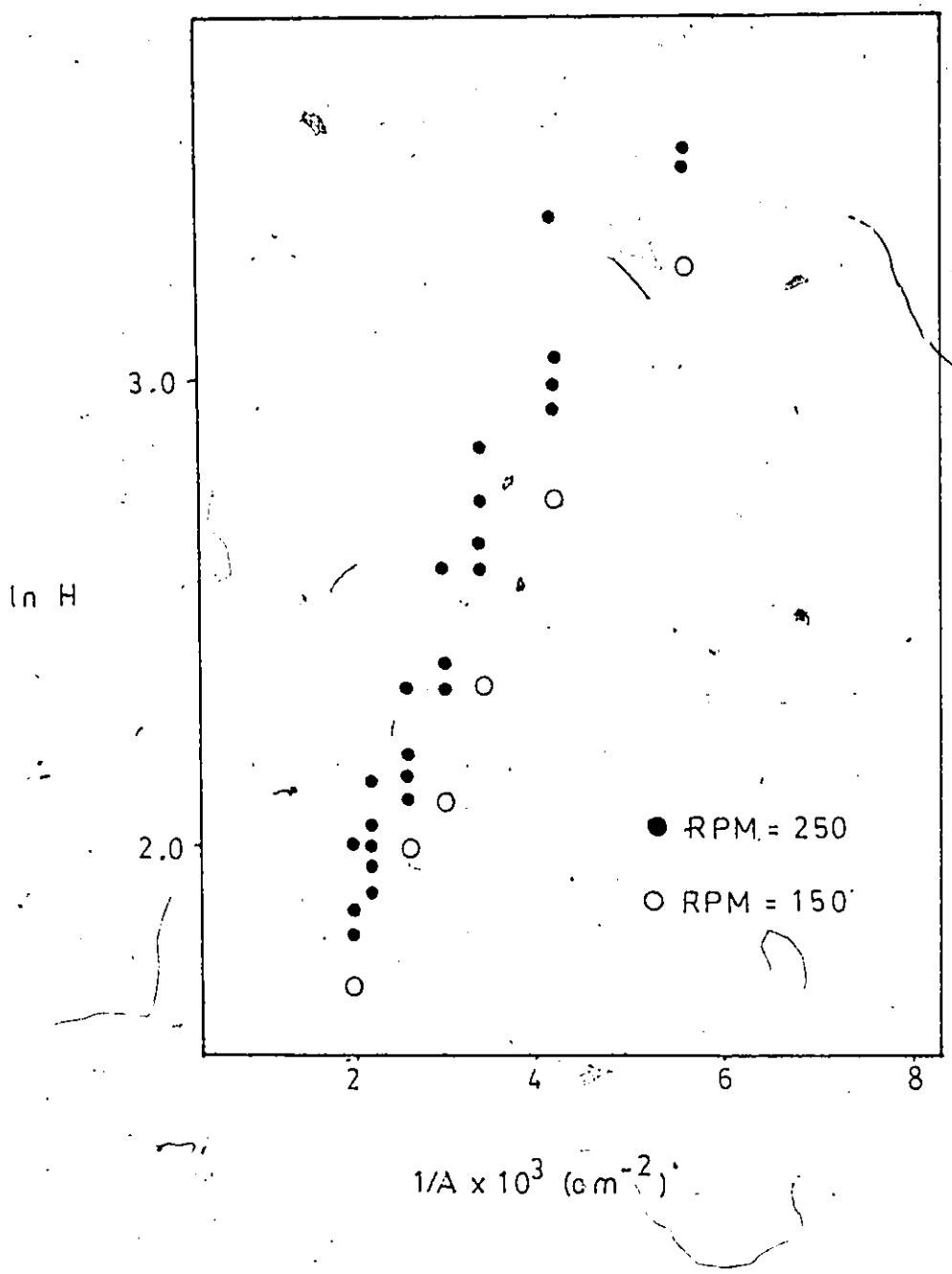

Figure D.5: ln H vs 1/A, Q=1500 $\phi d=.5$

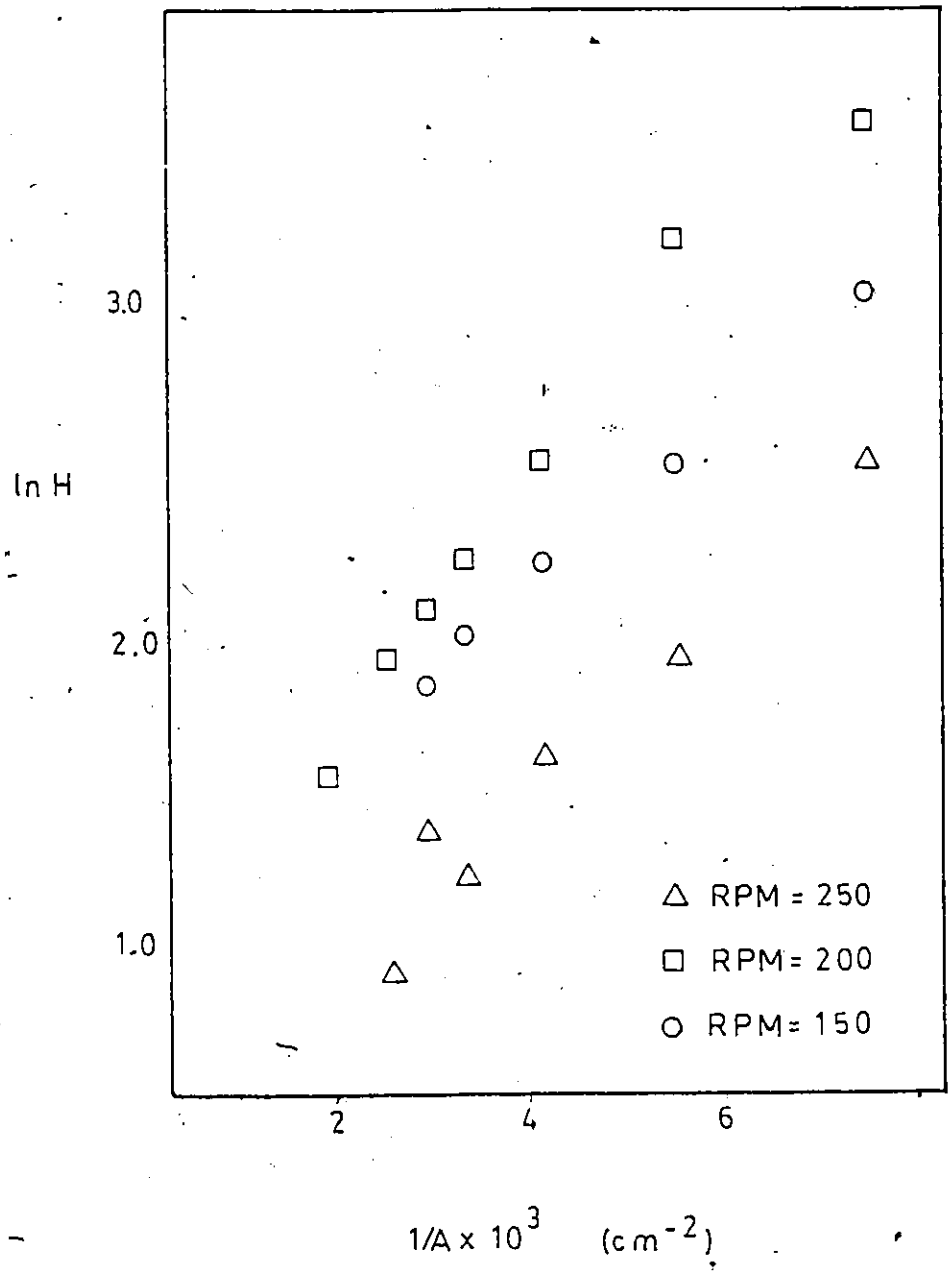

Figure D.6: ln H vs 1/A, Q=1500 ϕd=.4

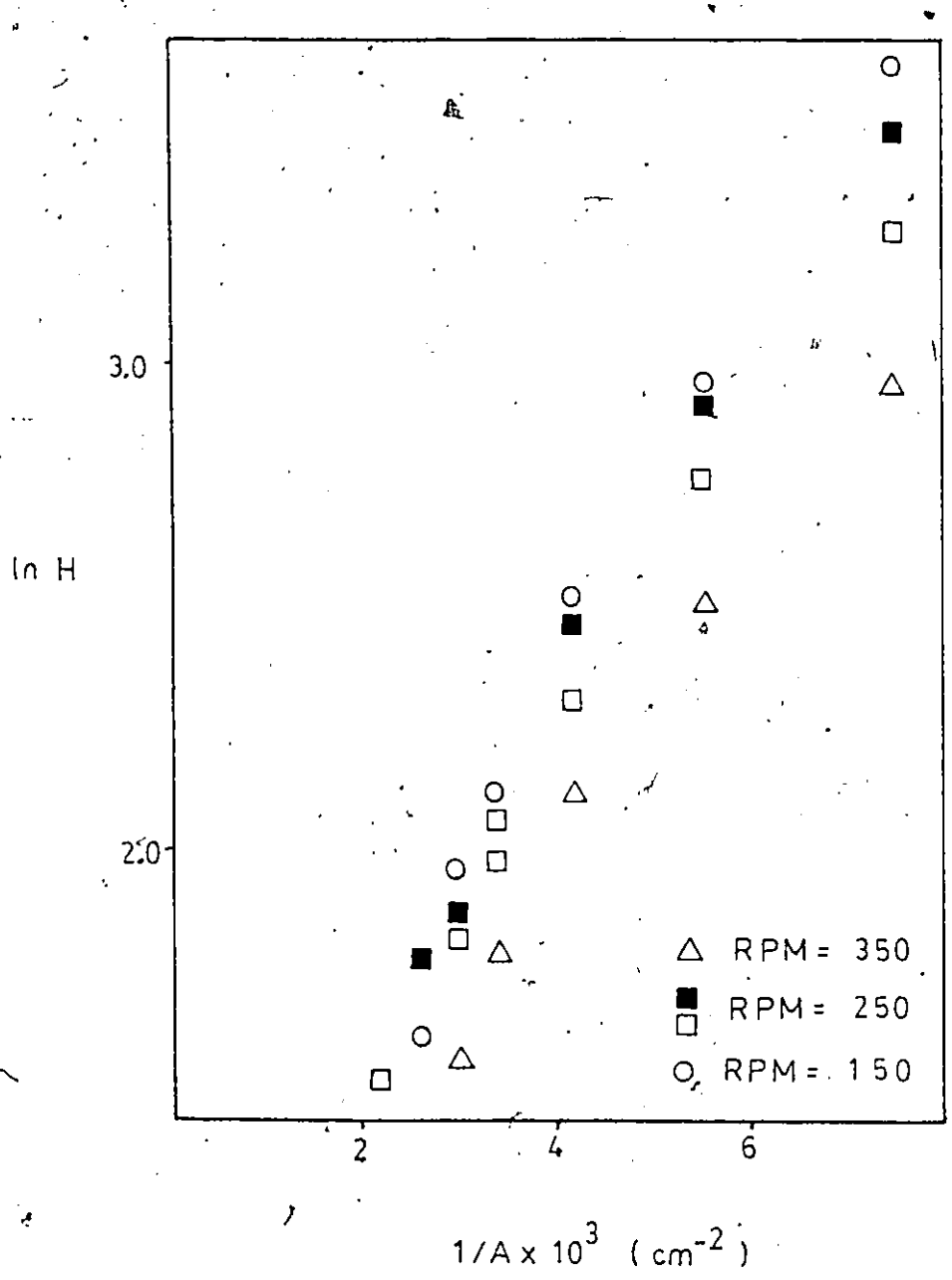

Figure D.7: ln H vs 1/A, Q=1000 ϕd=.6

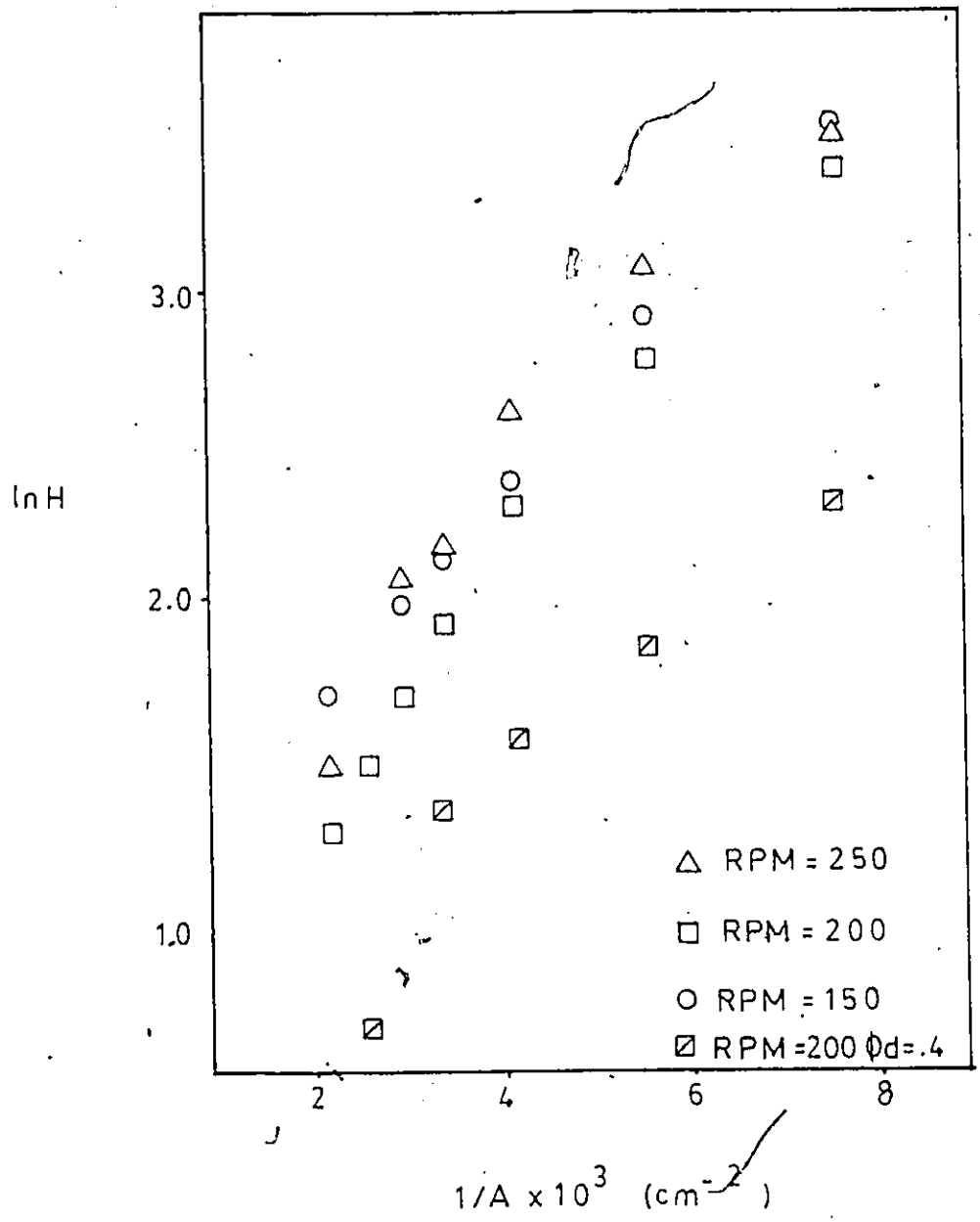

Figure D.8: ln H vs 1/A, Q=1000 ϕd=.5,.4

Appendix E

PLOTS OF LN H VS LN (1/A) FOR THE CYLINDRICAL DATA

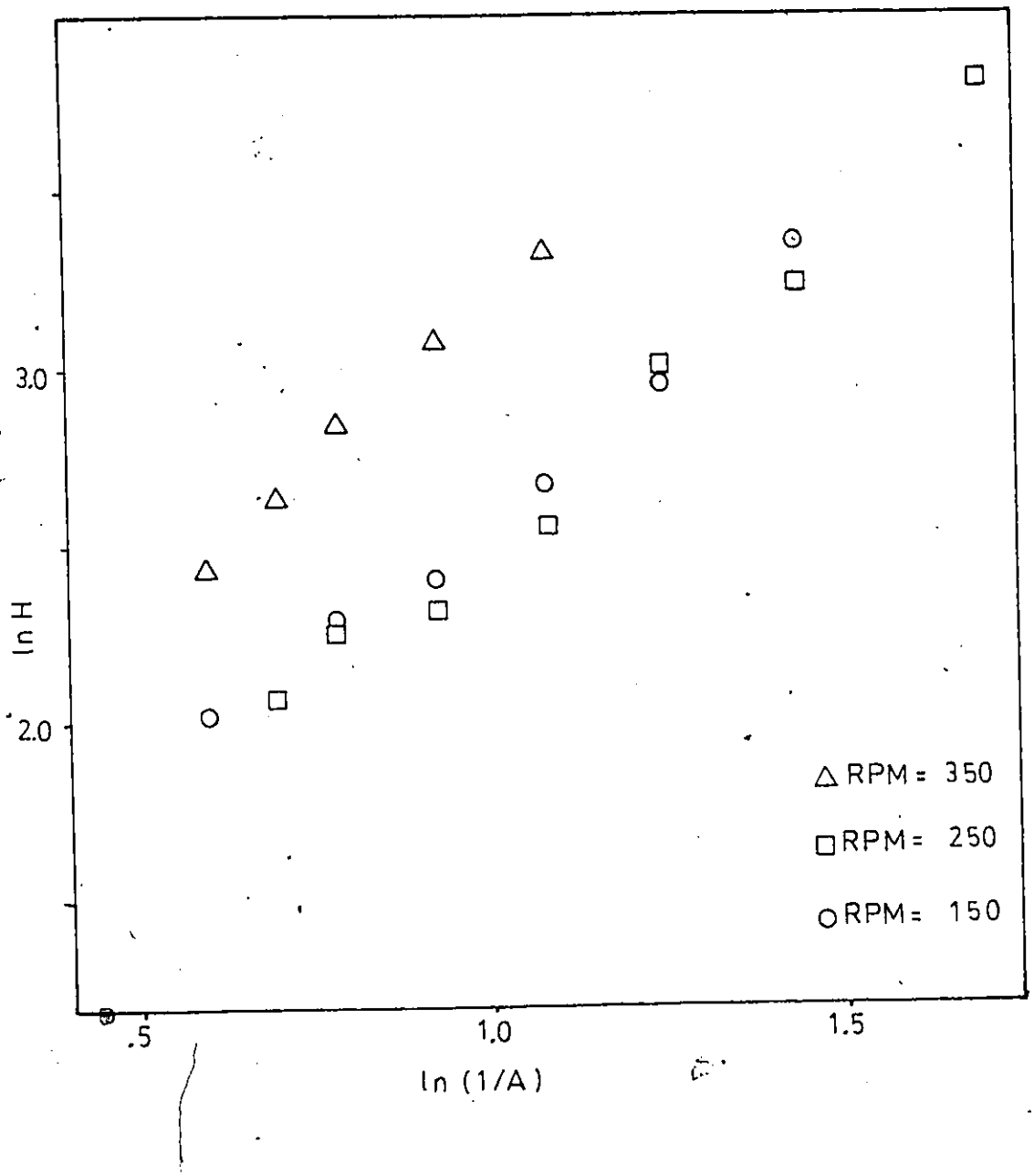

Figure E.1: ln H vs ln(1/A), Q=2000 ϕd=.6

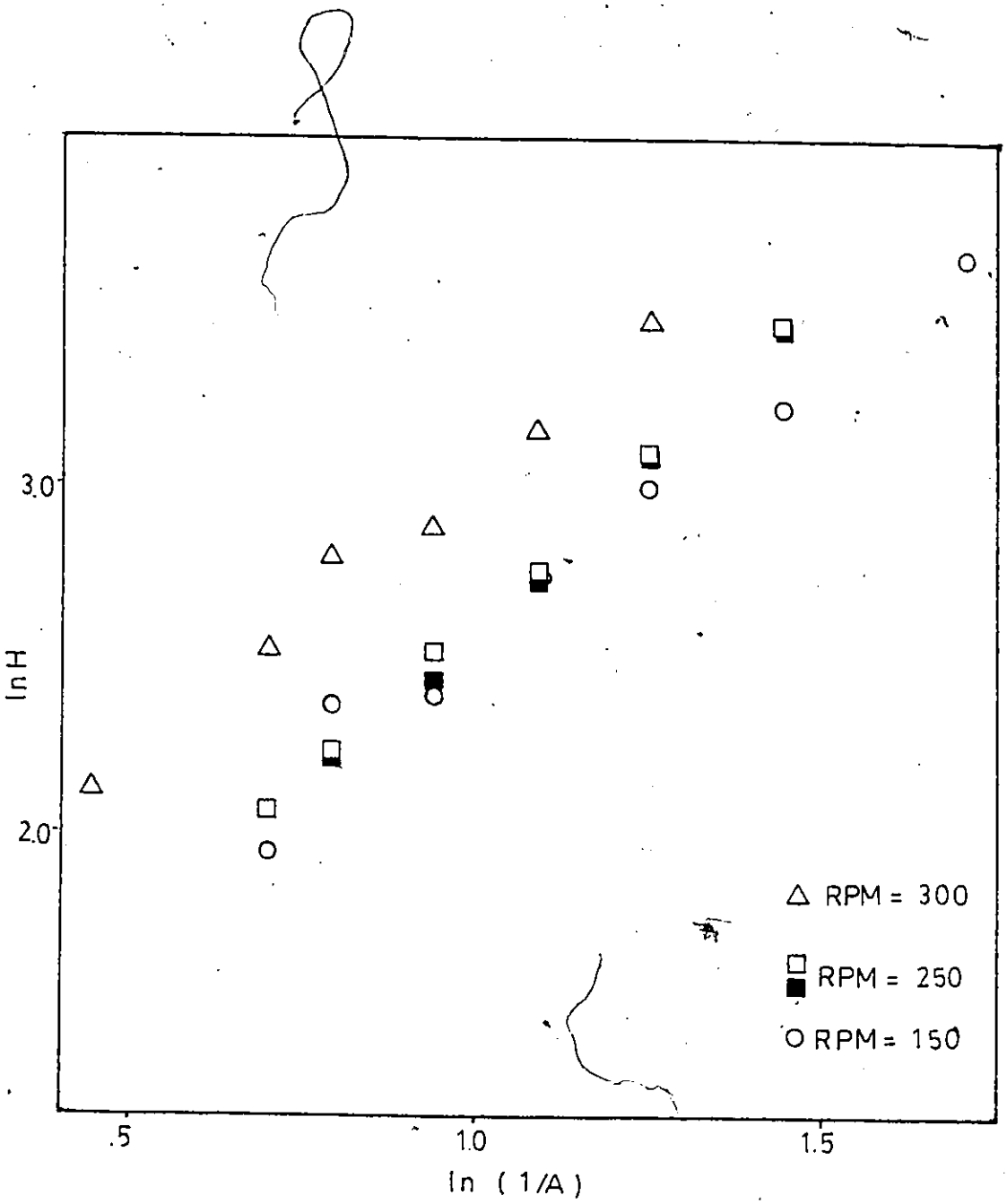

Figure E.2: ln H vs ln(1/A), Q=2000 ϕd=.5

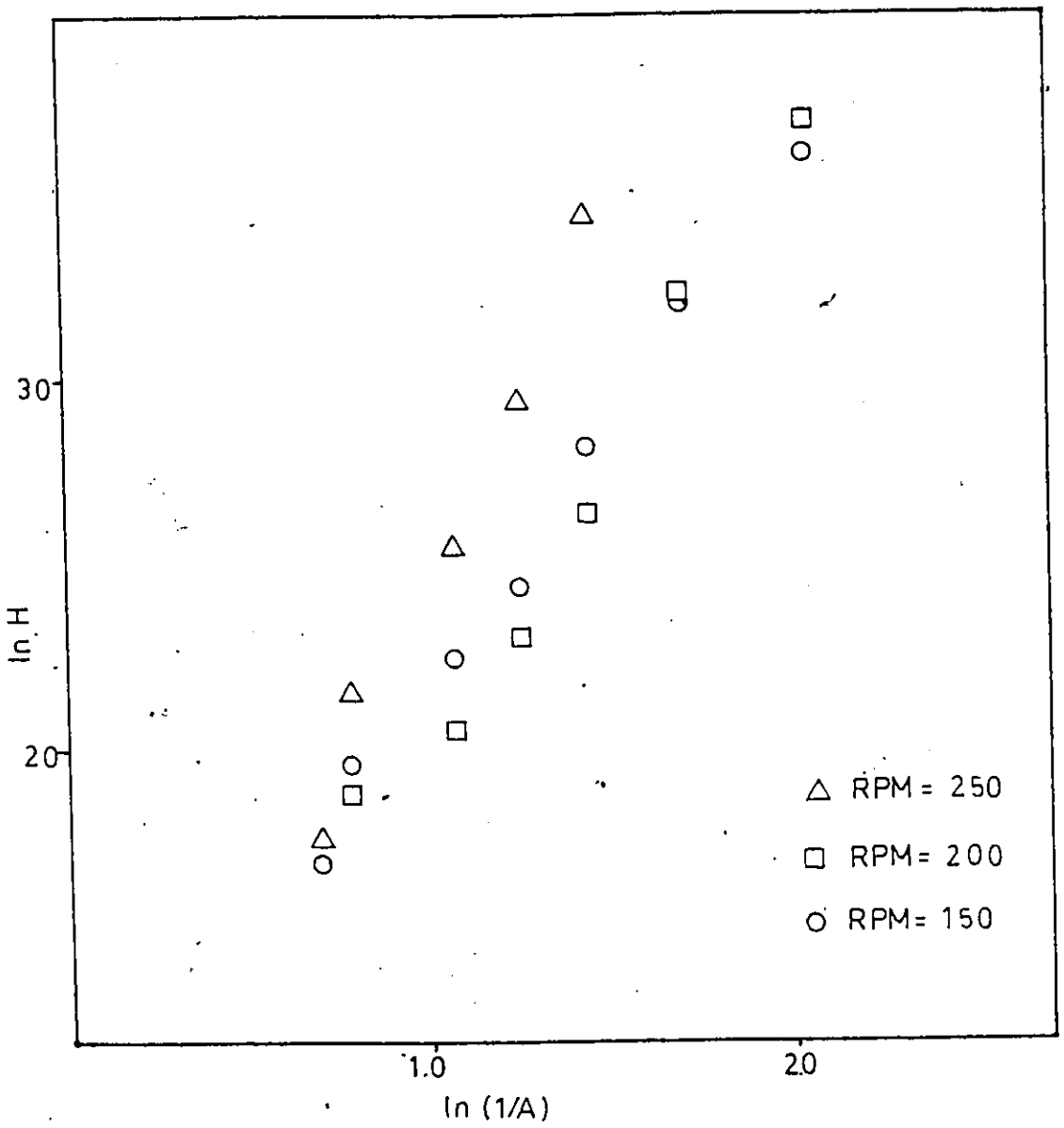

Figure E.3: ln H vs ln(1/A), Q=2000 ϕd=.4

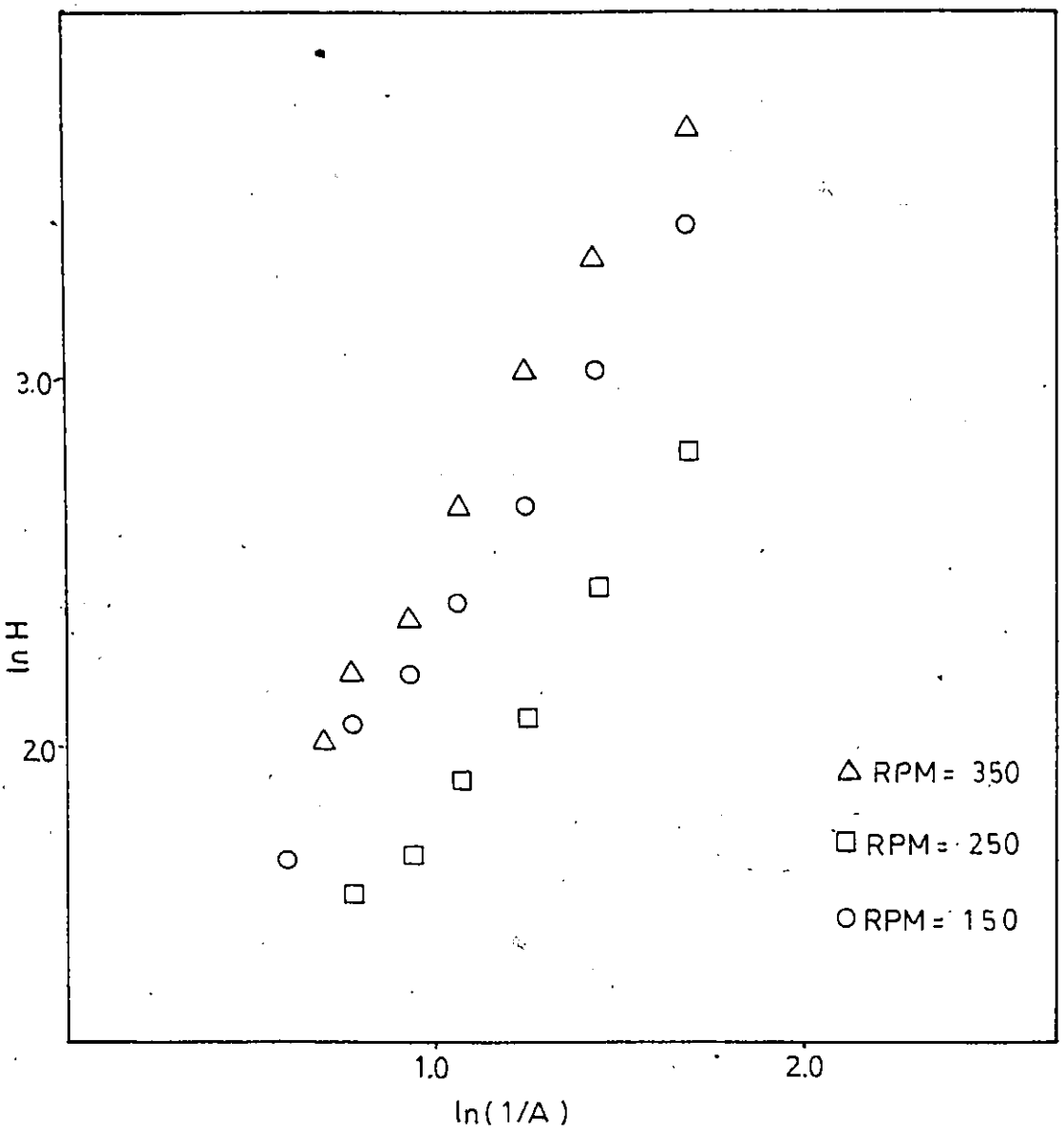

Figure E.4: ln H vs ln(1/A), Q=1500 ϕd=.6

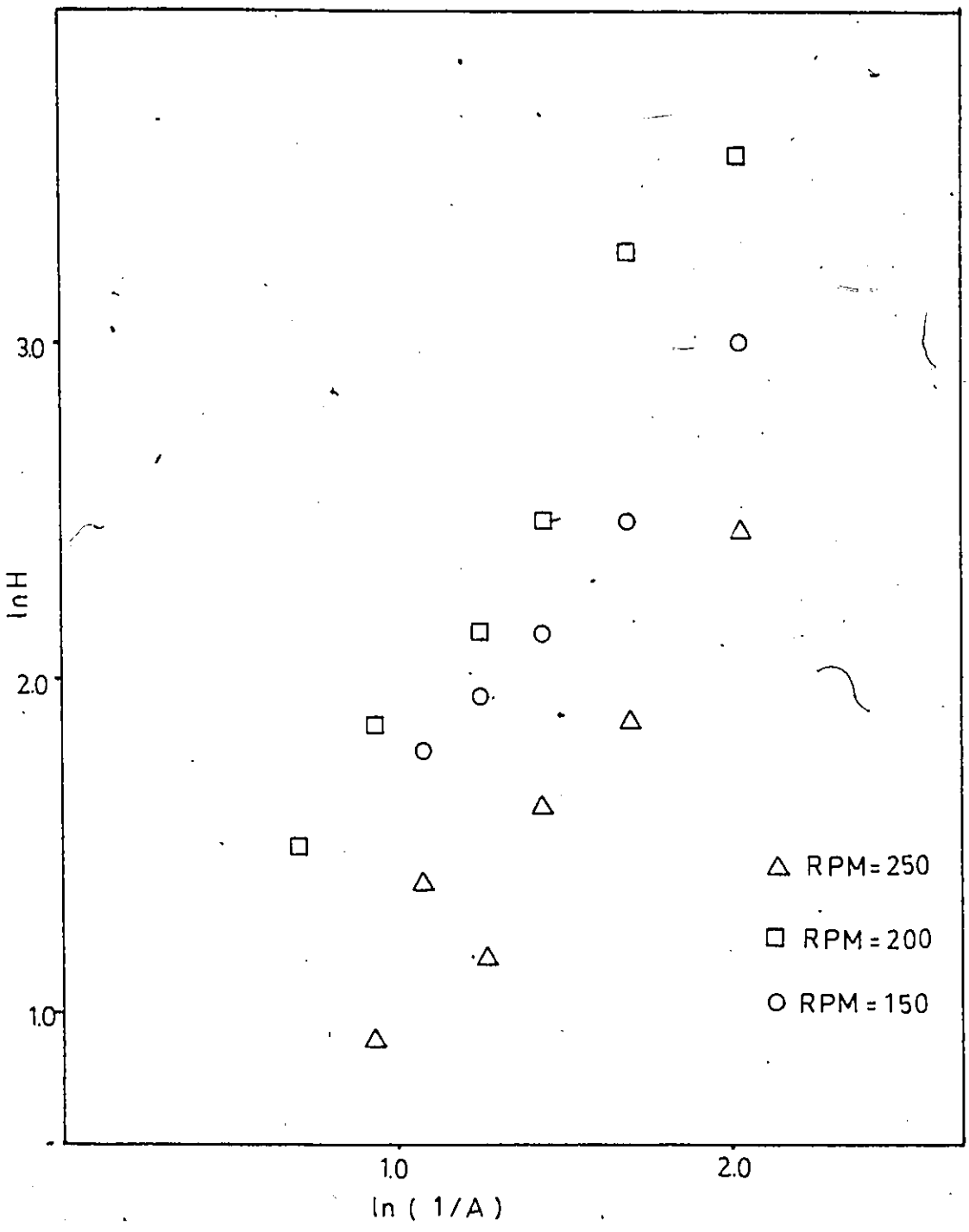

Figure E.5: ln H vs ln(1/A), Q=1500 ϕd=.4

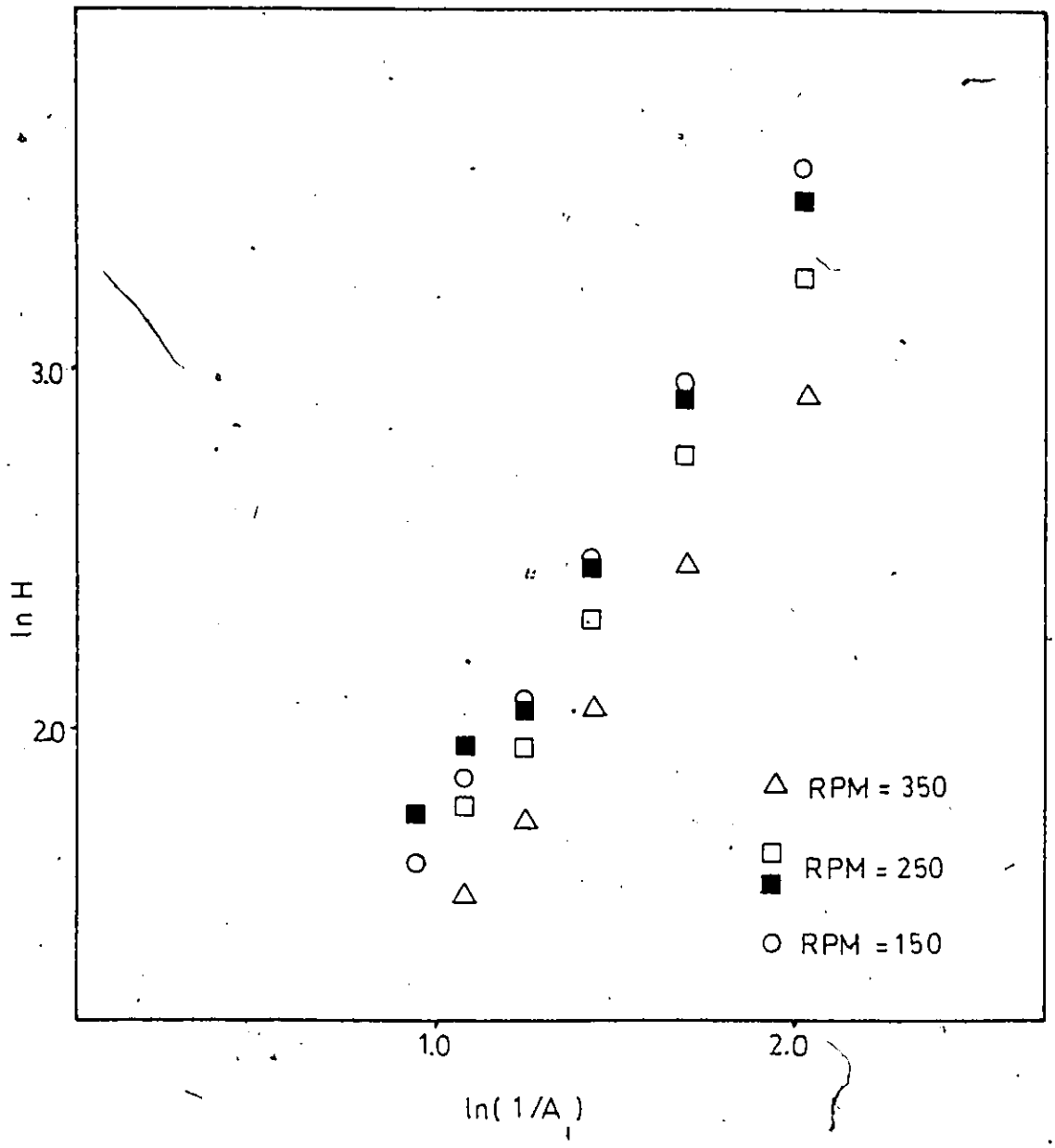

Figure E.6: ln H vs ln(1/A), Q=1000 ϕd=.6

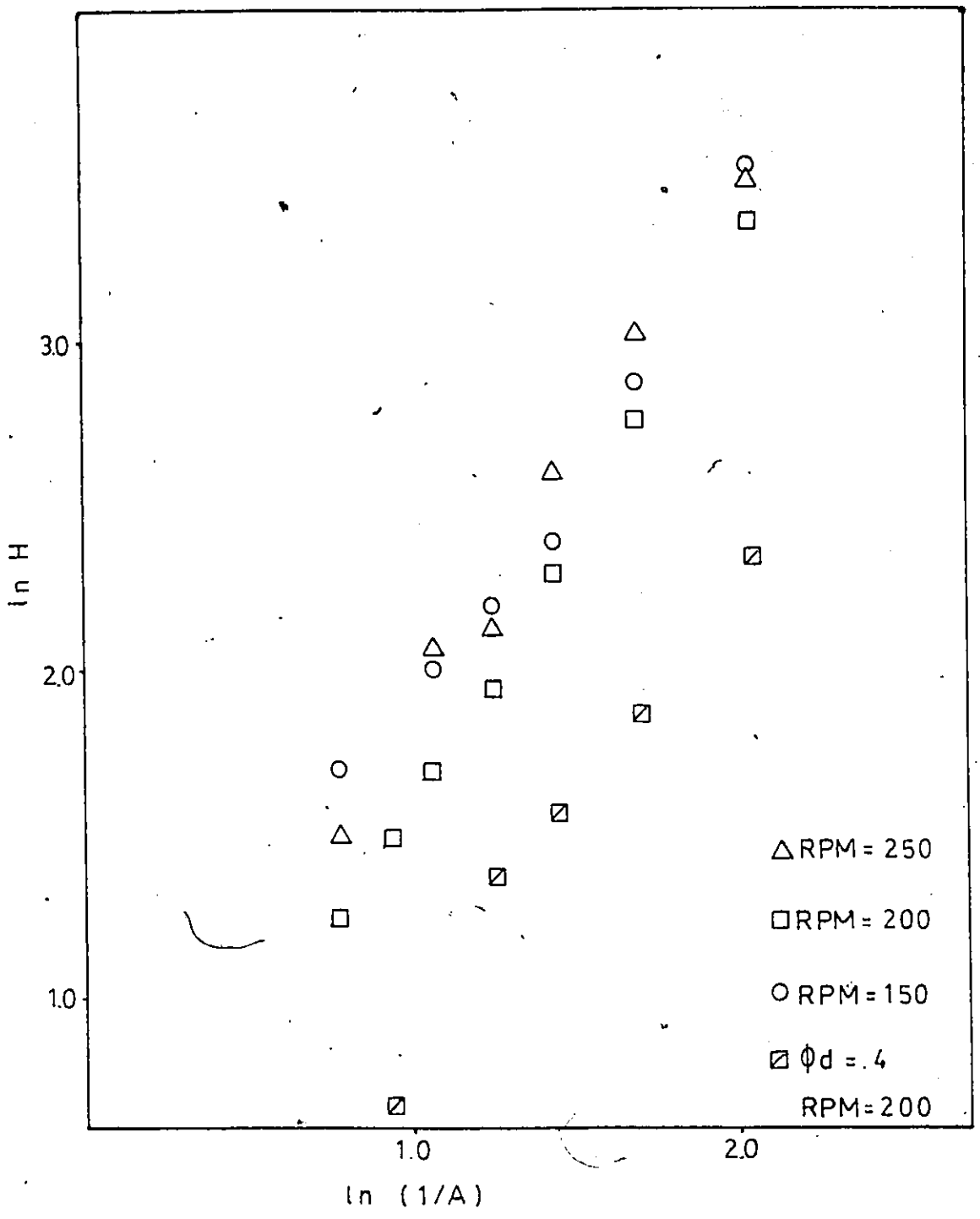

Figure E.7: ln H vs ln(1/A) Q=1000 ϕd=.5,.4

Appendix F

PLOTS OF V/Q VS H FOR THE CYLINDRICAL DATA

Vieler, Glasser, and Bryson proposed using $V/Q = aH + b$ to represent their continuous settler results. This linear equation can be rearranged.

using $V = AH$

$AH/Q = aH + b$

or $H(A/Q - a) = b$

$H = b/(A/Q-a)$

or $1/H = (A/Q - a)/b$

Q is constant for an individual run. Therefore,

$1/H = mA + b$

the equation of a straight line. Plotting 1/H vs A for the cylindrical data did not result in straight lines. This can be seen in the first plot in this appendix.

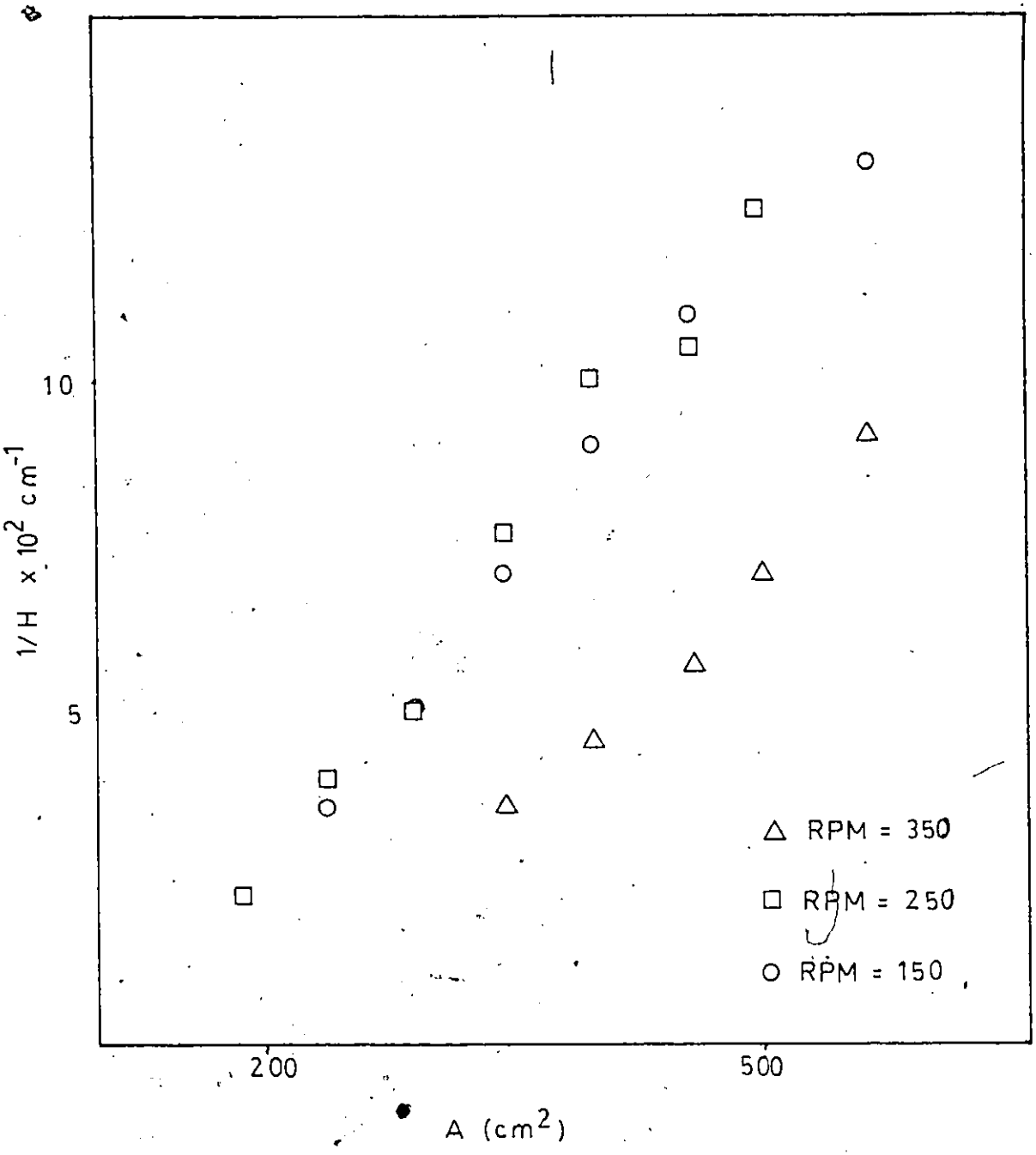

Figure F.1: 1/H vs A, Q=2000 ϕd=.6

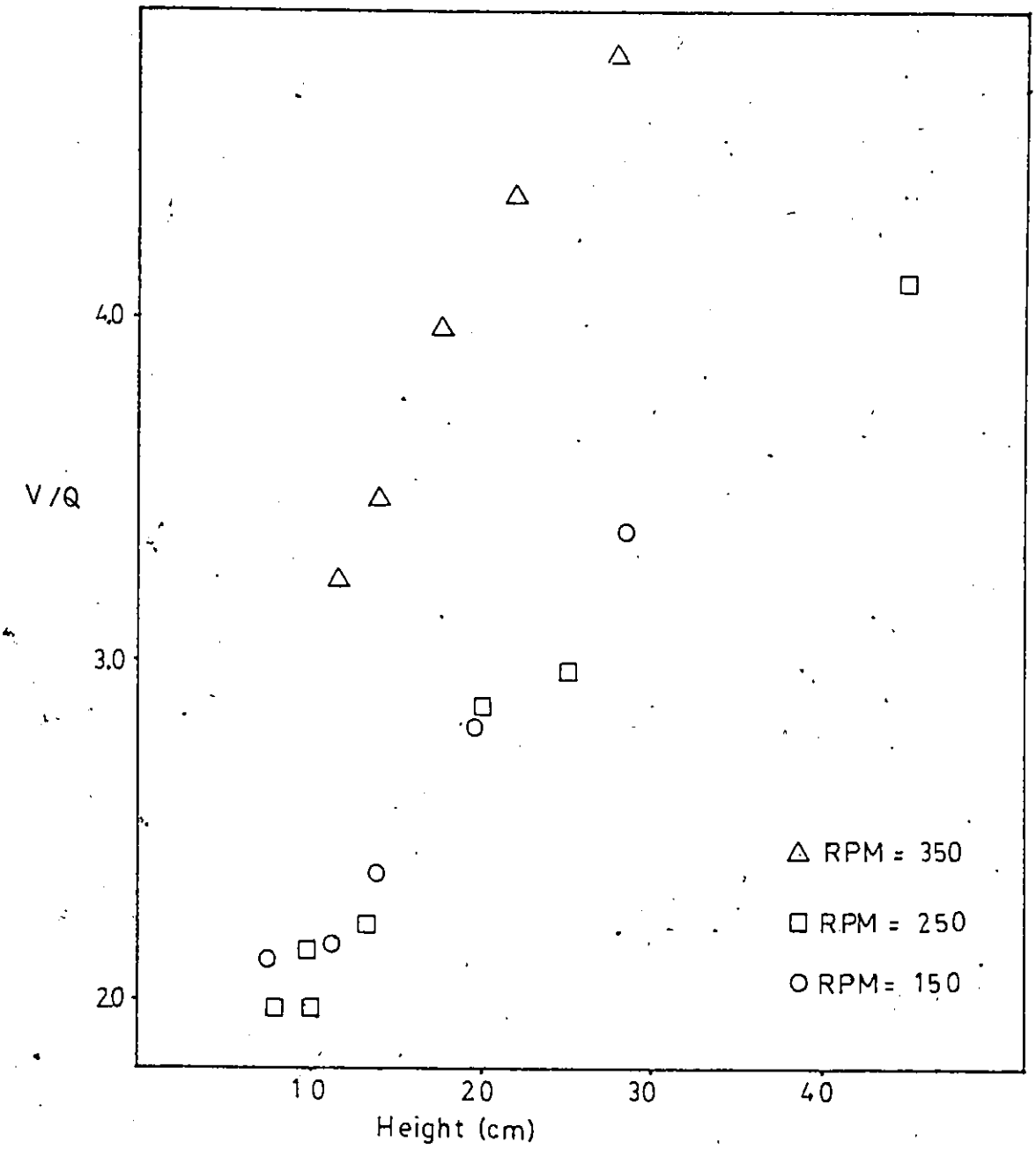

Figure F.2: V/Q vs H, Q=2000 ϕd=.6

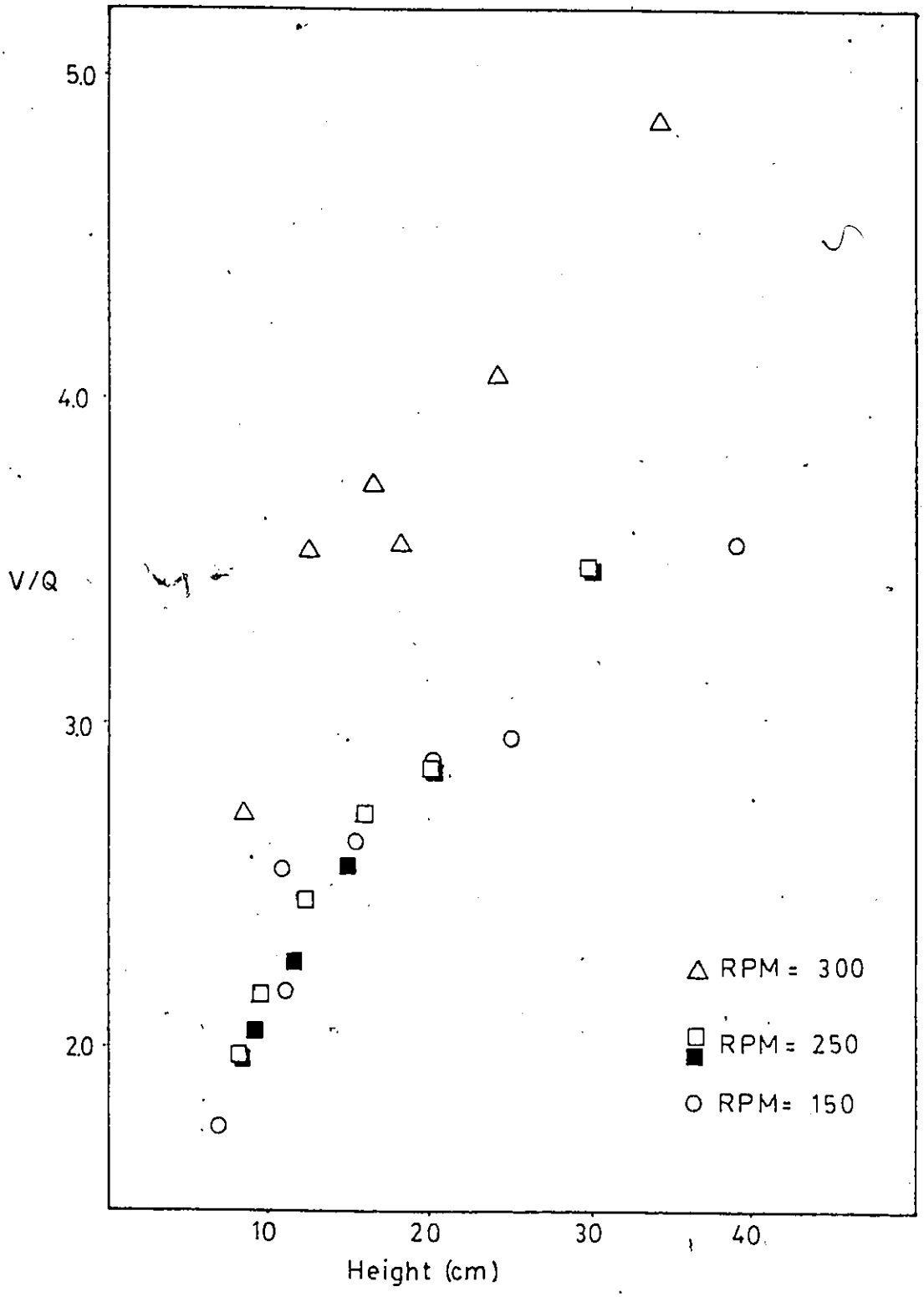

Figure F.3: V/Q vs H, Q=2000 ϕd=.5

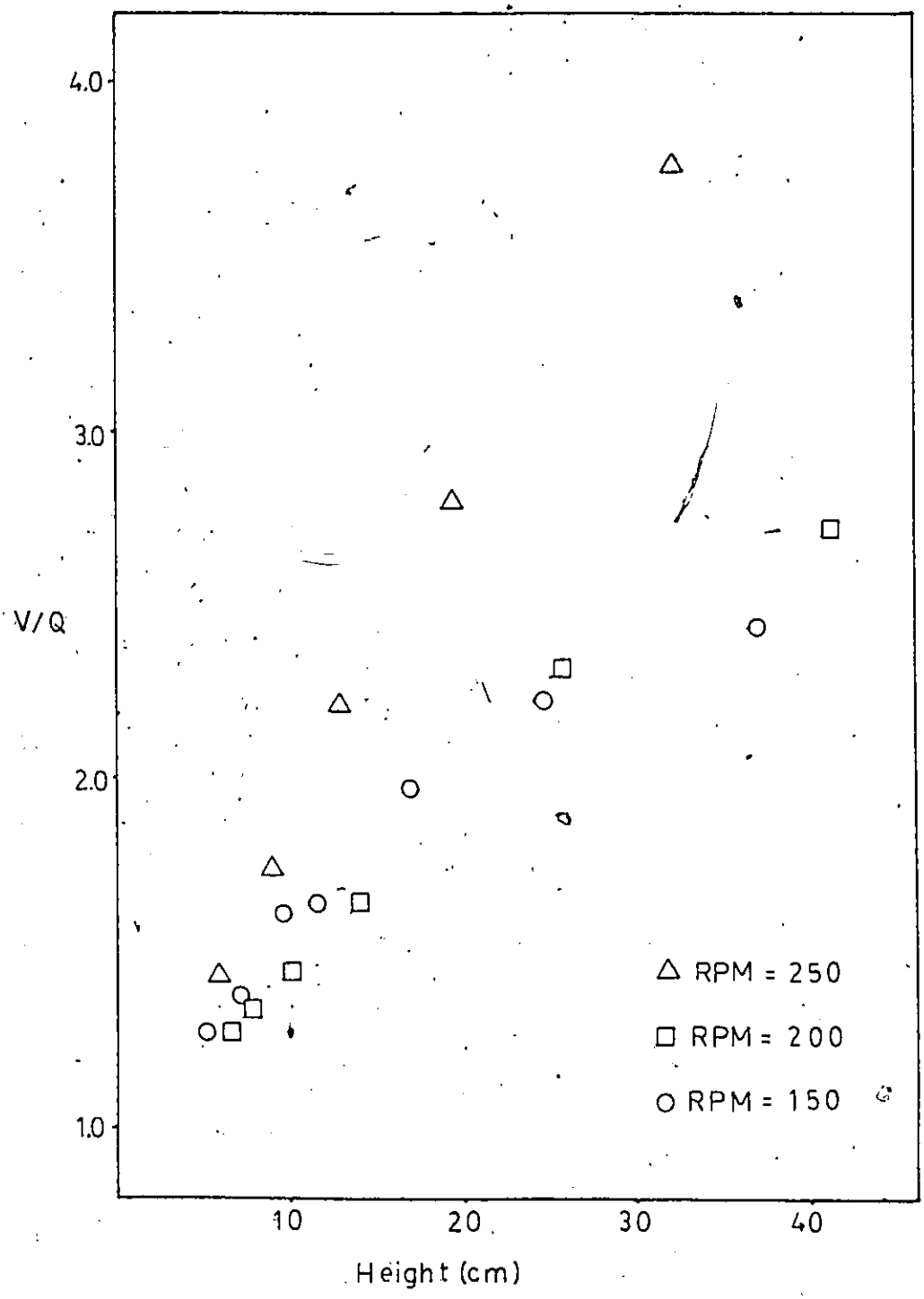

Figure F.4: V/Q vs H, Q=2000 ϕd=.4

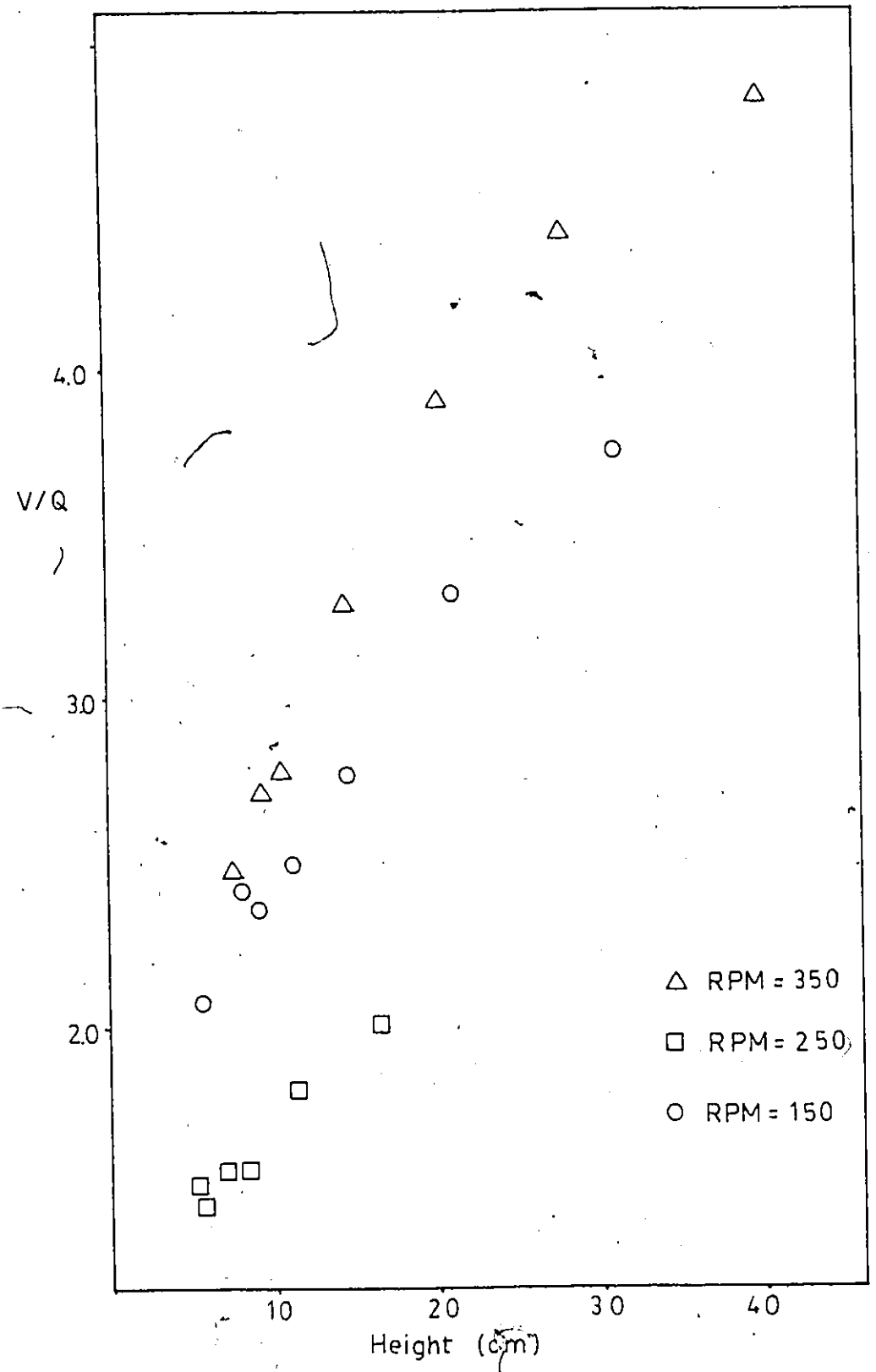

Figure F.5 V/Q vs H, Q=1500 ϕd=.6

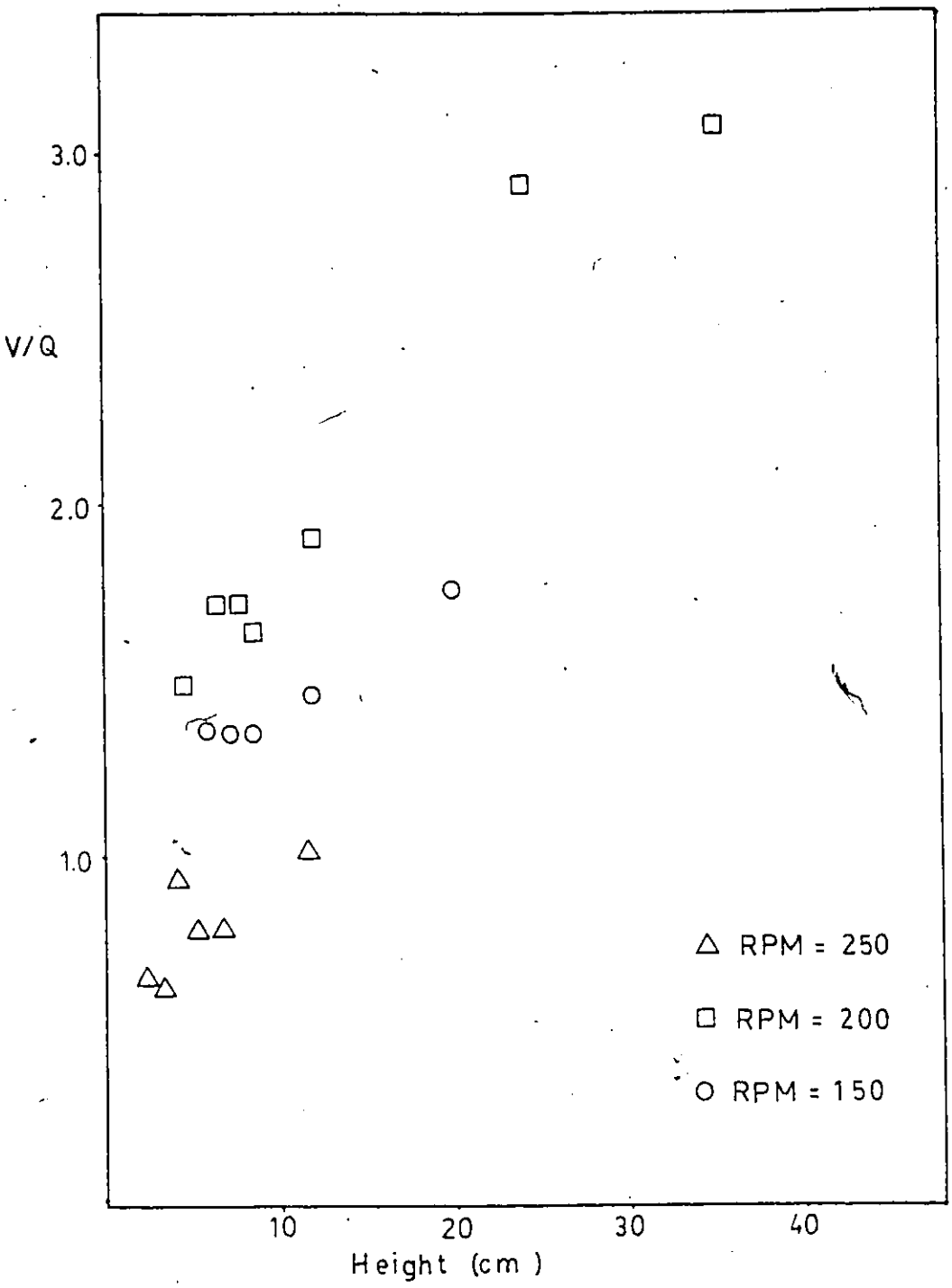

Figure F.6: V/Q vs H, Q=1500 ϕd=.4

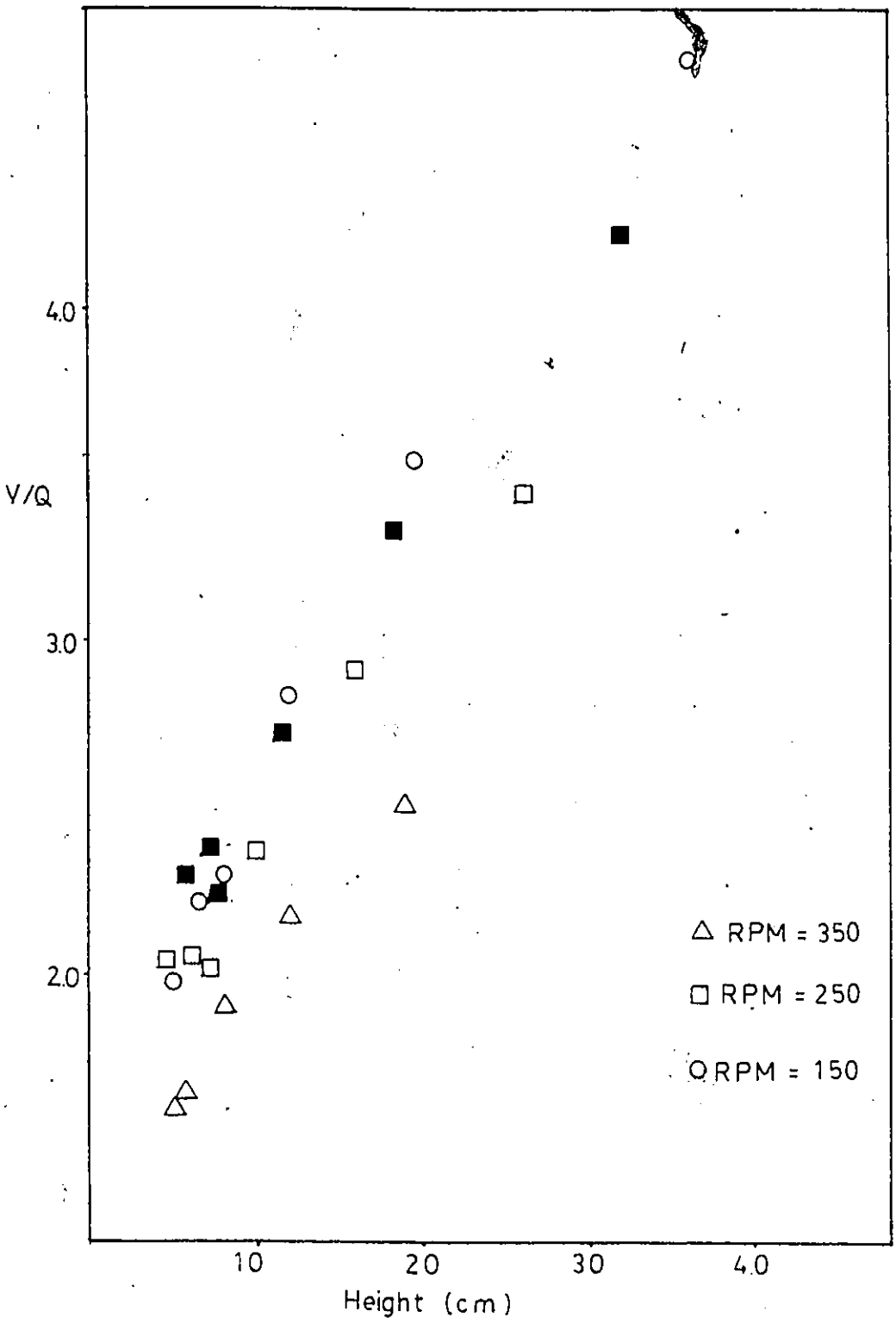

Figure F.7: V/Q vs H, Q=1000 ϕd=.6

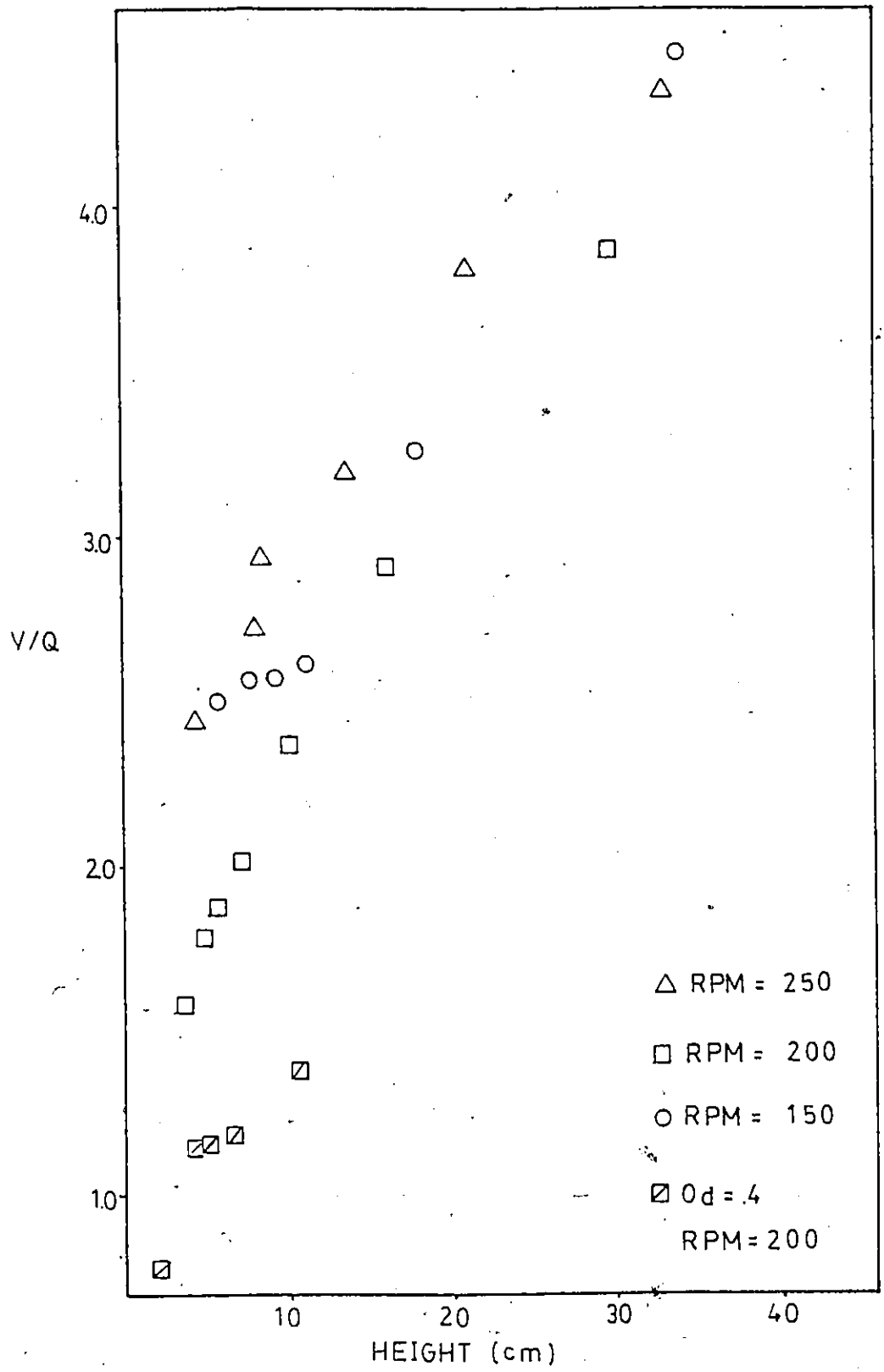

Figure F.8: V/Q vs H, Q=1000 ϕd=.5,.4

Appendix G

EQUIPMENT

Pumps	Masterflex peristaltic pumps with K 018 head
Rotameters	TRI-FLAT Fischer & Porter Co.
Impeller drive	Canlab RZR-50 variable speed mixer
Settler	Height 60 cm Full width Width 20 cm movable baffle Length 32 cm
Settling Areas	1 132 cm^2 2 182 3 237 4 287 5 341 6 396 7 455 8 497 9 547 10 641
Mixer A	volume 2500 ml^3 Square, open top 13.6 cm x 13.6 cm x 13.6 cm
Mixer B	volume 2500 ml^3 Cylindrical, closed top Height 14 cm, Diameter 15 cm

Impeller	6 Bladed turbine 5.2 cm O.D. Blades 1.73 wide x 1.4 cm high	
Phase Properties	Organic	density .80 g/cm³ viscosity 1.6 cp
	Aqueous	density 1.07 g/cm³ viscosity 1.0 cp
	Interfacial tension 40-50 dynes/cm	